Contrast Enhancement for Depolarizing Radar Targets

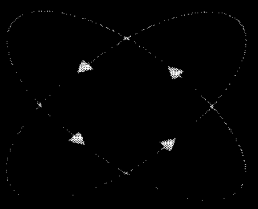

Dmitri N. Moisseev

TR 3863-5'

Propositions related to the dissertation

Contrast Enhancement for Depolarizing Radar Targets

by

Dmitri N. Moisseev

1. The general assumption that the polarization states of radar antennas are completely polarized is not valid. Moreover, this assumption can lead to poor calibration results and to misinterpretation of depolarization measurements.

2. Requiring the optimum polarization states to be completely polarized is not only unnecessary but it also limits the performance of polarimetric target contrast enhancement techniques.

3. The use of only second-order matrices calculated at zero lag to describe polarimetric properties of radar targets not only restrains the interpretation of polarimetric measurements but it also limits the performance of polarimetric contrast enhancement techniques.

4. Perfect objects for radar calibration should have not only very accurately known physical properties but also these properties should be identical to the properties of radar targets that one wishes to study.

5. The major irony of remote sensing is that the best measurements can be achieved only when the most *a priori* knowledge is available.

6. From the perspective of polarimetric radar measurements, ground echoes are less predictable than cloud echoes.

7. The major challenge in implementing polarimetric contrast enhancement techniques for ground clutter suppression is to develop appropriate adaptive processing techniques.

8. The art of drawing conclusions from experiments and observations consists in evaluating probabilities and in estimating whether they are sufficiently great or numerous enough to constitute proofs. This kind of calculation is more complicated and more difficult than it is commonly thought to be.

(Antoine Lavoisier)

9. The most exciting phrase to hear in science, the one that heralds new discoveries, is not 'Eureka!' but rather 'hmm...that's funny...'

(Isaac Asimov)

Stellingen behorende bij het proefschrift
Contrast Enhancement for Depolarizing Radar Targets
door
Dmitri N. Moisseev

1. De algemene aanname dat de polarisatiemodi van radarantennes volledig zijn gepolariseerd, is ongeldig. Bovendien kan deze aanname leiden tot slechte calibratieresultaten en tot een onjuiste interpretatie van depolarisatiemetingen.

2. Te eisen dat de optimale polarisatiemodi volledig gepolariseerd moeten zijn, is niet alleen onnodig, het beperkt ook de prestatie van polarimetrische doel-contrastverbeteringstechnieken.

3. Het gebruik van slechts tweede orde matrices, berekend voor vertraging nul en voor de beschrijving van de polarimetrische eigenschappen van radardoelen, beperkt niet alleen de interpretatie van polarimetrische metingen; het begrenst ook de prestatie van polarimetrische contrastverbeteringstechnieken.

4. Perfecte radarcalibratie-objecten moeten niet alleen eigenschappen hebben die zeer nauwkeurig bekend zijn, maar deze eigenschappen moeten ook identiek zijn aan die van het radardoel dat men wil studeren.

5. De grote ironie van remote sensing is dat de beste metingen alleen bereikt kunnen worden als de meeste *a- priori* kennis beschikbaar is.

6. Vanuit het perspectief van polarimetrische radarmetingen zijn grondecho's minder voorspelbaar dan wolkecho's.

7. De grootste uitdaging bij het implementeren van polarimetische contrastverbeteringstechnieken voor bodemclutter onderdrukking is het ontwikkelen van geschikte adaptieve bewerkingstechnieken.

8. De kunst om conclusies te trekken uit experimenten en observaties bestaat uit het evalueren van waarschijnlijkheden en het inschatten of deze voldoende groot zijn voor een bewijs. Deze manier van berekenen is gecompliceerder en moeilijker dan dat men algemeen aanneemt.

(Antoine Lavoisier)

9. In de wetenschap is de meest gehoorde opwindende zin die een nieuwe ontdekking aankondigt niet "Eureka!" maar eerder "hmm ...dat is grappig ..."

(Isaac Asimov)

Contrast Enhancement for Depolarizing Radar Targets

Contrast Enhancement for Depolarizing Radar Targets

PROEFSCHRIFT

ter verkrijging van de graad van doctor
aan de Technische Universiteit Delft,
op gezag van de Rector Magnificus prof. dr. ir. J.T. Fokkema,
voorzitter van het College voor Promoties,
in het openbaar te verdedigen op maandag 13 mei 2002 om 13.30 uur

door

Dmitri Nikolayevich MOISSEEV

Master of Science, Moscow Institute of Physics and Technology
geboren te Bolshevo, Rusland

Dit proefschrift is goedgekeurd door de promotor:

Prof. Dr. Ir. L. P. Ligthart

Toegevoegd promotor: Dr. Ir. H. W. J. Russchenberg

Samenstelling promotiecommissie:

Rector Magnificus	voorzitter
Prof. Dr. Ir. L. P. Ligthart	Technische Universiteit Delft, promotor
Dr. Ir. H. W. J. Russchenberg	Technische Universiteit Delft, toegevoegd promotor
Prof. Ir. P. van Genderen	Technische Universiteit Delft
Prof. Dr. E. Pottier	University of Rennes - 1, France
Prof. Dr. F. Yanovsky	National Aviation University, Ukraine
Prof. Dr. G. Brussaard	Technische Universiteit Eindhoven
Prof. Ir. P. Hoogeboom	Technische Universiteit Delft (reservelid)

Contrast enhancement for depolarizing radar targets / D.N. Moisseev

Includes bibliographical references and Dutch summary.

Keywords: Radar, Remote Sensing, Radar Polarimetry, Clutter Suppression, Target Enhancement, Doppler processing, Atmospheric Radar

ISBN 90-77017-64-X

Printed by Optima Grafische Communicatie, Rotterdam

to my mother and my father

Contents

Summary

Polarimetric measurements of radar objects play a more and more important role in radar research. The growing interest can be easily understood if the information content of the polarization measurements is considered. The polarization diversity do not only enable better retrieval of microphysical properties of radar objects such as shape and orientation, but they also give extra information on the time behavior of the radar objects and on properties of the radio wave propagation media. Radar polarimetry also becomes an important tool for improving of the quality of radar measurements; it can, for example, be used to increase the signal-to-noise ratio and the contrast between a target and background. The main questions which are studied in this Ph.D. project are the polarimetric calibration of radars and the use of Doppler polarimetry for characterizing and enhancing targets.

The first questions which arise when any measurement technique is used, are: how accurate are our measurements and how can we improve them? These simple questions have led to the development of a new polarimetric radar calibration procedure. The need for the calibration of any polarimetric system is based on the fact that the actual transmit and receive polarization states of the system differ from the ideal states. Generally, polarimetric calibration techniques are only optimal for point-target measurements. Since most of the atmospheric objects are distributed, an improved polarimetric calibration technique dedicated to measurements of extended objects was developed. This study is described in Chapter 2.

Because of the recent advances in radar technology that enable simultaneous Doppler and polarimetric measurements, the greater part of this thesis is dedicated to the use of both Doppler and polarimetry for characterizing time-varying radar objects better. The main results of this study are described in Chapter 5.

One of the main problems of radar observations is that the measured radar signal does not only contain responses from the wanted radar objects, but also from their surroundings. As the result the signals from building, trees, cars, birds,

insects, etc. occur in the echoes measured from atmospheric phenomena. Of all these unwanted targets, ground clutter plays the dominant role. The main challenge in the suppression of ground clutter is to reduce the clutter without affecting the weather echoes even when the Doppler spectrum properties of clutter and atmospheric phenomena are similar. In Chapters 4, and 6 three new polarimetric methods which address this problem are presented. In Chapter 4 it is shown that by subtracting the mean signal, the stable part of ground clutter can be suppressed and the remaining fluctuating part can be reduced by the wave decomposition technique. The result of this technique is an average improvement of the signal-to-clutter ratio of 16 dB. Chapter 6 shows that by combining Doppler and polarimetric information one can identify the Doppler velocity cells affected by ground clutter and suppress them. Moreover in this chapter a new polarimetric contrast enhancement technique is presented. This technique is based on the novel approach of decorrelating ground-clutter measurements by means of polarimetric transformation. It is shown that the signal-to-clutter ratio can drastically be improved even in the case of highly depolarizing clutter.

Chapter 1

Introduction

1.1 Motivation of research

Radar systems have proven to be a valuable tool for many remote sensing applications. By transmitting and receiving electromagnetic waves they allow us to study physical properties of remote objects. The applications of radar systems range from atmospheric and geophysical studies to surveillance and navigation tasks. By building more sensitive radar systems it becomes possible to study more remote and smaller objects. However, often the main factor that limits the use of radar is not the strength of the signal compared to noise, but the visibility of a target from the background reflections. Enhancing the visibility of targets is of paramount importance for improving the performance of the current radar systems.

The main topic of this Ph.D. thesis is to find new ways to discriminate between wanted and unwanted radar targets. Even though the main emphasis in this research lies on the suppression of ground clutter for atmospheric studies, most of the developed techniques can be applied to many other radar remote sensing scenarios.

1.2 Problem formulation

A radar is an active remote sensing instrument; it transmits and receives electromagnetic waves to measure physical properties of remote objects. Antennas are used to direct the radiation and to improve the sensitivity of the radar sys-

tem. However, due to the finite size of the antennas and the wave nature of EM radiation, radars transmit signals propagate in all directions from the antenna. Of course most of the energy is transmitted in the narrow beam around in one direction, but still some part of the transmitted signal escapes from this narrow beam. As a result radar can "see" objects even in the opposite direction. Another problem is that not only objects of interest are present in the radar beam and thus the radar signal contains also responses from unwanted targets. The separation of wanted and unwanted radar targets is very important for the improvement of all radar measurements.

In order to approach this problem let us first recall the information content of radar signals. Usually the radar wave is regarded to be a quasi monochromatic oscillation and thus it has the following characteristics: frequency, phase and amplitude. Moreover, since electromagnetic waves are transversal they also manifest vector properties and thus we have one more parameter for describing a radar wave: the polarization. So these four properties of the wave are the parameters which are used in radar remote sensing to study remote objects. Those are also the parameters which can be used to distinguish between different targets. Of course the easiest way to distinguish between two is to see if are they located at two different distances with respect to the radar. Nevertheless, in many cases this approach does not work. Another approach is to use the frequency changes induced by Doppler effect in the received signal. This approach allows one to separate two objects at the same range if they have different radial velocities with respect to the radar. However, the limitation of this technique is that if two objects have similar Doppler properties, the distinction between them becomes problematic. Another way to handle this problem is to use polarization properties to improve contrast between two radar targets. If shapes of these targets are different, it is possible by selecting the right polarization states of the antenna on the transmit and receive side to cancel the radar signal from one of them. However, if these targets shapes are not constant over the observation time or if orientations of these targets change over time this technique does not give the appropriate solution.

Based on the above we can formulate the scientific challenge addressed in this thesis study: How to improve the contrast between collocated radar targets in case they have similar Doppler velocities and their polarimetric properties are stochastic?

1.3 Thesis outline

In the study presented in this thesis the emphasis lie on the use of polarization diversity for enhancing radar targets.

In *Chapter 2*, we analyze the accuracy of polarimetric radar measurements of extended targets. It is shown that the common approach to describe antenna polarization states as completely polarized is not valid for distributed target measurements. This finding is very important for polarimetric measurements of atmospheric targets. In order to compensate for the deviations we propose a new polarimetric calibration procedure. This procedure is based on measurements of a known point-like target and of light rain. It is shown that the proposed calibration method allows us to improve the polarization isolation of the radar.

In *Chapter 3* a short overview of current clutter suppression techniques is given. It focuses on the polarimetric target contrast enhancement techniques. Cases of stationary and non stationary radar targets are discussed. It is shown that the target covariance matrix optimization technique is preferable for most applications. However, in the case of stationary targets this optimization leads to unpolarized states as optimum antenna polarization states.

Chapter 4 presents a novel technique for ground-clutter suppression for atmospheric radars. It is shown that by means of Doppler processing the polarimetric properties of the clutter can be modified. This technique is especially valuable if the Doppler frequencies of ground clutter are similar to the frequencies of atmospheric echoes.

In *Chapter 5* a new polarimetric formulation which combines both Doppler and polarimetric properties of targets is introduced. It is shown that this novel formalism, radar Doppler polarimetry, characterizes radar targets more completely and includes a common polarimetric formalism as a limiting case. Based on this new formulation the improved target enhancement technique is developed.

In *Chapter 6* the discussion on using polarimetry to improve the current Doppler clutter suppression technique is presented. It is shown that polarimetry is very convenient tool for identifying Doppler cells affected by ground clutter. Based on this study it is shown that this combination of Doppler and polarimetry results in a new clutter suppression technique which can succeed the common Doppler clutter suppression technique in the future. Further the worst case scenario for any target enhancement technique is presented. In this extreme case target and clutter Doppler properties are considered to be similar and clutter is highly depolarizing. Usually for this case neither Doppler nor polarimetric con-

trast technique will give a satisfactory result. However, it is shown that by using two pairs of transmit and receive polarizations to obtain measurements in such a way that clutter is decorrelated for these measurements, a high contrast between target and clutter can be achieved. The performance of this novel technique is demonstrated on the measurements of ground clutter.

In *Chapter 7* the main results of this Ph.D. research are summarized and conclusions are drawn. Also recommendations for future studies are given.

Chapter 2

Improved polarimetric calibration for extended targets

Abstract: Polarization properties of radar waves that are scattered from atmospheric objects are of great interest in meteorological studies. However, polarimetric radar measurements are often not sufficiently accurate for retrieving physical properties of targets. To compensate for errors, radar polarimetric calibration is applied. Typical calibrations are performed based on measurements of point targets with known scattering matrices located in the boresight of the antenna. Such calibration takes into account the polarization state of the antenna pattern only at one point. Since radar measurements of atmospheric phenomena involve distributed targets which fill the full antenna beam, point target radar calibrations are inadequate for meteorological studies.

This paper explains in detail the effects of the complete antenna patterns on weather echoes. It is shown that the conventional polarimetric calibration can be drastically improved by incorporating light rain (<20 dBZ) measurements into the calibration procedure. As a result the sensitivity of cross-polar measurements can be improved by 7 dB on average. Also it is shown that the bias in co-cross-polar correlation coefficient can be reduced.

2.1 Introduction

During recent years there has been a growing interest in the use of radar polarimetry for atmospheric studies. It has resulted in the use of various polarimetric parameters for the characterization of the studied media (Zrnic and Ryzhkov 1999). However, little attention has been given to the polarimetric calibration of atmospheric radars. Current calibration techniques are based on the measurement of known point targets. This approach uses the assumption that the polarimetric measurements with the radar can be described by the polarimetric properties of only one point of the radar antenna pattern. However, atmospheric radars most of the time are used for studies of extended radar objects and thus full antenna pattern information must be taken into account.

The main goal of using calibration methods based on point-target measurements is to estimate the distortion matrices (McCormick 1981), which characterize the transmit and receive channels of the system. Many different approaches are described in the literature to retrieve these distortion matrices. The main difference between them lies in the assumptions which are used in order to simplify the calibration procedure. It was shown by Sarabandi and Ulaby (1990) that if the antenna system and two orthogonal channels of the radar system are modeled as a four-port passive network, the calibration can be simplified to the measurement of a metallic sphere. Another approach is to assume a good polarization isolation of the system (>25 dB); then the polarimetric calibration can be done by using a metallic sphere and an unknown highly depolarizing target (Sarabandi et al. 1990). The use of the assumption of reciprocity of the antenna system was demonstrated in (Unal et al. 1994), and because of this assumption the polarimetric calibration can be carried out by using a single rotatable dihedral corner reflector. The use of weather echoes for calibration was demonstrated in (Hubbert and Bringi 2001). However, in this paper the point target calibration formalism was also employed as the basis for the calibration procedure.

In this chapter we analyze errors which are implied by the point target calibration formalism. Based on this analysis a correction method for existing calibration procedures is proposed. It is demonstrated that by applying this correction we can obtain more accurate cross-polar measurements. This new polarimetric calibration procedure is demonstrated using a set of precipitation measurements collected with the Delft Atmospheric Research Radar (DARR). The DARR description is given by Ligthart and Nieuwkerk (1980).

2.2 Point target polarimetric calibration

For an ideal polarimetric system, the measured scattering matrix of an object, **M**, is identical to the actual scattering matrix, **S**. However, in real radar systems these matrices are different. Usually this difference is explained by the divergence of the expected transmit and receive polarization states from the actual ones. For example, a radar transmit (or receive) basis that is treated as a linear $h - v$ basis is in reality a non-orthogonal basis with polarization vectors which are slightly elliptical. In this case a measured scattering matrix can be represented as:

$$\mathbf{M} = \mathbf{RST}, \tag{2.1}$$

where **R** and **T** are the antenna distortion receive and transmit 2x2 matrices, or, in other words, the matrices that transform the desired polarimetric basis into the actual antenna basis. This equation introduces the basics for the point target polarimetric radar calibration. It can be seen that if no assumptions are made about the **R** and **T** matrices, three known point targets are required to retrieve all elements of the distortion matrices.

Following the assumption used by Unal et al. (1994) and Hubbert and Bringi (2001) that the radar can be considered to be reciprocal ($\mathbf{M}^T = \mathbf{M}$), the formulation can be simplified as

$$\mathbf{M} = \mathbf{T}^T\mathbf{ST}, \tag{2.2}$$

where

$$\mathbf{T} = T_{11} \cdot \begin{bmatrix} 1 & \delta_2 \\ \delta_1 & f \end{bmatrix} \tag{2.3}$$

and δ_1, δ_2 represent coupling terms between the radar polarization channels, f is the one-way co-polar channel imbalance, and T_{11} is the coefficient which combines the absolute calibration constant and the radio wave propagation coefficient. It should be noted that since we are only interested in relative polarimetric calibration, the coefficient T_{11} is not considered in our discussion for the sake of simplicity.

Using the formulation (2.2) and taking into account that the matrices **M** and

S are symmetric, we can rewrite (2.2) as

$$\vec{m} = \begin{bmatrix} 1 & 2\delta_1 & \delta_1^2 \\ \delta_2 & f + \delta_1\delta_2 & f\delta_1 \\ \delta_2^2 & 2f\delta_2 & f^2 \end{bmatrix} \cdot \vec{s}, \tag{2.4}$$

where $\vec{s}$ and $\vec{m}$ are vector representations of the matrices **M** and **S**,

$$\vec{s} = \begin{bmatrix} S_{hh} & S_{hv} & S_{vv} \end{bmatrix}^T \text{ and } \vec{m} = \begin{bmatrix} M_{hh} & M_{hv} & M_{vv} \end{bmatrix}^T.$$

It is common to use the polarimetric covariance matrix $\mathbf{C} = \langle \vec{s} \cdot \vec{s}^{+} \rangle$ for the description of atmospheric targets (Santalla et al. 1999; Ryzhkov 2001); here $^+$ is the Hermitian transpose operator and $\langle\rangle$ denotes ensemble average. In order to obtain the calibrated covariance matrix **C** we should change (2.4) as follows:

$$\vec{c}_m = \mathbf{D}\vec{c}_s, \tag{2.5}$$

where $\vec{c}_m$ and $\vec{c}_s$ are the vector representations of the measured and actual object's covariance matrices and **D** is the system distortion matrix, which is defined as

$$\mathbf{D} = \begin{bmatrix} 1 & 2\delta_1 & \delta_1^2 \\ \delta_2 & f + \delta_1\delta_2 & f\delta_1 \\ \delta_2^2 & 2f\delta_2 & f^2 \end{bmatrix} \otimes \begin{bmatrix} 1 & 2\delta_1 & \delta_1^2 \\ \delta_2 & f + \delta_1\delta_2 & f\delta_1 \\ \delta_2^2 & 2f\delta_2 & f^2 \end{bmatrix}^*. \tag{2.6}$$

Here $\otimes$ denotes the Kronecker matrix product and * denotes complex conjugation.

Assuming we know f, δ_1, and δ_2, we can use (2.5) to obtain a calibrated covariance matrix of a radar object. However, this approach is based on the assumption that it suffices to estimate the distortion matrix at only one point of the antenna pattern. This approach can be erroneous, especially for atmospheric studies, where the complete antenna pattern plays a role in the radar measurement.

2.3 Effect of complete antenna patterns on atmospheric measurements

2.3.1 Polarimetric measurements of distributed targets

For a distributed target measurement, the measured scattering matrix is related to the target scattering matrix as in (Blanchard and Jean 1983; Doviak and Zrnic 1993):

$$\mathbf{M} = \int\int [f_r(\theta,\phi)]\,\widetilde{\mathbf{S}}(\theta,\phi)\,[f_t(\theta,\phi)]\sin\theta d\theta d\phi, \tag{2.7}$$

where $[f_i(\theta,\phi)] = \begin{bmatrix} f_{hh}(\theta,\phi) & f_{hv}(\theta,\phi) \\ f_{vh}(\theta,\phi) & f_{vv}(\theta,\phi) \end{bmatrix}$ with $i = r, t$

is the receive (or transmit) distortion matrix whose elements are antenna patterns for all polarization states and $\widetilde{\mathbf{S}}(\theta,\phi)$ is the scattering matrix of an extended radar target for the azimuth angle θ and the elevation angle ϕ. This formulation gives the most general description of the influence of the radar system on polarimetric measurements. From (2.7) it follows that in order to perform an accurate polarimetric radar calibration, one requires knowledge of eight 2-D antenna patterns (four if the reciprocity assumption of the antenna system is used). However, measuring antenna patterns accurately is complicated and time consuming, and not an option for most atmospheric radars. That is why it is important to see how the antenna patterns influence the polarimetric measurements of atmospheric objects and what can be done to reduce this effect.

2.3.2 Co-polar channel imbalance

The channel imbalance f is an important parameter; it can be seen from (2.2) and (2.3) that for radars with good polarization isolation (small δ_1, δ_2) the accuracy of the measured differential reflectivity ($Zdr = \frac{\langle |M_{hh}|^2 \rangle}{\langle |M_{vv}|^2 \rangle}$) is directly related to f.

In order to see how the complete antenna pattern influences Zdr measurements, we used the antenna patterns (see Fig. 2.1) of DARR. Coherent measurements of the antenna patterns in principal and 45 degrees planes of DARR antenna patterns were available for this study. A detailed information on antenna pattern measurements technique can be found in (Aubry and Zijderveld 1999). But only the 45 degrees plane measurements in conjunction with the assumption of rotationally symmetric co-polar antenna patterns were used for this study. This assumption

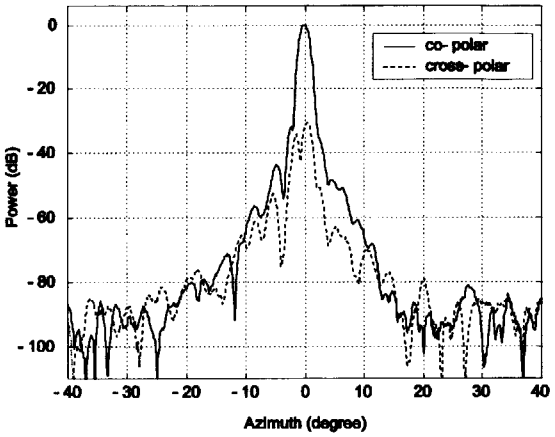

Figure 2.1: Two-way antenna patterns (45-degree plane). The solid line is the co-polar pattern and the dashed line is the cross-polar pattern.

was also confirmed by comparing the co-polar patterns measured in the principal and 45 degree planes. Using (2.7) we have estimated the measured Zdr value for a target with $Zdr = 0$ dB. Based on these calculations we have found that the difference between co-polar polarization channels due to the use of full antenna patterns is small and gives an uncertainty in Zdr measurements of about 10^{-2} dB.

Due to uncertainties in the used antenna pattern model and in the antenna measurements, especially for far side-lobes, this estimation does not give us the exact value of the influence of the complete antenna patterns on f. However, it does give us an estimate of the order of magnitude of this influence. Thus for most atmospheric studies the required Zdr accuracy of about 0.1 dB can be achieved by applying a point target polarimetric calibration.

2.3.3 Polarization isolation for a distributed target

The other important characteristic of an antenna system is the polarization isolation. The polarization isolation defines how pure the polarization state of a radar is. For atmospheric studies the polarization isolation of the radar determines the minimum possible measured linear depolarization ratio values ($Ldr = \frac{\langle |M_{vh}|^2 \rangle}{\langle |M_{hh}|^2 \rangle}$). If the point calibration notation is used, the polarization isolation ρ_a can be retrieved

as

$$\rho_a = \frac{\left\langle |M_{hh}|^2 \right\rangle}{\left\langle |M_{vh}|^2 \right\rangle} = \frac{|1+\delta_1^2|^2}{|\delta_2 + f\delta_1|^2} \simeq |\delta_2 + f\delta_1|^{-2}, \tag{2.8}$$

where $\left\langle |M_{hh}|^2 \right\rangle$ and $\left\langle |M_{vh}|^2 \right\rangle$ are averaged measured powers of hh, and vh elements of the scattering matrix of a polarimetrically isotropic non-depolarizing target ($\left\langle |S_{vh}|^2 \right\rangle = 0$, $\left\langle |S_{hh}|^2 \right\rangle = \left\langle |S_{vv}|^2 \right\rangle$). It can be seen that the smallest measurable Ldr value is fully defined by the antenna isolation value. Based on the point target calibration (Unal et al. 1994) it was determined that this value is 33 dB for DARR.

However, many atmospheric measurements with DARR showed that this value is never achieved and the minimum measured Ldr value is only -27.5 dB. This Ldr value does not represent the characteristic of atmospheric echoes, but the antenna polarization isolation. This difference between the predicted and measured polarization isolation was first described by Blanchard and Jean (1983). It was shown that this discrepancy can be explained by the difference in the estimations of the polarization isolation; whether it is estimated on measurements at one point at the boresight of the antenna or estimated by taking into account complete antenna patterns.

Similar to (2.8) we can define the polarization isolation for an extended target

$$\widetilde{\rho}_a = \frac{\left\langle |M_{hh}|^2 \right\rangle}{\left\langle |M_{vh}|^2 \right\rangle} \tag{2.9}$$

$$\left\langle |M_{hh}|^2 \right\rangle \simeq \left\langle \left| \int \widetilde{S}_{hh}(\theta,\phi) \cdot f_{thh}(\theta,\phi) f_{rhh}(\theta,\phi) d\Omega \right|^2 \right\rangle$$

$$\left\langle |M_{vh}|^2 \right\rangle \simeq \left\langle \left| \begin{array}{l} \int \widetilde{S}_{hh}(\theta,\phi) \cdot f_{thh}(\theta,\phi) f_{rvh}(\theta,\phi) d\Omega + \\ + \int \widetilde{S}_{vv}(\theta,\phi) \cdot f_{tvh}(\theta,\phi) f_{rvv}(\theta,\phi) d\Omega \end{array} \right|^2 \right\rangle$$

where Ω is the solid angle and $d\Omega = \sin\theta d\theta d\phi$. Using (2.9) we estimated the polarization isolation for DARR; it was found to be about 27 dB. This value of the polarization isolation is in good agreement with the atmospheric measurements.

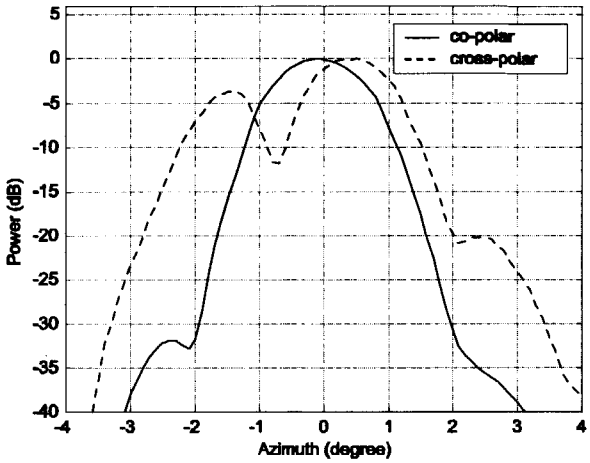

Figure 2.2: Two-way antenna patterns (45-degree plane). The cross-polar pattern is normalized to have the same maximum value as the co-polar pattern.

2.3.4 Difference between co- and cross-polar antenna patterns

The measurements of any element of the scattering matrix are influenced by the co- and cross-polar antenna patterns (Fig. 2.1). These antenna patterns determine the spatial structure of the co-polar and cross-polar channel responses and are represented in the distortion matrices as f_{thh}, f_{tvv}, f_{rhh}, f_{rvv} for co-polar patterns and f_{thv}, f_{tvh}, f_{rhv}, f_{rvh} for the cross-polar ones. In the cross-polar measurement of weakly depolarizing targets (most atmospheric objects), the influence of the cross-polar channel response is strong. Compensation of this influence is an important part of any calibration procedure. In a point target calibration procedure, co-polar and cross-polar channel responses are assumed to have no spatial dependences. However, in reality, this can be an erroneous assumption. From Fig. 2.1 and in more detail from Fig. 2.2 it can be seen that the co- and cross-polar antenna patterns have different shapes and as a result the observed volumes are also different.

The effect of the difference between these antenna patterns can clearly be seen in the observations of the magnitude of cross-correlation coefficient $|\rho_{xh}(0)| =$

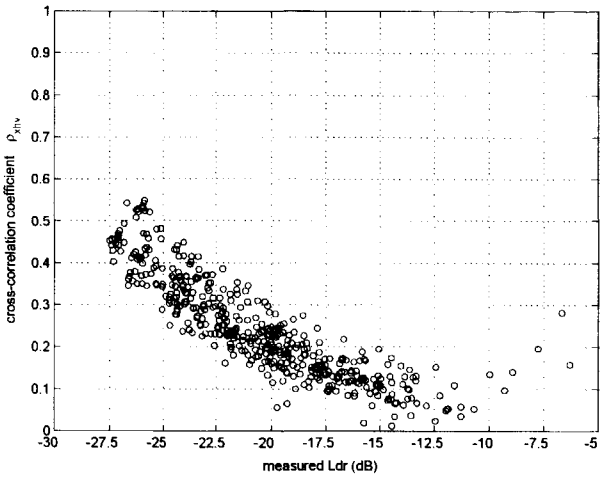

Figure 2.3: Dependence of the cross-correlation coefficient $|\rho_{xh}(0)|$ on *Ldr* for precipitation measurements.

$\left|\frac{\langle M_{hh} M_{vh}^* \rangle}{\sqrt{\langle |M_{hh}|^2 \rangle \langle |M_{vh}|^2 \rangle}}\right|$ (or $|\rho_{xv}(0)|$) between co-polar and cross-polar measurements of atmospheric objects. Fig. 2.3 shows the dependence between the cross-correlation coefficient and the measured *Ldr* values. This figure represents the calculations based on 6 different measurements of light rain, in 5 cases the radar pointed to the zenith and in one case it had an 80 degrees elevation angle. This figure shows measurement points that correspond not only to the light rain but also to the melting layer. For the case of light rain, the measurements with $Ldr \approx -27$ dB had a signal-to-noise ratio for cross-polar measurements of about 15 dB. More details about the signal processing which was applied to calculate this correlation coefficient can be found in section 2.4.2 of this chapter.

It is common to assume that the correlation coefficient between pure co-polar and cross-polar measurements of precipitation to be zero (Antar and Hendry 1985; Brussaard 1976). Even though, recent studies by Ryzhkov (2001) have shown that in some cases this correlation coefficient can differ from zero, but we do not expect that this effect will be significant for the zenith measurements of precipitation. So if this assumption is used, the further behavior of the scatter plot is clear and shows that with the increase of the *Ldr* values the correlation coefficient should

decrease. However, the value of the cross-correlation coefficient for Ldr values close to -27 dB requires more explantation.

While the co-polar measurements are mainly determined by the co-polar response of the target, the cross-polar measurements are strongly affected by coupling between the polarization channels. Thus, if the measurements of the target are performed with $Ldr = -\infty$ dB, the expected value of $|\rho_{xh}(0)|$ from the point of view of point target calibration will be 1, since it does not have any spatial dependence and the measured cross-polar values are determined purely by the coupling from the co-polar channel. But if the complete antenna patterns are taken into account, this value will be defined by the mismatch between the co- and cross-polar antenna patterns. In this case the co- and cross-polar measurements correspond to different radar volumes, and this results in the decorrelation between these two measurements.

To check whether this effect is strong enough to explain the obtained values of the cross-correlation coefficient, we used the measured antenna patterns. For such calculations knowledge of the two-dimensional antenna patterns $[f(\theta, \phi)]$ is needed. In our case only principal plane and 45-degree plane measurement of the antenna patterns were available. It is a good approximation to assume that the 2-D co-polar antenna pattern can be obtained by the rotation of the measured pattern in one plane, as we have done in section 2.3.2. This assumption, however, is not generally valid for the cross-polar antenna patterns, but can be used for the purpose of this chapter, as shown below.

The two-dimensional distribution of the gain function of the cross-polar response of the antenna has 4 clear maxima: 2 in the 45-degree plane (see Fig. 2.2) and 2 in the 135-degree plane; for the other angles the cross-polar gain becomes smaller, reaching its minimum in the main planes. As a result, if we used rotationally symmetric patterns obtained from the 45-degree plane antenna pattern, the intersection between the radar volumes for the co-polar and cross-polar measurements is larger than in reality; hence we overestimate the correlation between the co-polar and the cross-polar reflections. And thus if the estimated magnitude of the correlation coefficient will be significantly smaller than unity it will prove our hypothesis.

Let us calculate the correlation coefficient between cross-polar and co-polar signals. By using (2.7), the receive averaged power of co-polar reflections can be written as

$$\langle M_{hh}M_{hh}^{*}\rangle = \iint \left\langle \widetilde{S}_{hh}(\theta,\phi)\widetilde{S}_{hh}^{*}(\theta\prime,\phi\prime)\right\rangle \times \\ \times f_{thh}(\theta,\phi)f_{rhh}(\theta,\phi)\times \\ \times f_{thh}(\theta\prime,\phi\prime)f_{rhh}(\theta\prime,\phi\prime)d\Omega d\Omega\prime. \tag{2.10}$$

We should note that due to the fact that reflections from different volumes are uncorrelated, we can write the following $\left\langle \widetilde{S}_{hh}(\theta,\phi)\widetilde{S}_{hh}^{*}(\theta\prime,\phi\prime)\right\rangle = 2\sigma_{\Omega}^{2}\cdot\delta(\theta-\theta\prime,\phi-\phi\prime)$, $2\sigma_{\Omega}^{2}$ is the power per unit solid angle. Then, assuming uniform beam filling, (2.10) can be rewritten as

$$\left\langle |M_{hh}|^{2}\right\rangle = 2\sigma_{\Omega}^{2}\int f_{thh}^{2}(\theta,\phi)f_{rhh}^{2}(\theta,\phi)d\Omega \tag{2.11}$$

For the cross-polar averaged power we have

$$\left\langle |M_{vh}|^{2}\right\rangle = 2\sigma_{\Omega}^{2}\int f_{thh}^{2}(\theta,\phi)f_{rvh}^{2}(\theta,\phi)d\Omega+ \\ +4\sigma_{\Omega}^{2}\int f_{thh}(\theta,\phi)f_{rvh}(\theta,\phi)\times \\ \times f_{tvh}(\theta,\phi)f_{rvv}(\theta,\phi)d\Omega+ \\ +2\sigma_{\Omega}^{2}\int f_{tvh}^{2}(\theta,\phi)f_{rvv}^{2}(\theta,\phi)d\Omega. \tag{2.12}$$

To obtain (2.12) we have assumed that $\left\langle |S_{hh}|^{2}\right\rangle = \left\langle |S_{vv}|^{2}\right\rangle$ and $\frac{\langle S_{hh}S_{vv}^{*}\rangle}{\sqrt{\langle |S_{hh}|^{2}\rangle\langle |S_{vv}|^{2}\rangle}} = 1$. Finally the covariance is

$$\langle M_{hh}M_{vh}^{*}\rangle = 2\sigma_{\Omega}^{2}\int |f_{thh}(\theta,\phi)|^{2}\, f_{rhh}(\theta,\phi)\times \\ \times f_{rvh}^{*}(\theta,\phi)d\Omega+ \\ +2\sigma_{\Omega}^{2}\int f_{thh}(\theta,\phi)f_{rhh}(\theta,\phi)\times \\ \times f_{tvh}^{*}(\theta,\phi)f_{rvv}^{*}(\theta,\phi)d\Omega. \tag{2.13}$$

Using (2.11), (2.12) and (2.13) we calculated the cross-correlation coefficient and it is found to be equal to 0.74. This value, as it was expected, is larger than

the measured value of 0.5 (see Fig. 2.3), but it proves that mismatching of the antenna patterns can have a significant influence on $|\rho_{xh}(0)|$.

Based on the above-presented studies we can conclude that:

- for the *Zdr* measurements, a common point target calibration can be used
- polarization isolation and thus the coupling terms (δ_1 and δ_2) are strongly dependent on the complete antenna pattern.

2.4 Improvement of the polarimetric radar calibration procedure

2.4.1 Use of light-rain zenith measurements for improvement of the calibration

The above-presented study shows that the polarimetric radar calibration procedure based on point target measurements does not give an adequate description of the influence of the radar antennas on cross-polar properties of atmospheric echoes. It was also indicated that if a point target calibration procedure is combined with measurements of a known distributed target, a much better description of the effect of the radar system on polarimetric measurements can be achieved. However, the main problem of this approach is the availability of a distributed target with known polarimetric characteristics.

The most obvious candidate for the role of a known distributed target is light rain measured with a radar pointing to the zenith. Generally, we would expect that for this type of measurement the light rain will behave as a polarimetrically isotropic non-depolarizing target, meaning that the actual *Ldr* of light rain is much smaller than the antenna limit. However, this assumption can be violated in some special cases. It was shown by Ryzhkov et al. (1999) that hydrometeors can have a non-zero mean canting angle which will result in non-zero *Ldr* values even for the vertically pointing radar. This is usually caused by windshear or updraft. Another effect (Jameson and Durden 1996) which can contribute to the failure of our assumption is that large raindrops can oscillate (change their shape). This oscillation will result in the increase of the *Ldr* values. These two effects can put a restriction on the use of light rain for calibration. A reduction of these effects is feasible, however.

The oscillation of raindrops as well as a non-zero canting angle mainly contribute to the changes of polarimetric properties of large raindrops. This can

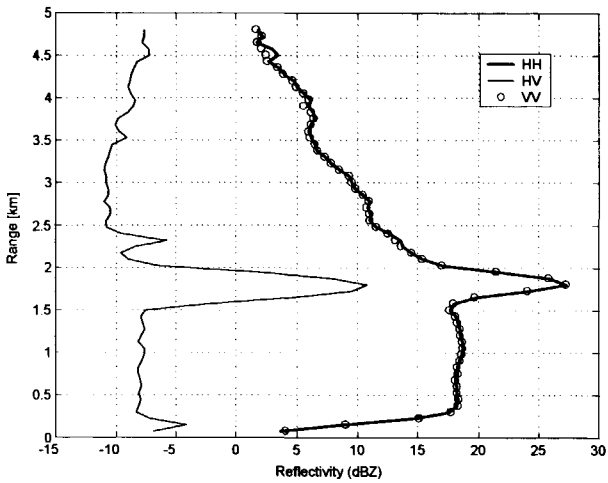

Figure 2.4: A typical vertical profile of rain. Only the absolute calibration is applied.

be efficiently reduced by applying Doppler processing. Furthermore, these effects were mainly seen for strong rain intensities (reflectivity above 30dBZ), while we use only light-rain data with values of reflectivities not larger than 20 dBZ, see Fig. 2.4.

2.4.2 Signal processing used for the estimation of the polarimetric properties of rain

Several signal processing algorithms were applied to reduce the influence of the following four effects:

- ground clutter
- noise
- change of the polarimetric properties of large raindrops
- staggered polarimetric measurements

Since very accurate measurements of the small cross-polar signal are paramount for the calibration procedure the appropriate clutter suppression should be

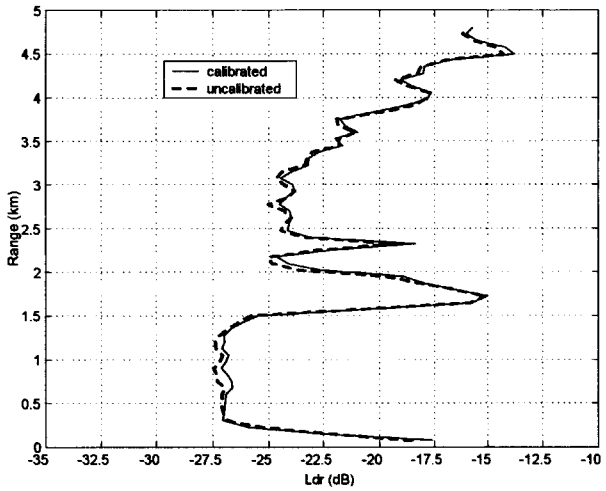

Figure 2.5: *Ldr* profile of precipitation. The dashed line represents the uncalibrated *Ldr* and the solid line shows the calibrated *Ldr*. The point target calibration technique was used. Steady increase of *Ldr* values in the cloud region is caused by a decrease in signal-to-noise ratio.

applied even to 90 degree elevation measurements of rain. The employed clutter suppression is based on the use of the co-polar correlation coefficient (Ryzhkov and Zrnic 1998; Moisseev et al. 2000) calculated for every Doppler resolution cell. For ground clutter these values are generally smaller than 0.7 and for atmospheric objects they are higher than 0.8. Thus, the Doppler cells which are contaminated by ground clutter can be successfully identified and suppressed. We should note that this processing also rejects cells with a poor signal-to-noise ratio (SNR). For further reduction of the noise, the averaged noise power was subtracted from all power measurements. Moreover, for all measurements presented in this paper averaging over 40 s was used.

In Fig. 2.4 the averaged vertical profiles of precipitation are given. It should be noted that in the cloud above the melting layer signal-to-noise ratio decreases, as a result the SNR is almost unity for cross-polar measurements at the height of 4.5 km. This effect also causes a steady increase of *Ldr* values above the melting layer in Fig. 2.5. Therefore, for our analysis only data of rain and melting layer, where SNR is better than 15 dB for cross-polar measurements, were used.

Presence of distorted large raindrops is controlled by examining the behavior of Zdr and Ldr as functions of Doppler velocity (Unal et al. 2001). As a result, Doppler spectra, where changes in these parameters for different Doppler resolution cells are observed, were discarded.

Since DARR has only one channel receiver all covariances in the measured covariance matrix, $\mathbf{C}_m$, are obtained at non zero time lag. Thus, it is necessary to estimate the values of these covariances at zero time lags. It can be shown that the difference between the cross-correlation calculated at zero time lag and at the time lag τ is an extra phase component $\omega\tau$ in the cross spectrum (Unal and Moisseev 2002). Thus, by compensating this phase difference on a calculated cross-spectrum and performing inverse FFT we can obtain a very accurate estimate of a covariance at zero time lag, for more information see (Unal and Moisseev 2002). Applying this step to all covariances in $\mathbf{C}_m$ we obtain a covariance matrix of precipitation as if all elements of the scattering matrix were measured simultaneously.

2.4.3 Improved calibration procedure and calibration results

From the above presented study we can conclude that point target calibration uses the assumption that antenna polarization states are completely polarized and thus they can be fully characterized by two 2x2 matrices, $\mathbf{T}$ and $\mathbf{R}$. It was also shown that in the case of distributed target measurements the correlation coefficient between direct and coupling terms of antenna polarization states is not equal to unity, and thus the assumption of antenna polarization states being completely polarized is not valid. Thus, in order to describe such partially polarized states the combined second-order distortion matrix should be used. Moreover, it should be noted that this distortion matrix cannot be determined from $\mathbf{T}$ and $\mathbf{R}$ alone, but needs to be corrected based on actual measurements to take into account the full antenna pattern. In this section the procedure to improve calibration results for atmospheric studies based on measurements of light rain added to the results of the point target calibration is discussed.

As is shown above, the channel imbalance obtained from the point target calibration is precise enough to retrieve the Zdr values. On the other hand, the cross-polar measurements are very sensitive to the calibration procedure and thus the polarimetric calibration should be modified in order to improve the accuracy of these measurements. Based on this, we can postulate that from the point target calibration the channel imbalance f can be retrieved and the light-rain measure-

ment data can be used to improve the cross-polar measurements.

Generally, the cross-polar voltage will be defined as a sum of integrals of $f_{xx}(\theta,\phi)f_{xy}(\theta,\phi)$, where the subscripts xx and xy correspond to any co-polar and cross-polar antenna pattern and the co-polar voltage is defined by $f_{xx}(\theta,\phi)f_{xx}(\theta,\phi)$. Based on this, we can conclude that a co-cross-polar covariance is defined by the sum of the integrals with the elements under the integral sign that are analogous to $f_{xy}(\theta,\phi)$ (or $f^*_{xy}(\theta,\phi)$). This can be seen in (2.13). In terms of the point target calibration these elements are similar to δ_i (or δ_i^*), where $i = 1,2$. Under the current assumption of reciprocity of the radar system, the co-cross-polar covariances should be equal for the measurements of light rain; this also is confirmed by our measurements. Therefore, the decorrelation between co-polar and cross-polar measurements due to the antenna pattern is characterized by one correlation coefficient $|\rho_{xh}(0)|$, it should be noted that we neglect the higher-order effects such as coupling of the cross-polar signal into the co-polar channel. In order to take this decorrelation into account one should multiply the elements of the matrix $\mathbf{D}$ which are proportional to δ_i (or δ_i^*) by the cross-correlation coefficient $|\rho_{xh}(0)|$ obtained from the light-rain measurements. As a result we can obtain the modified distortion matrix, $\widehat{\mathbf{D}}$, as:

$$\widehat{\mathbf{D}} = \begin{pmatrix} 1 & |\rho_{xh}(0)| & 1 & |\rho_{xh}(0)| & 1 & 1 & 1 & 1 & 1 \\ |\rho_{xh}(0)| & 1 & |\rho_{xh}(0)| & 1 & |\rho_{xh}(0)| & 1 & 1 & 1 & 1 \\ 1 & |\rho_{xh}(0)| & 1 & 1 & 1 & |\rho_{xh}(0)| & 1 & 1 & 1 \\ |\rho_{xh}(0)| & 1 & 1 & 1 & |\rho_{xh}(0)| & 1 & |\rho_{xh}(0)| & 1 & 1 \\ 1 & |\rho_{xh}(0)| & 1 & |\rho_{xh}(0)| & 1 & |\rho_{xh}(0)| & 1 & |\rho_{xh}(0)| & 1 \\ 1 & 1 & |\rho_{xh}(0)| & 1 & |\rho_{xh}(0)| & 1 & 1 & 1 & |\rho_{xh}(0)| \\ 1 & 1 & 1 & |\rho_{xh}(0)| & 1 & 1 & 1 & |\rho_{xh}(0)| & 1 \\ 1 & 1 & 1 & 1 & |\rho_{xh}(0)| & 1 & |\rho_{xh}(0)| & 1 & |\rho_{xh}(0)| \\ 1 & 1 & 1 & 1 & 1 & |\rho_{xh}(0)| & 1 & |\rho_{xh}(0)| & 1 \end{pmatrix} .*\mathbf{D}, \tag{2.14}$$

where .* denotes the operator of element by element matrix multiplication.

A second step to improve polarimetric calibration is to compensate for the difference between the polarization isolation estimations, (2.8) and (2.9). At the first glance one can conclude that this can be done by solving (2.5) for adequate δ_1 and δ_2. However, this solution is sensitive to the accuracy of f and it depends on the decorrelation compensation. Although the estimation of f from the point target calibration is accurate enough for the Zdr measurements, the order of magnitude of its error is comparable to the magnitudes of coupling terms δ_1 and δ_2. It means that the accurate solution of (2.5) for δ_1 and δ_2 is impossible. However, the difference between two polarization isolation estimates can effectively be reduced just by multiplying δ_1 and δ_2 by $\sqrt{\frac{\widetilde{\rho}_a}{\rho_a}}$, as follows from (2.8). The complete antenna polarization isolation $\widetilde{\rho}_a$ is equal to $\frac{1}{Ldr}$, and Ldr is determined from the

light-rain zenith measurements. By doing so we keep phases of δ_1 and δ_2 and the ratio δ_1/δ_2 as determined from point target calibration measurements and we only adjust the amplitudes of the coupling terms to include complete antenna patterns gain distribution.

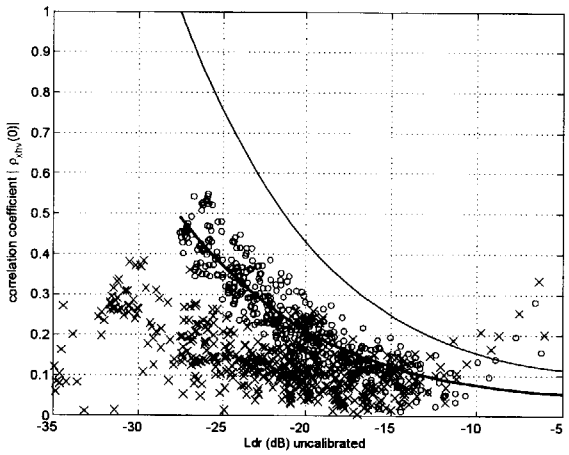

Figure 2.6: The magnitude of cross-correlation coefficient between cross- and co-polar measurements as a function of *Ldr*. The thin solid line shows prediction of this behavior if no decorrelation compensation is applied. The thick solid line represents prediction obtained from the final calibration model. The o-shaped markers show the behavior of the correlation coefficient before calibration (same as Fig. 2.3) and the x-shaped markers show the behavior of the correlation coefficient $|\rho_{xh}(0)|$ after the calibration.

These two simple procedures allow us to compensate for some discrepancy between the point target calibration and the measurements of extended targets. Of course, the assumptions underlying the current polarimetric calibration might not be valid for all cases, however, in our opinion the use of these assumptions allows us to improve the polarimetric calibration method dramatically and these assumptions are less strong than the ones which are used when the point target calibration is applied to the polarimetric measurements of distributed targets.

In total six precipitation measurements were used to demonstrate the performance of the improved polarimetric calibration method. Two measurements were carried out on November 27, 1997 and the other four on December 23, 1997. Five of these measurements were obtained with the radar pointing to the zenith and one with a radar elevation angle of 80 degrees.

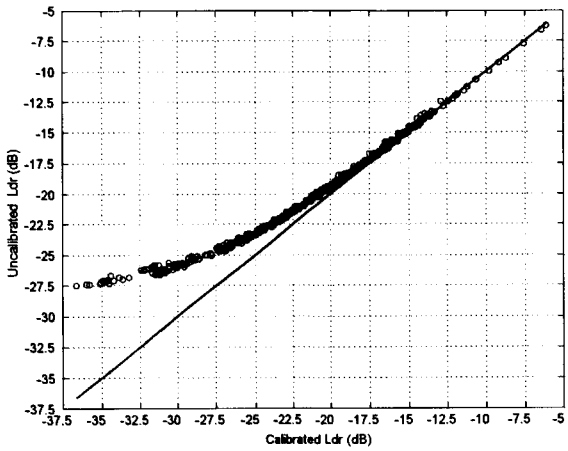

Figure 2.7: Uncalibrated *Ldr* values of different precipitation measurements as a function of the calibrated *Ldr*. The solid line is given to facilitate the interpretation of the graph and shows a one-to-one relation between the calibrated and uncalibrated *Ldr* values. It can be seen that the new calibration procedure increases sensitivity of cross-polar measurements by more than 7 dB. It should also be noted that uncalibrated Ldr values have a bias of more than 1 dB for targets that have *Ldr* values below -20 dB

In Fig. 2.5 one of the zenith measurements is used to show the result of the point target calibration procedure. It can be seen that the *Ldr* values have hardly changed after the calibration.

The scatter plot of the cross-correlation coefficient between cross- and co- polar measurements as a function of the *Ldr* values obtained for all the measurements is shown in Fig. 2.6. Also two curves that represent the predicted behavior of the correlation coefficient are shown; the thin line shows the prediction for the calibration procedure if no decorrelation compensation is applied and the thick line shows the results of the improved calibration procedure. These lines are obtained by applying the distortion matrices, $\mathbf{D}$ and $\widehat{\mathbf{D}}$, with and without decorrelation compensation, to the modeled covariance matrix of precipitation, as:

$$\overrightarrow{c}_m = \mathbf{D}\,\overrightarrow{c}_s \text{ or } \overrightarrow{c}_m = \widehat{\mathbf{D}}\,\overrightarrow{c}_s$$

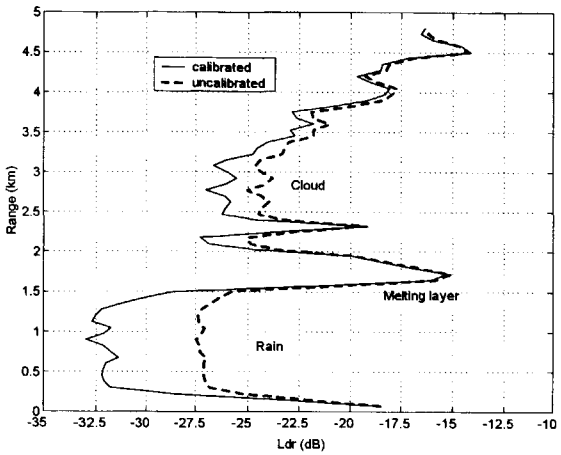

Figure 2.8: Comparison between calibrated *Ldr* and uncalibrated *Ldr* values for a typical vertical precipitation profile. The improved polarimetric calibration procedure is used.

where the covariance matrix, $\mathbf{C}_s$, is given as follows:

$$\mathbf{C}_s = \begin{pmatrix} 1 & 0 & 1 \\ 0 & Ldr & 0 \\ 1 & 0 & 1 \end{pmatrix}, \tag{2.15}$$

and the *Ldr* values vary from -60 dB to -5 dB. It can be seen that if no decorrelation compensation is used, the calibration prediction gives wrong estimates of the measured correlation coefficient. It can be also seen that the cross-correlation coefficient obtained by applying the new polarimetric calibration is less biased, ideally calibrated values should be equal to zero. The other important conclusion which we can draw from this figure is that if the co-cross-polar correlation coefficient is used for the description of the media, extreme care should be taken. This is because even for rather high *Ldr* values (such as -15 dB), the antenna has a non-negligible effect on these measurements.

In Fig. 2.7 the scatter plot of the resulting *Ldr* values for all six measurements is shown. It can clearly be seen that the proposed calibration procedure gives an

improvement of about 7 dB in antenna isolation. The result of the new polarimetric calibration is demonstrated on the single precipitation profile and is shown in Fig. 2.8.

2.5 Summary and conclusions

In this chapter the effect of complete antenna patterns on the polarimetric measurements of atmospheric phenomena was analyzed. This study is based on the use of the measured antenna patterns as well as on the analysis of the precipitation measurements with DARR. The goal of this paper was to investigate the sensitivity of the polarimetric calibration to complete antenna patterns for atmospheric radars. It was shown that the common polarimetric calibration techniques, which imply that the polarimetric imperfection of a radar can be described from the measurements of known targets located at the boresight direction of the antenna, are not valid for the polarimetric measurements of atmospheric objects. The limitation of this assumption can clearly be seen in cross-polar measurements. It was also demonstrated that due to the antenna effects, both the *Ldr* values and the co-cross-polar correlation coefficient $|\rho_{xh}(0)|$ values are biased. This means that due to imperfection of the polarization channels, below about -20 dB the *Ldr* measurements have a non-negligible bias for DARR The co-cross-polar correlation coefficient has a bias of more than 0.1 even for the melting-layer measurements with *Ldr* values of -15 dB.

Based on this study a new polarimetric radar calibration procedure is proposed. This new calibration method uses light-rain measurements in order to take into account the extended nature of weather echoes. This combination of a point target calibration method and light-rain measurements has led to a substantial improvement in the cross-polar measurements of atmospheric objects. This improvement mainly manifests itself in an increase of sensitivity of the cross-polar measurements by more than 7 dB and in a reduction of the effects of the antenna on the co-cross-polar correlation coefficient $|\rho_{xh}(0)|$ measurements. We propose the use of this technique to reduce the influence of imperfection of a radar system on polarimetric measurements of weather echoes.

It should be noted, however, that the obtained data should carefully be analyzed; this is needed because polarimetric measurements are affected not only by an imperfection of the polarization channels, but also by noise, variance of the estimates of a covariance matrix elements, time changes of radar system characteristics, etc. All these effects can influence the performance of the polarimetric calibration and should be the topic of future study.

References

Antar, Y. M. M. and A. Hendry: 1985, Correlation measurements in precipitation at linear polarization using dual-channel radar. *Electron. Lett.*, **21**, 1052–1054.

Aubry, P. and J. H. Zijderveld: 1999, TARA reflector radiation pattern measurements. Technical Report S010-99, IRCTR, Delft University of Technology.

Blanchard, A. J. and B. R. Jean: 1983, Antenna effects in depolarization measurements. *IEEE Trans. Geosci. Remote Sens.*, **21**, 113–117.

Brussaard, G.: 1976, A meteorological model for rain-induced cross polarization. *IEEE Trans. Antennas Propagat.*, **24**, 5–11.

Doviak, R. J. and D. S. Zrnic: 1993, *Doppler Radar and Weather Observations*. Academic Press, Inc., London.

Hubbert, J. C. and V. N. Bringi: 2001, Estimation of polarization errors from covariance matrices of CSU-CHILL radar data. *Proc. Of 30th Conf. On Radar Meteorology*, Amer. Meteor. Soc., Munich, Germany, 44–46.

Jameson, A. R. and S. L. Durden: 1996, A possible origin of linear depolarization observed at vertical incidence in rain. *J. Appl. Meteor.*, **35**, 271–277.

Ligthart, L. P. and L. R. Nieuwkerk: 1980, FM-CW Delft atmospheric research radar. *IEE Proc. F. Commun. Radar Signal Process.*, **127**, 421–426.

McCormick, G. C.: 1981, Polarization errors in a two-channel system. *Radio Sci.*, **16**, 67–75.

Moisseev, D., C. Unal, H. Russchenberg, and L. Ligthart: 2000, Doppler polarimetric ground clutter identification and suppression for atmospheric radars based on co-polar correlation. *Proc. MIKON*, Wroclaw, Poland, 94–97.

Ryzhkov, A., D. Zrnic, E. Brandes, J. Vivekanandan, V. Bringi, and G. Huang: 1999, Characteristics of hydrometeor orientation obtained from radar polarimetric measurements in a linear polarization basis. *Proc. IGARSS*, Hamburg, Germany, 702–704.

Ryzhkov, A. V.: 2001, Interpretation of polarimetric radar covariance matrix for meteorological scatterers: Theoretical analysis. *J. Atmos. Oceanic Technol.*, **18**, 315–328.

Ryzhkov, A. V. and D. S. Zrnic: 1998, Polarimetric rainfal estimation in the presence of anomalous propagation. *J. Atmos. Oceanic Technol.*, **15**, 1320–1330.

Santalla, V., Y. M. M. Antar, and A. G. Pino: 1999, Polarimetric radar covariance matrix algorithms and applications to meteorological radar data. *IEEE Trans. Geosci. Remote Sens.*, **37**, 1128–1137.

Sarabandi, K. and F. T. Ulaby: 1990, A convenient technique for polarimetric calibration of single-antenna radar systems. *IEEE Trans. Geosci. Remote Sens.*, **28**, 1022–1033.

Sarabandi, K., F. T. Ulaby, and M. A. Tassoudji: 1990, Calibration of polarimetric radar system with good polarization isolation. *IEEE Trans. Geosci. Remote Sens.*, **28**, 70–75.

Unal, C. M. H. and D. N. Moisseev: 2002, Improved Doppler processing for polarimetric radars: Application to precipitation measurements. *Proc. Of URSI-F Open Symp. Propagat. and Remote Sens. (CDROM).*

Unal, C. M. H., D. N. Moisseev, F. J. Yanovsky, and H. W. J. Russchenberg: 2001, Radar Doppler polarimetry applied to precipitation measurements: Introduction of the spectral differential reflectivity. *Proc. Of 30th Conf. On Radar Meteorology*, Amer. Meteor. Soc., Munich, Germany, 316–318.

Unal, C. M. H., R. J. Niemeijer, J. S. V. Sinttruyen, and L. P. Ligthart: 1994, Calibration of a polarimetric radar using a rotatable dihedral corner reflector. *IEEE Trans. Geosci. Remote Sens.*, **32**, 837–845.

Zrnic, D. S. and A. V. Ryzhkov: 1999, Polarimetry for weather surveillance radars. *Bull. Amer. Meteor. Soc.*, **80**, 389–406.

Chapter 3

Overview of radar target enhancement techniques

Abstract: This chapter gives a short overview of target enhancement techniques. The main focus is on polarimetric contrast enhancement methods, but the use of Doppler information for ground clutter suppression also got attention. Both coherent (stable targets) and incoherent (random targets) cases are discussed. Most attention is given to the case of random radar targets. In this case two approaches are presented: the Kennaugh matrix and the covariance matrix approaches. It is shown that the covariance matrix approach is more advantageous for the case of random targets. The realizability issue of the optimum polarization states obtained with the covariance matrix polarimetric optimization is also discussed. It is shown that in some cases the covariance matrix optimization could deliver unpolarized optimum polarization states.

3.1 Introduction

The ability for detection of small objects embedded in clutter as well as for the study radar targets when strong clutter is present is paramount for modern radar systems. Probably the most common technique for clutter suppression is Doppler processing. It is based on the assumption that target signal and clutter have different Doppler properties, e.g. mean velocities. However, if this is not the case, the problem of clutter suppression can possibly be solved by using polarimetric properties of radio waves. In this chapter a short overview of Doppler and polarimetric enhancement techniques is given.

In section 3.2 the polarimetric contrast enhancement approach for the case of stable radar targets is presented. The polarization target formalism for the case of random targets is given in section 3.3. In this section Mueller, Kennaugh and covariance matrices are introduced for the characterization of radar targets. Moreover, these matrix formalisms are used to solve the problem of enhancing the contrast between random target and non stationary clutter. Also, the question whether the covariance matrix optimization solution gives the realizable polarization states vectors is discussed in great detail. It is shown that there is a general misunderstanding about the use of the covariance matrix for polarimetric optimization. This misunderstanding is clarified in section 3.3. Section 3.4 describes the Doppler clutter suppression technique and also addresses the limitations of this processing method. It is shown that for ground-clutter suppression the performance of this technique is strongly affected by weather conditions and thus has some limitations for real-time radar applications.

3.2 Polarimetric target enhancement; coherent case

3.2.1 Optimization of the received signal power

When the radar wave of polarization $\vec{e}_t$ illuminates a target, the polarization state of the scattered wave, $\vec{e}_s$, will be determined as:

$$\vec{e}_s = \mathbf{S}\vec{e}_t \tag{3.1}$$

where $\mathbf{S} = \begin{pmatrix} S_{xx} & S_{xy} \\ S_{yx} & S_{yy} \end{pmatrix}$ is the scattering matrix of the radar target, given in the basis $\{x, y\}$. Since for our study the case of monostatic backscattering from reciprocal targets is of main interest, in the rest of the thesis the reciprocity relation (Ulaby and Elachi 1990), $S_{xy} = S_{yx}$, will be assumed.

If radar targets can be considered stable during radar observations they are completely defined by their scattering matrices. In this case the measured voltage, v, on the receiving antenna terminals is defined as:

$$v = \vec{h}^T \mathbf{S} \vec{e}_t \tag{3.2}$$

where $\vec{h}$ is the antenna polarization state (Kostinski and Boerner 1986).

Now, if we want to optimize the received power, we should follow the polarization procedure which was originally introduced by Kennaugh (1952), who has shown that the optimum transmit polarization state vector, $\vec{x}$, can be found by solving the quasi eigenvector problem:

$$\mathbf{S}\vec{x} = \mu\vec{x}^* \tag{3.3}$$

Alternatively the optimum transmit polarization can also be defined as the eigenvector of the Graves power matrix $\mathbf{G} = \mathbf{S}^+\mathbf{S}$ (Kostinski and Boerner 1986):

$$\{\mathbf{G} - \lambda\mathbf{I}\}\,\vec{e}_{t,opt} = 0 \tag{3.4}$$

here $^+$ denotes Hermitian conjugate and * denotes complex conjugation. The (3.4) follows directly from the power optimization problem of the scattered wave

$$P = \vec{e}_s^{\,+}\vec{e}_s = (\mathbf{S}\vec{e}_t)^+(\mathbf{S}\vec{e}_t) = \vec{e}_t^{\,+}\mathbf{G}\vec{e}_t \tag{3.5}$$

Once we have found the optimum transmit polarization by using (3.3) or (3.4), we can write the formulation for the corresponding polarization state of the receiver antenna as:

$$\vec{h} = \frac{(\mathbf{S}\vec{e}_{t,opt})^*}{\|\mathbf{S}\vec{e}_{t,opt}\|} \tag{3.6}$$

where $\|\vec{x}\|$ indicates the norm of the vector $\vec{x}$. Sometimes formulation (3.6) is called the polarization matching condition after Kostinski and Boerner (1986).

The equations (3.4) and (3.6) give a solution to the general problem of maximizing the received power from an arbitrary reciprocal radar target. It should be noted that generally the polarization states $\vec{h}$ and $\vec{e}_t$ are different.

3.2.2 Optimum polarization states; COPOL-Null, COPOL-Max, XPOL-Null and XPOL-Max

It is convenient to describe a radar target by its characteristic polarization states. The idea of describing the radar objects by their optimum polarization states originates from the work of Huynen (1970), who has introduced the polarization fork concept. This concept basically is the representation of the optimum polarization states on the Poincare sphere. It is known that for an reciprocal target there are 6 unique optimum polarizations (Huynen 1970; Kanareykin et al. 1966; Boerner

et al. 1981; Boerner 1981). These are COPOL-max, COPOL-saddle (they coincide with XPOL-nulls), COPOL-nulls and XPOL-max. It was shown that except for some special cases the quasi-eigenvectors of the scattering matrix **S** are unique, orthogonal and are the XPOL null polarizations. Moreover, one of the vectors defines the COPOL-max and the other vector COPOL-saddle point. And the eigenvalues are uniquely related to the COPOL-null polarizations, as shown by Boerner et al. (1991).

It should be noted that these optimum polarizations have less degrees of freedom since the relationship between the transmit and receive polarizations states is fixed, e.g. the COPOL optimum states correspond to the same polarization states on transmit and receive sides and the XPOL optimum states have orthogonal antenna polarization states.

3.2.3 Contrast enhancement

Let us consider the case where the radar volume contains of two stable radar targets, and the signal of one of them needs to be separated. This is a typical radar problem where a target is measured in a clutter environment, e.g. an underground target signal contaminated by surface clutter (Moriyama et al. 1995) or detection of weather objects in case of strong sea clutter (Tkhin and Yanovsky 1993). In this case of stable radar targets the concept of optimum polarization states can be the instrument to suppress the signal from one of the targets. The problem is identical to the optimization problem

$$\max_{\vec{e}_t, \vec{h}} \frac{|\vec{h}^T \mathbf{S}_t \vec{e}_t|^2}{|\vec{h}^T \mathbf{S}_c \vec{e}_t|^2} \tag{3.7}$$

where $\mathbf{S}_t$ is the target scattering matrix and $\mathbf{S}_c$ is the scattering matrix of the unwanted object. Obviously if we find such $\vec{h}$, $\vec{e}_t$ that

$$|\vec{h}^T \mathbf{S}_c \vec{e}_t|^2 = 0 \tag{3.8}$$

these polarization vectors will give a solution to (3.7) and thus the sough optimum polarization states. It should be noted that there are an infinite number of possible polarization states to satisfy this condition, (3.8). Nonetheless, if we consider the case where the transmit and receive polarizations are identical then the solution of (3.8) will coincide with the COPOL-null of the clutter term.

Although the above-presented formulation is an important tool for characteriz-

ing radar targets and for enhancing the contrast between radar targets it is limited to the stable-targets case, i.e. a target which polarimetric properties do not change in time. This limitation is rather severe, since most of the real-life targets have time-varying scattering matrices. Moreover, it was shown by Mieras (1983) that even rigid targets show rather difficult polarimetric signatures due to changes in the aspect angle of the radar.

3.3 Polarimetric target enhancement; incoherent case

3.3.1 Mueller matrix approach

Until now we only considered the coherent case where the radar waves are completely polarized and the radar targets are stable. However, if we consider scattering of radar waves from random radar targets a new polarimetric formulation should be adopted. One of the most used polarimetric formulations for the description of partially polarized waves and random targets are the Stokes vector and the Mueller matrix, respectively.

We consider a quasi-monochromatic wave, which can be described by its Jones vector , $\vec{e}(t)$, (Chandrasekhar 1950; Born and Wolf 1965):

$$\vec{e}(t) = \begin{bmatrix} e_h(t) \\ e_v(t) \end{bmatrix} = \begin{bmatrix} |e_h(t)| \cdot e^{j\delta_h t} \\ |e_v(t)| \cdot e^{j\delta_v t} \end{bmatrix} e^{j\omega t} \tag{3.9}$$

where ω is the carrying frequency of the wave, and the maximum spectrum width $\Delta\omega$ is much smaller than ω. For this wave representation we can introduce the Stokes vector, $\vec{g}(0)$, which is related to the elements of the Jones vector (3.9) as follows:

$$\vec{g} = \vec{g}(0) = \begin{bmatrix} g_0 \\ g_1 \\ g_2 \\ g_3 \end{bmatrix} = \begin{bmatrix} \langle |e_h|^2 \rangle + \langle |e_v|^2 \rangle \\ \langle |e_h|^2 \rangle - \langle |e_v|^2 \rangle \\ 2\,\mathrm{Re}\,\langle e_h e_v^* \rangle \\ 2\,\mathrm{Im}\,\langle e_h e_v^* \rangle \end{bmatrix} \tag{3.10}$$

where $\vec{g}(0)$ corresponds to the calculations of covariances and variances in (3.10) at zero time lag and $\langle ... \rangle$ denotes ensemble average.

Using new this formulation we can write the Stokes vector of the scattered wave as follows:

$$\overrightarrow{g_s} = \mathbf{M}_4 \overrightarrow{g}_t \tag{3.11}$$

where $\mathbf{M}_4$ is the Mueller matrix. The Mueller matrix can be related to the scattering matrix as (Boerner et al. 1991):

$$\mathbf{M}_4 = \mathbf{A}(x,y)\left\{\mathbf{S}(x,y) \otimes \mathbf{S}(x,y)^*\right\}\mathbf{A}(x,y)^{-1} \tag{3.12}$$

where $\otimes$ is the Kronecker (direct) matrix multiplication and $\mathbf{A}(x,y)$ is the Kronecker expansion matrix given in the $\{x,y\}$ polarization basis. And $\mathbf{A}(x,y)$ has the following form in $\{h,v\}$ basis:

$$\mathbf{A}(h,v) = \begin{pmatrix} 1 & 0 & 0 & 1 \\ 1 & 0 & 0 & -1 \\ 0 & 1 & 1 & 0 \\ 0 & j & -j & 0 \end{pmatrix} \tag{3.13}$$

The formulation (3.11) is given in the wave coordinate system and if we want to translate it into the radar coordinate system, the Kennaugh matrix , $\mathbf{K}_4$ is used (Ulaby and Elachi 1990) and than (3.11) becomes:

$$\begin{aligned} \overrightarrow{g_s} &= \mathbf{K}_4 \overrightarrow{g}_t \\ \mathbf{K}_4 &= \mathbf{A}(x,y)^*\left\{\mathbf{S}(x,y) \otimes \mathbf{S}(x,y)^*\right\}\mathbf{A}(x,y)^{-1} \end{aligned} \tag{3.14}$$

Formulation (3.14) is commonly used in radar polarimetry for describing the scattered waves from time-varying targets.

Polarimetric optimization and contrast enhancement

Adopting the new formulation (3.14) we can express the power of the received radar signal in terms of the Kennaugh matrix and Stokes vectors (Giuli 1986):

$$P = \overrightarrow{g}_r^T \mathbf{K}_4 \overrightarrow{g}_t, \tag{3.15}$$

it should be noted that for the sake of simplicity we do not consider calibration and propagation factors in this relation. Using this expression we can formulate

the polarimetric optimization procedure as finding a $\overrightarrow{g}_t$ and $\overrightarrow{g}_r$ that maximize (or minimize) P. It should be noted that since most of the current radar systems are able to produce only completely polarized states, the following constraints on Stokes vectors $\overrightarrow{g}_t$ and $\overrightarrow{g}_r$ should be applied

$$\begin{aligned} \overrightarrow{g}_r^T \mathbf{R} \overrightarrow{g}_r &= 0 \\ \overrightarrow{g}_t^T \mathbf{R} \overrightarrow{g}_t &= 0 \end{aligned} \tag{3.16}$$

$$\text{where } \mathbf{R} = \begin{pmatrix} 1 & 0 & 0 & 0 \\ 0 & -1 & 0 & 0 \\ 0 & 0 & -1 & 0 \\ 0 & 0 & 0 & -1 \end{pmatrix}$$

Combining (3.15) and (3.16) we can write the Lagrangian, L, as (Searle 1982):

$$L = \overrightarrow{g}_r^T \mathbf{K}_4 \overrightarrow{g}_t + \lambda_1 \overrightarrow{g}_r^T \mathbf{R} \overrightarrow{g}_r + \lambda_2 \overrightarrow{g}_t^T \mathbf{R} \overrightarrow{g}_t \tag{3.17}$$

And as a result, the optimum polarization states can be obtained by finding extrema of (3.17). The use of this formalism for finding optimum co-polar polarization states was demonstrated by van Zyl et al. (1987). The more general problem of maximizing the signal-to-clutter power ratio was addressed in (Ioannidis and Hammers 1979). In this case the maximum of the ratio $\left(\overrightarrow{g}_r^T \mathbf{K}_{4t} \overrightarrow{g}_t\right) / \left(\overrightarrow{g}_r^T \mathbf{K}_{4c} \overrightarrow{g}_t\right)$ is sought, where $\mathbf{K}_{4t}$ and $\mathbf{K}_{4c}$ are the Kennaugh matrices of the target and the clutter respectively.

The other approach to solve the polarimetric optimization problem was proposed by Poelman (1980) and Boerner et al. (1991). This method consists of two stages:

1. In the first stage the polarization of transmitted wave is chosen such that the degree of polarization, $p = \frac{\sqrt{\overrightarrow{g}_{i1}^2 - \overrightarrow{g}_{i2}^2 - \overrightarrow{g}_{i3}^2}}{\overrightarrow{g}_{i0}}$, of the scattering wave reaches its maximum.

2. In the second stage the polarization state of the receive antenna is chosen such that it matches (or is orthogonal to) the polarized component of the scattered wave.

As a result, when the receive polarization state matches the polarized component of the scattered wave, the maximum of received power is achieved. And if we

select for the reception the polarization state which is orthogonal to the polarized component of the scattered wave, we can minimize the received signal from a target, and thus this approach can be used to solve the target contrast enhancement problem (Poelman 1980).

The Kennaugh matrix and Stokes vector formalism enables characterization of both random and stable radar targets. However, no close-form solution of the polarimetric optimization problem is available in the literature, which leads to the use of numerical techniques to find characteristic polarizations.

3.3.2 Covariance matrix approach

The other common technique for describing a random target is the use of the covariance matrix, $\mathbf{C}_4(0)$. This matrix can be derived from the voltage equation (3.2) as follows

$$V(t) = \vec{h}^T \mathbf{S(t)} \vec{e}_t = (\vec{h}^T \otimes \vec{e}_t^T) \begin{pmatrix} S_{xx}(t) \\ S_{yx}(t) \\ S_{xy}(t) \\ S_{yy}(t) \end{pmatrix} = \tag{3.18}$$

$$= (\vec{h}^T \otimes \vec{e}_t^T)\vec{s}(t) = \vec{w}_4^+ \vec{s}(t)$$

Then the average receive power can be found as:

$$\langle VV^+ \rangle = \langle \vec{w}_4^+ \vec{s}(t)(\vec{w}_4^+ \vec{s}(t))^+ \rangle = \langle \vec{w}_4^+ \vec{s}(t)\vec{s}(t)^+ \vec{w}_4 \rangle \tag{3.19}$$

$$= \vec{w}_4^+ \mathbf{C}_4(0) \vec{w}_4$$

where

$$\mathbf{C}_4(0) = \left\langle \begin{pmatrix} S_{xx}S_{xx}^* & S_{xx}S_{yx}^* & S_{xx}S_{xy}^* & S_{xx}S_{yy}^* \\ S_{yx}S_{xx}^* & S_{yx}S_{yx}^* & S_{yx}S_{xy}^* & S_{yx}S_{yy}^* \\ S_{xy}S_{xx}^* & S_{xy}S_{yx}^* & S_{xy}S_{xy}^* & S_{xy}S_{yy}^* \\ S_{yy}S_{xx}^* & S_{yy}S_{yx}^* & S_{yy}S_{xy}^* & S_{yy}S_{yy}^* \end{pmatrix} \right\rangle \tag{3.20}$$

In the monostatic backscattering case the target covariance matrix $\mathbf{C}_4(0)$ is singular and can be simplified to the 3x3 form (Lüneburg et al. 1991):

$$\mathbf{C}_3(0) = \left\langle \begin{pmatrix} S_{xx}S_{xx}^* & \sqrt{2}S_{xx}S_{xy}^* & S_{xx}S_{yy}^* \\ \sqrt{2}S_{xy}S_{xx}^* & 2S_{xy}S_{xy}^* & \sqrt{2}S_{xy}S_{yy}^* \\ S_{yy}S_{xx}^* & \sqrt{2}S_{yy}S_{xy}^* & S_{yy}S_{yy}^* \end{pmatrix} \right\rangle \tag{3.21}$$

then polarization vector $\vec{w}_4$ can also be rewritten as:

$$\vec{w}_3 = [\ h_x e_x \quad \tfrac{1}{\sqrt{2}}(h_x e_y + h_y e_x) \quad h_y e_y\ ]^+ \tag{3.22}$$

Target contrast enhancement

Let us now solve the problem of enhancing the contrast between two radar objects with covariance matrices $\mathbf{C}_{3t}(0)$ and $\mathbf{C}_{3c}(0)$. The ratio of the powers received from these targets is

$$R_{tc} = \frac{\vec{w}_3^+ \mathbf{C}_{3t}(0)\vec{w}_3}{\vec{w}_3^+ \mathbf{C}_{3c}(0)\vec{w}_3} \tag{3.23}$$

If we want to increase the contrast of the target given by the covariance matrix $\mathbf{C}_{3t}(0)$ with respect to the clutter, $\mathbf{C}_{3c}(0)$, we should maximize the ratio R_{tc} (Swartz et al. 1988). This process can be carried out by applying the method of the Lagrangian multipliers. In this case the Lagrangian, L, is:

$$L = \vec{w}_3^+ \mathbf{C}_{3t}(0)\vec{w}_3 + \lambda(\vec{w}_3^+ \mathbf{C}_{3c}(0)\vec{w}_3 - c) \tag{3.24}$$

where λ is the Lagrangian multiplier and c is a constant. We can solve this maximization problem by setting the partial derivative $\frac{\partial L}{\partial \vec{w}_3^+}$ to zero:

$$\frac{\partial L}{\partial \vec{w}_3^+} = \mathbf{C}_{3t}(0)\vec{w}_3 + \lambda \mathbf{C}_{3c}(0)\vec{w}_3 = 0 \tag{3.25}$$

This leads to the generalized eigenvalue problem (Searle 1982)

$$\mathbf{C}_{3t}(0)\vec{w}_3 = -\lambda \mathbf{C}_{3c}(0)\vec{w}_3 \tag{3.26}$$

and thus the optimum polarization vectors $\vec{w}_{3opt}$ are the eigenvectors determined from (3.26). The maximum ratio R_{tc} is given by the maximum eigenvalue. It

should be noted that the problem of maximizing the received power of one target can be considered as the limiting case of (3.23), where $\mathbf{C}_{3c}(0)$ is the identity matrix and represents the covariance matrix of the white noise. From (3.26) it follows that in this case the optimum polarization states $\vec{w}_{3opt}$ are the eigenvectors of the target covariance matrix $\mathbf{C}_{3t}(0)$. The same approach can be used for the case of non-monostatic scattering or of non-reciprocal radar targets if the target covariance matrix $\mathbf{C}_3(0)$ is substituted by $\mathbf{C}_4(0)$.

Possible misinterpretations of the polarimetric optimization results

Even though the covariance matrix approach is commonly used for target contrast enhancement (Boerner et al. 1998; Mott 1995; Swartz et al. 1988) there is an issue which has not been addressed in the literature so far. Generally speaking, the optimum polarization vectors $\vec{w}_{3opt}$ contain the second-order moment of the antenna polarization states, $\vec{h}$ and $\vec{e}_t$. As can be seen in (3.19) we have put the polarization vector $\vec{w}_4$ outside of the averaging operator, assuming that the polarization antenna states $\vec{h}$ and $\vec{e}_t$ do not depend on time. However, the solutions to (3.26) do not necessary correspond to the completely polarized states $\vec{h}$ and $\vec{e}_t$ (Bebbington 2002). This misunderstanding about the polarization contrast enhancement method can lead to misinterpretation of the results. In (Cloude 1990) author has discussed the problem that the polarization vector $\vec{w}_{3opt}$ is not unitary, even though the antenna polarization states are. In his opinion, this could lead to the bias in the estimation of optimum polarization states of the antenna if they are retrieved from $\vec{w}_{3opt}$. He supported his argument with an example in which he tries to solve the power optimization problem for a stable radar target with the scattering matrix

$$\mathbf{S} = \begin{pmatrix} a & 0 \\ 0 & b \end{pmatrix} \tag{3.27}$$

where a and b are some real numbers. The covariance matrix in this case would be

$$\mathbf{C}_3(0) = \begin{pmatrix} a^2 & 0 & ab \\ 0 & 0 & 0 \\ ab & 0 & b^2 \end{pmatrix} \tag{3.28}$$

and the resulting optimum vector $\vec{w}_{3opt}$ and the eigenvalue $\lambda_{\max}$ are

$$\vec{w}_{3opt} = \frac{1}{\sqrt{a^2+b^2}} \begin{pmatrix} a \\ 0 \\ b \end{pmatrix} \tag{3.29}$$

$$\lambda_{\max} = a^2 + b^2.$$

It can be seen that from (3.29) and (3.22) we cannot obtain the optimum polarization states, $\begin{pmatrix} 1 \\ 0 \end{pmatrix}$ or $\begin{pmatrix} 0 \\ 1 \end{pmatrix}$, which can be given by the Graves solution (3.4), however. And thus the conclusion of this article (Cloude 1990) was that the eigenvector method for optimization in radar polarimetry gives biased estimates of the antenna polarization states. However, in our opinion Cloude missed the main problem, because it was hidden by the 3-dimensional representation of the covariance matrix. If we rewrite the same covariance matrix into a 4-dimensional form, there is a direct one-to-one relation between the unity of the antenna polarization states $\vec{h}$, $\vec{e}_t$ and the unity of $\vec{w}_4$, where we obtain:

$$\mathbf{C}_4(0) = \begin{pmatrix} a^2 & 0 & 0 & ab \\ 0 & 0 & 0 & 0 \\ 0 & 0 & 0 & 0 \\ ab & 0 & 0 & b^2 \end{pmatrix} \tag{3.30}$$

$$\vec{w}_{4opt} = \frac{1}{\sqrt{a^2+b^2}} \begin{pmatrix} a \\ 0 \\ 0 \\ b \end{pmatrix}$$

Using (3.18) and (3.30) we can find the system of equations which should lead to the solution to elements of $\vec{h}$, $\vec{e}_t$:

$$\begin{aligned} h_x e_x &= \frac{a}{\sqrt{a^2+b^2}} \\ h_x e_y &= 0 \\ h_y e_x &= 0 \\ h_y e_y &= \frac{b}{\sqrt{a^2+b^2}} \end{aligned} \tag{3.31}$$

It can clearly be seen that also this system of equations does not provide the solution to the elements of the antenna polarization states $\vec{h}$, $\vec{e}_t$. However, the result (3.31) becomes clear if the polarization states are considered to be partially polarized. Then all the elements $h_i e_j$ $(i,j = x,y)$ of the vector $\vec{w}_{4opt}$ can be interpreted as the covariances $\langle h_i e_j \rangle$, and thus these elements are allowed to be zero even if neither h_i nor e_j are zero. This observation also clarifies the value of the eigenvalue, which is equal to the radar cross section of the target for the case where the antenna polarization states are completely unpolarized.

One of the ways to eliminate this problem is to use constraints on $\vec{w}_{opt}$ to ensure that the optimum polarizations only correspond to the completely polarized antenna states. It should be noted that we have already used such constraints (3.16) when we solved the polarization optimization problem using the Kennaugh matrix formalism. However, there is no simple mathematical expression for such a constraint for $\vec{w}_{opt}$. An alternative approach was employed by Tragl (1990), who limited the possible optimum polarization vectors $\vec{w}_{opt}$ to only the case of co-pol or cross-pol extrema. As a result of such a limitation the polarization ratio formalism (Agrawal and Boerner 1989) can be used to provide a direct one-to-one relation between the elements of the optimum vectors $\vec{w}_{opt}$. However, the disadvantage of such an approach is that it cannot be used to achieve maximum possible contrast enhancement values; this was also mentioned by Tragl.

Clarification of the polarimetric optimization results

Any time-dependent scattering matrix can be written as the sum of the linear independent scattering matrices such that (Cloude and Pottier 1996):

$$\mathbf{S}(t) = \sum_{i=1}^{k} \gamma_i(t) \mathbf{S}_i \tag{3.32}$$

where $\gamma_i(t)$ are complex time-dependent processes and $\langle \gamma_i \gamma_j^* \rangle = 0$ if $i \neq j$, $\mathbf{S}_i$ is the scattering matrix of the i characteristic target and k determines the degrees of freedom of the random target. It should be noted that in the monostatic backscattering case the maximum value of k is 3. The covariance matrix $\mathbf{C}_3(0)$ of this random target can be written as follows:

$$\mathbf{C}_3(0) = \sum_{i=1}^{3} \mathbf{C}_{3i}(0) = \sum_{i=1}^{3} \lambda_i \vec{w}_{3i} \vec{w}_{3i}^{+} \tag{3.33}$$

where λ_i are the eigenvalues of the covariance matrix $\mathbf{C}_3(0)$ and $\vec{w}_{3i}$ are the corresponding eigenvectors. The relation between (3.32) and (3.33) is given as:

$$\begin{aligned} \lambda_i &= \left\langle |\gamma_i(t)|^2 \right\rangle, \ i = 1..3 \\ \vec{s}_i &= \vec{w}_{3i} \end{aligned} \tag{3.34}$$

where $\vec{s}_i = vec(\mathbf{S}_i)$.

The recent work (Yang et al. 2001) shows that for the case of symmetric scattering matrices there are only two unique polarization states vectors, $\vec{a}$ and $\vec{b}$, such that

$$\begin{aligned} \vec{a}^T \mathbf{S}_1 \vec{b} &= 0 \text{ and} \\ \vec{a}^T \mathbf{S}_2 \vec{b} &= 0 \end{aligned} \tag{3.35}$$

where $\mathbf{S}_1$, $\mathbf{S}_2$ are the scattering matrices of two different radar targets. These polarization vectors $\vec{a}$ and $\vec{b}$ are the eigenvectors of the generalized eigenvalue problem of two matrices $\mathbf{S}_1$, $\mathbf{S}_2$. It is also known (Kostinski and Boerner 1986; Yang et al. 2001) that there is an infinite number of vectors $\vec{a}$ and $\vec{b}$ which insures that there is no signal from one stable radar target.

It can be shown that $[\, a_{ix}b_{ix} \ \ \frac{1}{\sqrt{2}}(a_{ix}b_{iy} + a_{iy}b_{ix}) \ \ a_{iy}b_{iy} \,]^+$ are the eigenvectors of the target covariance matrix $\mathbf{C}_3(0)$, where $\vec{a}_i$ and $\vec{b}_i$ $(i = 1..3)$ are the null polarization vectors of the characteristic target scattering matrices $\mathbf{S}_j, \mathbf{S}_k$ ($j, k = 1, 2, 3$; $j \neq k$; $i \neq j, k$) as given in (3.32). Thus the eigenvectors of the target covariance matrix $\mathbf{C}_3(0)$ determine the null polarizations of the characteristic targets in (3.32).

Let us consider three possible cases:

1. The target covariance matrix $\mathbf{C}_3(0)$ has three different eigenvalues. For that

reason there are three unique eigenvectors $\vec{w}_{3i}$ and hence there are three unique characteristic scattering matrices. As a result, all $\vec{a}_i$ and $\vec{b}_i$ null vectors are uniquely defined and give direct solution for the optimum antenna polarization states. And the maximum eigenvalue of the covariance matrix gives the maximum received power.

2. The target covariance matrix $\mathbf{C}_3(0)$ has only two different eigenvalues. Then there are only two unique eigenvectors $\vec{w}_{3i}$ which define the plane in the three-dimensional space; the third eigenvector, which corresponds to the zero eigenvalue, is orthogonal to this plane and thus is defined up to some proportionality coefficient. As a result one of the characteristic scattering matrices and two pairs of $\vec{a}_i$ and $\vec{b}_i$ are also defined up to some proportionality coefficient, but they can still give us solution for the optimum antenna polarization states.

3. The target covariance matrix $\mathbf{C}_3(0)$ has only one unique eigenvalue. This is the case of the stable radar target, which was used as a example and treated above. Then there is only one unique eigenvector and two other eigenvectors, which correspond to zero eigenvalues, lie in the plane which is orthogonal to this unique eigenvector. As a result there is an infinite number of different eigenvectors and there is no unique solution for $\vec{a}_i$ and $\vec{b}_i$. This, as we have already discussed, is the case when the polarization state vectors are not defined, and correspond to the unpolarized waves.

It was shown that the target covariance matrix approach is a very useful tool for solving the contrast enhancement problem in the case of random targets. However, in the case of stable radar targets this technique does not provide the realizable polarization state vectors.

3.4 Doppler clutter suppression

One of the most common techniques for the suppression of unwanted reflections in radar studies is Doppler processing. If the target and clutter have different Doppler velocities, they can effectively be separated in a Doppler power spectrum. This technique is widely used in meteorological radars where the main clutter is caused by the ground and the signal comes from weather objects. Since ground targets are usually stationary their Doppler spectrum will have a narrow distribution around zero Doppler velocity. Weather echoes, on the other hand, have a wide spectrum

with a non-zero mean velocity. In this case, ground clutter can be suppressed efficiently by applying a notch filter (Groginsky and Glover 1980; Doviak and Zrnic 1993) around zero Doppler frequency. The width of this filter is defined by the width of the ground clutter.

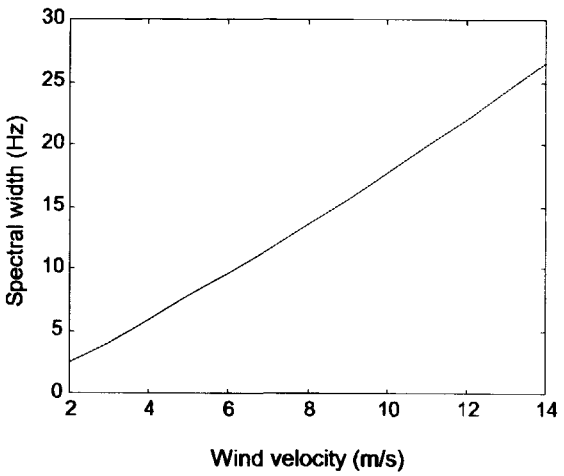

Figure 3.1: Dependence of ground clutter spectrum width on wind velocity. The spectrum width is calculated for a radar with 10 cm wavelength.

The main disadvantage of this method is that the spectrum width of the ground clutter and thus the width of the notch filter depends on the weather conditions. For example, due to the wind the foliage will move. Since the amplitude of the foliage fluctuations depends on the wind speed, it has also a direct influence on the ground clutter spectrum width (Groginsky and Glover 1980). In Fig. 3.1 the empirical relation (Doviak and Zrnic 1993) between the ground-clutter spectrum width and the wind speed is plotted. It can be seen that for high wind speeds the Doppler width of ground clutter is comparable to that of atmospheric echoes, e. g. clouds (Venema et al. 1999). And thus if in this case the mean velocities of clouds were close to zero, most of the signal would be suppressed by the Doppler processing.

3.5 Conclusions

This chapter presented a short overview of the existing clutter suppression techniques. It was shown that polarimetric contrast-enhancement techniques can be used for clutter suppression. For this purpose the Kennaugh or covariance matrix formalism should be employed. It was also indicated that the covariance matrix approach gives a much simpler solution for optimum polarization states. However, this solution leads to unpolarized antenna states in the case of stable targets. Thus the use of the covariance matrix method for target enhancement is recommended only in the case of random radar targets, whereas the scattering matrix formalism is advised for the contrast enhancement of stationary radar targets.

It is shown that Doppler processing is an useful tool for ground clutter suppression. However, the main problem of this technique is the dependence of the processing on the weather conditions, which limits the performance of this method in real-time applications.

References

Agrawal, A. P. and W.-M. Boerner: 1989, Redevelopment of Kennaugh's target characteristic polarization state theory using the polarization transformation ratio formalism for the coherent case. *IEEE Trans. Geosci. Remote Sens.*, **27**, 2–14.

Bebbington, D. H. O.: 2002, Generalized optimal polarizations. A unified geometric approach. *Proc. Of URSI-F Open Symp. Propagat. and Remote Sens. (CDROM)*, Germany.

Boerner, W.-M.: 1981, Use of polarization in electromagnetic inverse scattering. *Radio Sci.*, **16**, 1037–1045.

Boerner, W.-M., M. B. El-Arini, C.-Y. Chan, and P. M. Mastoris: 1981, Polarization dependence in electromagnetic inverse problems. *IEEE Trans. Antennas Propagat.*, **29**, 262–271.

Boerner, W.-M., H. Mott, E. Luneburg, C. Livingstone, B. Brisco, R. Brown, and J. S. Paterson: 1998, *Manual of Remote Sensing. Principles and Applications of Imaging Radar*, John Wiley and Sons., chapter 5. Polarimetry in Radar Remote Sensing: Basic and Applied Concepts. 271–357.

Boerner, W.-M., W.-L. Yan, A.-Q. Xi, and Y. Yamaguchi: 1991, On the basic principles of radar polarimetry: The target characteristic polarization state theory of Kennaugh, Huynen's polarization fork concept, and its extension to the partially polarized case. *Proc. IEEE*, **79**, 1538–1550.

Born, M. and E. Wolf: 1965, *Principles of Optics*. Pergamon Press Ltd., London.

Chandrasekhar, S.: 1950, *Radiative Transfer*. Oxford Clarendon, Oxford, UK.

Cloude, S. R.: 1990, Polarimetric optimization based on the target covariance matrix. *Electron. Lett.*, **26**, 1670–1671.

Cloude, S. R. and E. Pottier: 1996, A review of target decomposition theorems in radar polarimetry. *IEEE Trans. Geosci. Remote Sens.*, **34**, 498–518.

Doviak, R. J. and D. S. Zrnic: 1993, *Doppler Radar and Weather Observations*. Academic Press, Inc., London.

Giuli, D.: 1986, Polarization diversity in radars. *Proc. IEEE*, **74**, 245–269.

Groginsky, H. L. and K. M. Glover: 1980, Weather radar canceler design. *Proc. Of 19th Radar Meteorol. Conf.*, 192–198.

Huynen, J. R.: 1970, *Phenomenological Theory of Radar Targets*. Ph.D. thesis, Delft University of Technology.

Ioannidis, G. A. and D. E. Hammers: 1979, Optimum antenna polarizations for target discrimination in clutter. *IEEE Trans. Antennas Propagat.*, **27**, 357–363.

Kanareykin, D. B., N. F. Pavlov, and V. A. Potechin: 1966, *Polarization of Radio Signals*. Sovetskoe Radio, Moscow, [in Russian].

Kennaugh, E. M.: 1952, Polarization properties of radar reflections. Project Rep. 389-12, Ohio State Univ.

Kostinski, A. B. and W.-M. Boerner: 1986, On foundations of radar polarimetry. *IEEE Trans. Antennas Propagat.*, **34**, 1395–1404.

Lüneburg, E., V. Ziegler, A. Schroth, and K. Tragl: 1991, Polarimetric covariance matrix analysis of random radar targets. *Target and Clutter Scattering and Their Effects on Military Radar Performance*, AGARD-CP-501, Ottawa, Canada, 27–1–27–12.

Mieras, H.: 1983, Optimal polarizations of simple compound targets. *IEEE Trans. Antennas Propagat.*, **31**, 996–999.

Moriyama, T., Y. Yamaguchi, H. Yamada, and M. Sengoku: 1995, Reduction of surface clutter by a polarimetric FM-CW radar in undeground target detection. *IEICE Trans. Commun.*, **E78-B**, 625–629.

Mott, H.: 1995, Polarimetric contrast optimization. *IGARSS*, 2011–2013.

Poelman, A. J.: 1980, Study of controllable polarization applied to radar. *Military Microwaves' 80 Conf. Rec.*, London, U.K., 389–404.

Searle, S. R.: 1982, *Matrix Algebra Useful for Statistics*. Wiley Series in Probability and Mathematical Statistics, John Wiley and Sons, Inc., New York.

Swartz, A. A., H. A. Yueh, J. A. Kong, L. M. Novak, and R. T. Shin: 1988, Optimal polarizations for achieving maximum contrast in radar images. *J. Geophys. Res.*, **93**, 15252–15260.

Tkhin, V. K. and F. J. Yanovsky: 1993, Simulation of the algorithm of selecting radar signals reflected from hydrometeorological targets on the background of earth surface. *Statistical processing techniques of signals in avionics*, 40–47, in Russian.

Tragl, K.: 1990, Polarimetric radar backscattering from reciprocal random targets. *IEEE Tr. Geosci. Remote Sens.*, **28**, 856–864.

Ulaby, F. T. and C. Elachi, eds.: 1990, *Radar Polarimetry for Geoscience Applications*. Artech House, Inc., Norwood, MA.

van Zyl, J. J., C. H. Papas, and C. Elachi: 1987, On the optimum polarizations of incoherently reflected waves. *IEEE Trans. Antennas Propagat.*, **35**, 818–825.

Venema, V., H. Russchenberg, and L. Ligthart: 1999, Correction for clipping of doppler spectra from clouds and other atmospheric targets. *Proc. IGARSS*, Hamburg, Germany, 1180–1182.

Yang, J., Y. Yamaguchi, H. Yamada, W.-M. Boerner, H. Mott, and Y. Peng: 2001, Development of target null theory. *IEEE Trans. Geosci. Remote Sens.*, **39**, 330–338.

Chapter 4

Use of the wave decomposition for ground clutter suppression

Abstract: This chapter introduces a new ground clutter suppression technique which preserves weather echoes. This clutter suppression method uses both statistical and polarimetric properties of the target and clutter. This technique is intended for use in atmospheric studies for weather echoes, the spectral properties of which do not differ much from those of ground clutter. This technique can be applied both to the total signal or to its separate Doppler frequency components.

4.1 Introduction

The performance of a ground-based atmospheric radar is highly affected by ground clutter. Several clutter suppression techniques are used to reduce this influence. The most common ground-clutter suppression technique uses Doppler power spectrum information, that is, the mean Doppler velocity and the spectrum width (Doviak and Zrnic 1993). Ground echoes have a zero mean Doppler velocity and a narrow Doppler spectrum, and hence, reflections that have velocities close to zero are suppressed. It is more difficult to suppress the ground clutter if atmospheric targets have low radial velocities. Such targets, as for example clouds, also have Doppler velocities close to zero and narrow Doppler spectra. Another approach

to clutter suppression is to use polarization diversity to identify range resolution cells which are contaminated by ground clutter. For this approach different polarimetric parameters can be used, such as: co-polar correlation coefficient (Ryzhkov and Zrnic 1998; Zrnic and Ryzhkov 1999), the degree of polarization and circular depolarization rati (da Silveira and Holt 1997), linear depolarization ratio (Hagen 1997) and differential reflectivity (Vivekanandan et al. 1999). These techniques are only used to detect echoes contaminated by ground clutter and not to separate weather echoes from clutter in a mixture. An attempt to improve current clutter suppression techniques using both Doppler and polarimetry was made by Moisseev et al. (2000), however this technique also led to the loss of target information if target reflections and clutter occupied the same area in the Doppler spectrum.

This chapter introduces a new clutter suppression technique, which improves signal-to-clutter ratio even if ground clutter and weather echoes have similar Doppler velocities. The technique is optimal for non-scanning atmospheric radars. It improves the signal-to-clutter ratio with almost no effect on the reflections from weather targets.

Generally, waves scattered from radar objects are partially polarized. It is convenient to analyze partially polarized waves as a sum of two components: a stable and a fluctuating component. The stable component of the wave is scattered by targets that are constant over the observation time, for example, buildings, the earth's surface, etc.; these contribute to the ground clutter. The fluctuating component of the scattered radar wave consists of reflections from weather objects and the fluctuating part of the ground clutter, such as trees, grass; also reflections from the stable targets can fluctuate if the propagation path is changing. Since the stable and the fluctuating parts of the wave contain reflections of different types of ground clutter, in this chapter we will consider these two parts separately.

Section 4.2 discusses the first step of the processing: the suppression of stable clutter, which consists of removing a constant component of the reflected signals (Doviak and Zrnic 1993). When atmospheric targets have Doppler velocities close to zero, a part of the reflections can appear to be reflections from non-fluctuating targets and thus be affected by the stable clutter suppression. This technique is equivalent to the suppression of the zero Doppler velocity cell. The width of the cell is defined by the averaging time over which the stable signal is calculated, and thus the width can be manipulated to preserve weather signals. In this section the influence of stationary-clutter suppression on atmospheric targets is discussed based on two typical measurement situations: a vertical sensing of the cloud and a horizontal sensing of precipitation.

Table 4.1: Specifications of the Delft Atmospheric Research Radar

Radar parameter	Value
Radar frequency	3.3 GHz
Antenna beamwidth	1.8^0
Frequency modulation law	triangular
Number of samples per sweep	128
Frequency deviation	2 MHz
Sweep time	1.25 ms
Maximum range	9600 m
Range resolution	75 m
Polarization	linear
Cross-polar isolation (for distributed targets)	27 dB
Receiver	one channel
Measurement time of the scattering matrix	3.75 ms
Maximum unambiguous Doppler velocity	6 m/s
Doppler velocity resolution	4.7 cm/s
Observation time for one Doppler spectrum	0.96 s
Number of Doppler spectra used for averaging	8

Section 4.3 introduces a new method for the suppression of the fluctuating part of ground clutter. This step of the processing is based on polarimetric differences between atmospheric targets and the fluctuating part of the ground clutter. To improve the use of this clutter suppression for meteorological studies, Doppler polarimetry is introduced in Section 4.4.

For this research we used measurement data from the Delft Atmospheric Research Radar (DARR), the specifications of which are given in Table 4.1. DARR is an FM-CW (Frequency Modulated Continuous Wave) S-band radar located on the roof of the 92 meters high building of the Faculty of Information Technology and Systems. DARR is capable of carrying out Doppler and polarimetric target measurements simultaneously.

The proposed clutter suppression method is illustrated with two precipitation measurements. In the first case the precipitation event consists of three different groups of atmospheric targets, namely a precipitating cloud, a melting layer of the precipitation (bright band) and rain. Reflections from the melting layer show relatively strong polarimetric behavior in comparison with the other weather echoes. The second precipitation measurement is a drizzle measurement, in this case the atmospheric object of interest (drizzle) contains mainly spherical (polarimetrically isotropic) hydrometeors. For the drizzle measurement the radar is pointed to the zenith; for the first measurement the radar had a 20-degree elevation angle with the respect to the horizon. Thus in both cases ground clutter reflections were mainly due to the antenna side lobes.

4.2 Suppression of Stable Clutter

Suppression of stable clutter is based on the fact that the correlation time of clutter is much longer than the correlation time of atmospheric targets. So if coherent averaging is performed over a time period which is much longer than the correlation time of atmospheric targets, the reflections from the atmosphere will be canceled and only reflections from the stable part of the ground clutter will remain. Subtraction of these averaged reflections from measurement data will cancel stable clutter.

4.2.1 Zenith radar measurements: estimation of the correlation time of weather echoes

During the Dutch national measurements campaign CLARA (CLouds And RAdiation) (Lammeren et al. 1999) extensive information about cloud physics was collected. It was measured that typical Doppler spectra widths for zenith radar measurements of the clouds are between 0.18-0.3 m/s (Venema et al. 1999). It is known that the spectrum width of light rain caused by different fall velocities of hydrometeors is about 1 m/s (Doviak and Zrnic 1993). It is commonly assumed that Doppler spectra of clouds and rain have a Gaussian shape. Then, according to the Wiener-Khintchine theorem, the autocorrelation function of the weather echo signal can be estimated as

$$F(\omega) = 2 \cdot \int_{-\infty}^{\infty} R(\tau) \cdot e^{-i\omega\tau} d\tau \tag{4.1}$$
$$R(\tau) = \frac{1}{4\pi} \cdot \int_{-\infty}^{\infty} F(\omega) \cdot e^{i\omega\tau} d\omega$$

where ω is the Doppler frequency, $F(\omega)$ is the intensity spectrum, τ is the time delay and $R(\tau)$ is the correlation function. For the Gaussian spectrum we have

$$F(\omega) = \frac{1}{\sigma\sqrt{2\pi}} \cdot e^{-\frac{(\omega-\omega_0)^2}{2\sigma^2}} \tag{4.2}$$

where ω_0 is the mean Doppler frequency and σ is the spectrum width. The correlation function from (4.1) and (4.2) will be

$$R(\tau) = \frac{1}{4\pi} \cdot \exp[-\frac{1}{2}(\sigma\tau)^2] \cdot \exp[i\omega_0\tau] = \tag{4.3}$$
$$= \frac{1}{4\pi} \cdot \exp[-8(\pi\sigma_v\tau/\lambda)^2] \cdot \exp[i\frac{4\pi}{\lambda}V_0\tau]$$

where σ_v is the Doppler velocity spectral width, λ is the radar wavelength and V_0 is the mean radial velocity of the scattering particles.

One of the most difficult cases of ground clutter suppression is when the mean Doppler velocity of the target is close to zero. Then the correlation time is the time at which $\exp[-8(\pi\sigma_v\tau/\lambda)^2] = e^{-1}$. Thus the correlation time is

$$\tau_c = \frac{\lambda}{2\pi\sqrt{2}\sigma_v} \text{ or } \tau_c = \frac{\sqrt{2}}{\sigma} \tag{4.4}$$

From (4.4) follows that the correlation time of clouds is about 0.05 s and for vertical measurements of rain the correlation time is 0.01 s. The Doppler spectrum width of a weather echo is a function of both the radar parameters as, for example, the beam width, and of meteorological parameters that describe time behavior of the ensemble of hydrometeors. The above-mentioned calculations were performed for zenith radar measurements. Radar reflections measured at other elevation angles will have a different correlation time, since the part of the Doppler spectrum width that is due to different fall velocities of hydrometeors depends on the elevation angle of the radar. However, these calculations give an estimate of the correlation time for typical atmospheric targets.

4.2.2 Horizontally pointed radar measurements: estimation of the correlation time of rain

For measurements with horizontally pointing radar the width of the spectrum due to spread of hydrometeors velocities will be zero and other mechanisms of Doppler spectrum widening will dominate. Usually the Doppler spectrum width of a radar measurement of rain can be considered as a sum of independent contributions (Doviak and Zrnic 1993; Gossard and Strauch 1983)

$$\sigma^2 = \sigma_s^2 + \sigma_\alpha^2 + \sigma_d^2 + \sigma_o^2 + \sigma_t^2 \tag{4.5}$$

where σ_s^2 is due to wind shear, σ_α^2 to the finite antenna beamwidth, σ_d^2 to different fall velocities of hydrometeors, σ_o^2 to a change in orientation of the hydrometeors and σ_t^2 to turbulence. As was mentioned above for the horizontal sensing of precipitation, σ_d^2 is zero. Giving an estimation of all mechanisms which influence the width of the Doppler spectrum and the correlation time is not the purpose of this chapter so we will concentrate on the idealized situation when neither wind nor turbulence are present and the orientation of particles does not change over time. Under these circumstances the width of the Doppler spectrum is only defined by σ_α^2, where σ_α^2 is defined by the change of the path to a hydrometeor due to it movements through the radar volume. The Doppler frequency ω_d for a falling particle is

$$\omega_d = 2\pi \cdot \frac{2V_0}{\lambda} \cos\alpha \tag{4.6}$$

where α is the orientation angle of the radar relative to the zenith and V_0 is the mean fall velocity. For an antenna with a narrow beamwidth, a Doppler spectrum width could be estimated by taking a differential of (4.6)

$$\sigma_\alpha = \Delta\omega_d = 4\pi\frac{V_0}{\lambda}\theta \cdot \sin\alpha \tag{4.7}$$

$$\sigma_\alpha = 4\pi\frac{V_0}{\lambda}\theta \text{ or } \sigma_\alpha^v = V_0\theta$$

where $\theta \equiv \Delta\alpha$ is the 3 dB beamwidth of the antenna, σ_α is a Doppler frequency spectral width and σ_α^v is the corresponding Doppler velocity spectral width. Typically θ is about 3 degrees and the mean fall velocity of rain is approximately 4 m/s (Russchenberg 1992), which gives an estimate of the rain Doppler velocity spectral width for horizontal measurements equal to 0.2 m/s with a radar wavelength of

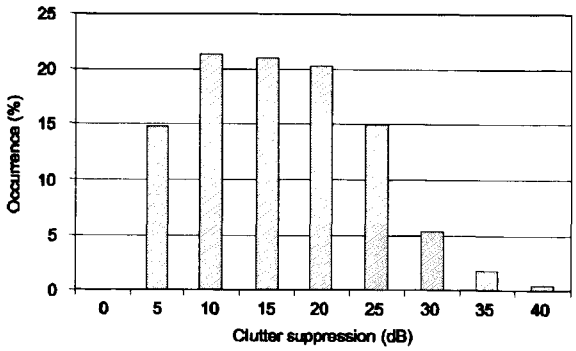

Figure 4.1: Reduction of ground-clutter power due to the stable clutter suppression

10 cm and the correlation time of about 0.05 s. So the longest correlation time we can expect for a weather echo is in the order of 0.05 s for clouds and a horizontal measurement of rain.

4.2.3 Results of stable clutter suppression

If the information from atmospheric targets is to be preserved, the averaging time, which is used to calculate the stable clutter component, should be so long that the effective width of the Doppler cell is much smaller than the Doppler width of weather echoes (in our case 0.18 m/s).

Fig. 4.1 gives the result of the stable clutter suppression. Ground-clutter reflections before and after clutter suppression are calculated and a histogram of the power ratios is given. These ground-clutter measurements were performed by DARR for different radar elevation angles and in different azimuth directions. The wind speed for all these measurements was between 3.5 and 8 m/s. In all analyzed cases ground clutter can be considered as an urban-area ground clutter. About eight seconds of data were used to calculate the average signal for processing. This averaging time gives an effective width of $5.9 \cdot 10^{-3}$ m/s for Doppler cells, since $\lambda = 0.09\ m$ and the observation time T_s is 7.96 s. Thus, the influence of this processing on the atmospheric targets signal is negligible.

The median value for the stable clutter suppression is about 13 dB. The spread in the histogram is caused by the presence of data with different ground-clutter content. High values of clutter suppression correspond to ground clutter with a

large stable part, which corresponds to the reflections from man-made objects. Low values of clutter suppression, on the other hand, correspond to clutter with a relatively large fluctuating part, which corresponds to natural objects such as trees.

4.3 Fluctuating Ground-Clutter Suppression

4.3.1 Short review of the theory of polarimetry

The electric-field vector of a wave scattered from a target is related to the transmitted wave electric-field vector by the scattering matrix of the target as

$$\begin{pmatrix} E_x \\ E_y \end{pmatrix} = \begin{pmatrix} S_{xx} & S_{xy} \\ S_{yx} & S_{yy} \end{pmatrix} \begin{pmatrix} E_x^t \\ E_y^t \end{pmatrix} \tag{4.8}$$

where (x, y) is an arbitrary orthonormal polarization basis. In most cases a radar target fluctuates over time, which implies changes of the scattering matrix and of the scattered wave. To describe a time-dependent wave, the coherence matrix is used

$$\mathbf{J}(\tau) = \left\langle \begin{pmatrix} E_x(t) \\ E_y(t) \end{pmatrix} \cdot \begin{pmatrix} E_x^*(t+\tau) & E_y^*(t+\tau) \end{pmatrix} \right\rangle = \tag{4.9}$$

$$= \begin{pmatrix} \langle E_x(t) \cdot E_x^*(t+\tau) \rangle & \langle E_x(t) \cdot E_y^*(t+\tau) \rangle \\ \langle E_y(t) \cdot E_x^*(t+\tau) \rangle & \langle E_y(t) \cdot E_y^*(t+\tau) \rangle \end{pmatrix}$$

where $\langle\rangle$ denotes ensemble averaging and τ is the time delay. The wave behavior is assumed to be a stationary random process. For the case of quasi monochromatic waves: if the time delays τ are restricted by $|\tau| \ll \frac{1}{\sigma}$, where σ is the width of the spectrum of the scattered wave, expression (4.9) will become (Perina 1972)

$$\mathbf{J}(0) = \mathbf{J} = \begin{pmatrix} \langle E_x(t) \cdot E_x^*(t) \rangle & \langle E_x(t) \cdot E_y^*(t) \rangle \\ \langle E_y(t) \cdot E_x^*(t) \rangle & \langle E_y(t) \cdot E_y^*(t) \rangle \end{pmatrix} = \begin{pmatrix} J_{xx} & J_{xy} \\ J_{yx} & J_{yy} \end{pmatrix} \tag{4.10}$$

This expression gives a more common notation of the wave coherence matrix and is widely used in radar polarimetry (Ulaby and Elachi 1990).

For a completely unpolarized wave, the coherence matrix **J** will become a diagonal matrix, since an unpolarized wave has no preferable polarization, which implies that $\left\langle |E_x|^2 \right\rangle = \left\langle |E_y|^2 \right\rangle$ and $\langle E_x E_y^* \rangle = 0$. A partially polarized wave can be represented as a sum of a completely polarized and a completely unpolarized wave; in mathematical form it can be written as (Potechin and Tatarinov 1978)

$$\mathbf{J} = \begin{pmatrix} A & 0 \\ 0 & A \end{pmatrix} + \begin{pmatrix} B & J_{xy} \\ J_{yx} & C \end{pmatrix} \tag{4.11}$$

where the first matrix represents the coherence matrix of the completely unpolarized wave and the second one that of the completely polarized wave. Following a well-known procedure (Potechin and Tatarinov 1978; Perina 1972) using the diagonalization of **J** we can find that

$$\begin{aligned} A &= \frac{1}{2}(Tr\mathbf{J} - \sqrt{Tr^2\mathbf{J} - 4\det\mathbf{J}}) \\ B &= \frac{1}{2}(J_{xx} - J_{yy}) + \frac{1}{2}\sqrt{Tr^2\mathbf{J} - 4\det\mathbf{J}} \\ C &= \frac{1}{2}(J_{yy} - J_{xx}) + \frac{1}{2}\sqrt{Tr^2\mathbf{J} - 4\det\mathbf{J}} \end{aligned} \tag{4.12}$$

where $Tr\mathbf{J}$ denotes the trace of the matrix **J** and $\det\mathbf{J}$ denotes determinant of **J**. The degree of polarization p of a wave is the ratio of the power in the polarized component of the wave I_{pol} and the total power of the wave I_{tot}. It can be written as

$$\begin{aligned} p &= \sqrt{1 - \frac{4\det\mathbf{J}}{Tr^2\mathbf{J}}} = \frac{\sqrt{(J_{xx} - J_{yy})^2 + 4 \cdot J_{xx}J_{yy}}}{J_{xx} + J_{yy}} = \\ &= \frac{I_{pol}}{I_{tot}} \end{aligned} \tag{4.13}$$

For an unpolarized wave $p = 0$, since $\frac{4\det\mathbf{J}}{Tr^2\mathbf{J}} = 1$ or $J_{xy} = J_{yx} = 0$ and $J_{xx} = J_{yy}$. For a completely polarized wave $p = 1$, since $\det\mathbf{J} = 0$.

4.3.2 Atmospheric targets and fluctuating ground clutter

Most of the atmospheric targets are characterized by the fact that cross-polar reflections in the $h-v$ linear polarization basis are much smaller than co-polar ones. For light rain and water clouds $Ldr = \frac{\langle |S_{hv}|^2 \rangle}{\langle |S_{hh}|^2 \rangle}$ is usually smaller than -30 dB, but for the melting layer of a precipitation event this value can lie in the order of -15 dB (Hagen 1997). It should be mentioned that the Ldr values in a melting layer belong to the highest values to be found in weather echoes. It is common to assume that the co-polarized and cross-polarized elements of the scattering matrix for ground clutter are uncorrelated (Borgeaud et al. 1987; Swartz et al. 1988). In the case of precipitation measurements, it was recently shown (Ryzhkov 2001) that the cross-correlation coefficient between these scattering matrix elements can be close to unity. However, in this chapter the assumption that the co-polarized and cross-polarized elements of the scattering matrix of precipitation are uncorrelated is used since it represents the less favorable case for the proposed clutter suppression method. Then, according to (4.10) and (4.8) the coherence matrix of an atmospheric target, expressed in $h-v$ linear polarization basis, when the transmitted wave is horizontally polarized, will be

$$\mathbf{J} = \begin{pmatrix} \langle |S_{hh}|^2 \rangle & 0 \\ 0 & \langle |S_{hv}|^2 \rangle \end{pmatrix} \tag{4.14}$$

and the degree of polarization according to (4.13) will be

$$p = \left| \frac{(1 - Ldr)}{(1 + Ldr)} \right| \tag{4.15}$$

Strictly speaking the matrix (4.14) is only proportional to the actual wave coherency matrix (4.10). However, we are only interested in relative polarimetric parameters and hence the coefficient of proportionality can be omitted here. Thus for atmospheric targets the limits of the degree of polarization will change in between 0.94, for a precipitation melting layer, and 1, for light rain and water clouds.

As was shown in the beginning of this chapter, stable-clutter suppression removes the monochromatic component of the wave scattered from the ground clutter. This component dominates reflections from the ground clutter and its suppression gives a reduction by 13 dB of the clutter signal. The residue part of the clutter varies over time and a wave reflected from it has nonzero spectrum width. These reflections come from small objects which fluctuate over time, i.e. trees,

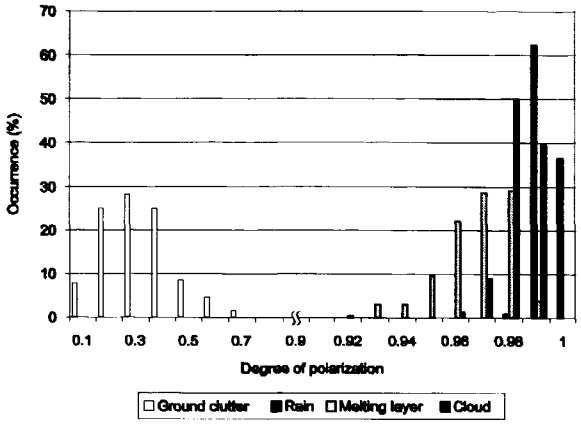

Figure 4.2: Degree of polarization for ground clutter, rain, melting layer and cloud

grass etc. A theoretical prediction of the degree of polarization for such targets is complicated. It is even more complicated by the fact that in most of the cases reflections from the ground clutter are obtained via the antenna side lobes. Thus the exact polarization basis of the radar sounding is unknown and antenna patterns for different polarizations are different.

Measurements of the degree of polarization of waves scattered by atmospheric targets as rain, precipitating cloud and melting layer of precipitation as well as data of the ground clutter were obtained during a measurements campaign in November 1997. These measurements were carried out using DARR. Scattering matrices of the precipitation were obtained in $h - v$ linear polarization basis. Since the exact polarization states of the side lobes of the antenna are unknown, reflections from the ground clutter were treated as if they were also obtained in $h - v$ linear polarization basis. It should be noted that even though the degree of polarization can change from basis to basis, it mainly depends on the time variations of the backscattered wave, which are defined by the variations of the target. The radar elevation angle for these measurements was 20 degrees with respect to the horizon. To calculate the degree of polarization approximately eight seconds of data were used. Prior to the calculation of the degree of polarization the stable clutter was suppressed. This processing removes the constant component of the signal, this component is completely polarized by definition.

Measurements results are presented in Fig. 4.2. As can be seen, the degree

of polarization for the atmospheric targets is close to unity, as expected. The mean value for the degree of polarization of clouds and rain is higher than 0.98. This value is expected to be an underestimation since cross-polar measurements of rain and water clouds are affected by the coupling of the polarization channels, see Chapter 2. The cross-polar isolation of DARR for distributed targets is -27 dB. The mean value of the degree of polarization of the melting layer is 0.97. This value is defined by physical processes in the melting layer itself, since the cross-polar reflections are about 10 dB higher than the antenna limit.

Fig. 4.2 also shows that the mean value of the degree of polarization of the ground clutter is about 0.3. That means that the waves scattered from the ground clutter are mainly depolarized. However, values of the degree of polarization for ground clutter were reported to be close to unity in (Giuli et al. 1991). These measurements were performed in the suburbs of Rome, Italy. Since in both cases we deal with the same type of ground clutter (urban-area ground clutter), differences in their physical properties cannot explain the discrepancy between the results. However, the difference between these and our results can be explained by the fact that reflections from an urban area are dominated by the reflections from the stable ground clutter. And in our case prior to the calculation of the degree of polarization, the stable ground clutter was suppressed. By this processing the stable part (and hence the completely polarized part) of the ground clutter was removed. This part dominates the ground-clutter reflections; it is 13 dB larger than the fluctuating part of ground clutter. Thus, this difference in the processing can explain the difference in results.

The degree of polarization gives a high contrast between ground clutter and weather echoes, as can be seen in Fig. 4.2. That gives the possibility to use the degree of polarization for detecting the range resolution cells which are affected by ground clutter. This approach was already discussed by da Silveira and Holt (1997). In this chapter, the difference in polarimetric properties of weather echoes and fluctuating ground clutter for clutter suppression is used by applying the wave decomposition theorem. The degree of polarization for ground clutter has the median value of 0.3 and for atmospheric targets the value of 0.97. Now, if the backscattered wave is decomposed in completely polarized and completely unpolarized waves, the amount of clutter power which will remain in the polarized part will be on average 5.2 dB lower than in the backscattered wave. Moreover, the power in the completely polarized part of the atmospheric signal will only be reduced by 0.13 dB.

The above-given values of the polarimetric clutter suppression correspond to

the reduction of the clutter power in the backscattered wave. The gain in the signal-to-clutter ratio for the co-polar element of the scattering matrix can be obtained from (4.15) assuming that $J_{xy} = J_{yx} = 0$. In this case the reduction of clutter is given by $(1 - Ldr)$, where Ldr is obtained from (4.15). This leads us to the final values of the fluctuating-clutter suppression using the wave decomposition theorem, which on average give 3.35 dB of ground clutter suppression and will reduce power in atmospheric signal by only 0.07 dB.

4.4 Wave decomposition in Doppler domain

The combination of stable-clutter suppression and wave decomposition is an attractive tool for ground-clutter suppression, as it results in about 16 dB of clutter suppression and preserves reflections from the atmospheric targets. The drawback of this method is that the output of this processing gives averaged intensities, so the Doppler spectrum information is lost. The solution to this problem lies in applying the method to Doppler spectra.

Let's introduce the spectral coherence matrix $\mathbf{F}(\omega)$ (Perina 1972), which is analogous to the wave coherence matrix (4.10) but defined for each Doppler frequency

$$\mathbf{F}(\omega) = \begin{pmatrix} F_{xx}(\omega) & F_{xy}(\omega) \\ F_{yx}(\omega) & F_{yy}(\omega) \end{pmatrix}, \tag{4.16}$$

where

$$F_{ij}(\omega) = 2\int_{-\infty}^{+\infty} J_{ij}(\tau)\exp(-i\omega\tau)d\tau. \tag{4.17}$$

The expression (4.17) relates the wave coherence matrix (4.9) to the spectral coherence matrix (4.16).

The relation between the matrix $\mathbf{J}(0)$ and the spectral coherence matrix is

$$J_{ij}(0) = \frac{1}{4\pi}\int_{-\infty}^{+\infty} F_{ij}(\omega)d\omega. \tag{4.18}$$

In the discrete form, if we take into account that the measurement time T is finite, the expression (4.18) can be rewritten as (Davenport and Root 1958)

$$J_{ij}(0) = \frac{1}{4\pi} \sum_k F_{ij}^{(T)}(\omega_k) \cdot \Delta\omega, \tag{4.19}$$

where $\Delta\omega \sim \frac{1}{T}$ denotes the spectral (Doppler) frequency resolution. Thus a wave coherence matrix is just the sum of coherence matrices of waves with frequencies ω_k and the spectrum width $\Delta\omega$. This result is logical since waves with different center frequencies are statistically independent and their cross-correlations are zero.

To clarify the physical meaning of (4.19) we consider two limiting cases.

1. If the observation time is small ($T \ll \frac{1}{\sigma_d}$, σ_d is the width of the Doppler spectrum), then the Doppler frequency resolution cell contains the complete Doppler spectrum of targets. Therefore the wave coherence matrix $\mathbf{J}(0)$ will coincide with the spectral coherence matrix $\mathbf{F}(\omega)$. In this case application of the wave decomposition theorem to the spectral coherence matrix will give the same results as its application to the wave coherence matrix.

2. An infinitely long observation time will lead to infinitesimal Doppler frequency resolution cells and hence every Doppler cell will represent a monochromatic wave. For example, if a wave consists of two equal intensity components with slightly different frequencies and having orthogonal polarizations, then according to the Stokes theorem (Chandrasekhar 1950) this wave will behave as a completely unpolarized wave. However, if spectral coherence matrices are calculated for a time interval that is long enough to separate these components of the wave, then the resulting two spectral coherence matrices will represent completely polarized waves. In this case application of the wave decomposition theorem in the time domain and in the frequency domain will give two completely different results.

Thus to be able to apply the wave decomposition theorem to the Doppler spectrum we should have Doppler resolution cells that are large enough to contain the complete spectrum of the ground clutter. And the Doppler spectrum resolution should be high enough to allow for a good estimation of widths and mean velocities of atmospheric targets.

4.5 Results of the wave decomposition

To test this new clutter suppression technique we have measured slant and vertical profiles of precipitation. The elevation angle of the radar for the slant profile

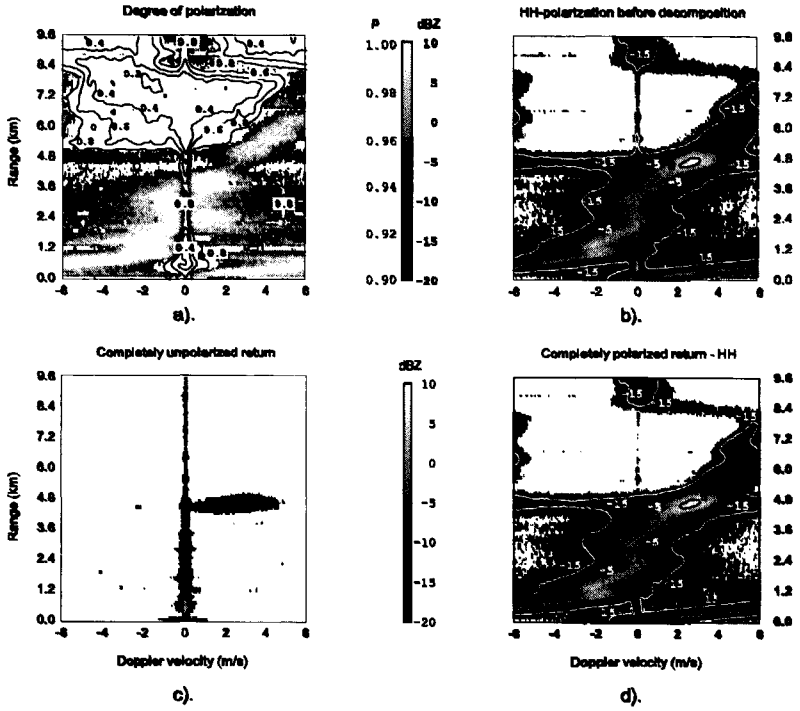

Figure 4.3: Slant profile of precipitation, 20 degrees elevation.

measurement was 20 degrees relative to horizon. The co-polar and cross-polar components of the scattered wave were measured by alternating linear polarizations on the receiving channel; the polarization state is switched every 1.25 ms. For both examples one minute of data is collected. Prior to the Doppler processing, stable-clutter suppression is performed. Coherent averages of the co-polar and cross-polar echoes for the stable-clutter suppression are computed using the complete data set. It is important to note that the coherence time of DARR is in the order of 3 minutes. The radar coherence time is inversely proportional to the spectrum width caused by the radar phase instability.

The Doppler spectrum of the coherence matrix is obtained each 0.96 s using 256 samples. The maximum unambiguous Doppler velocity for this setting is 6 m/s and the Doppler velocity resolution is 0.047 m/s. This number of samples is a trade-off between a high Doppler resolution for the retrieval of spectrum

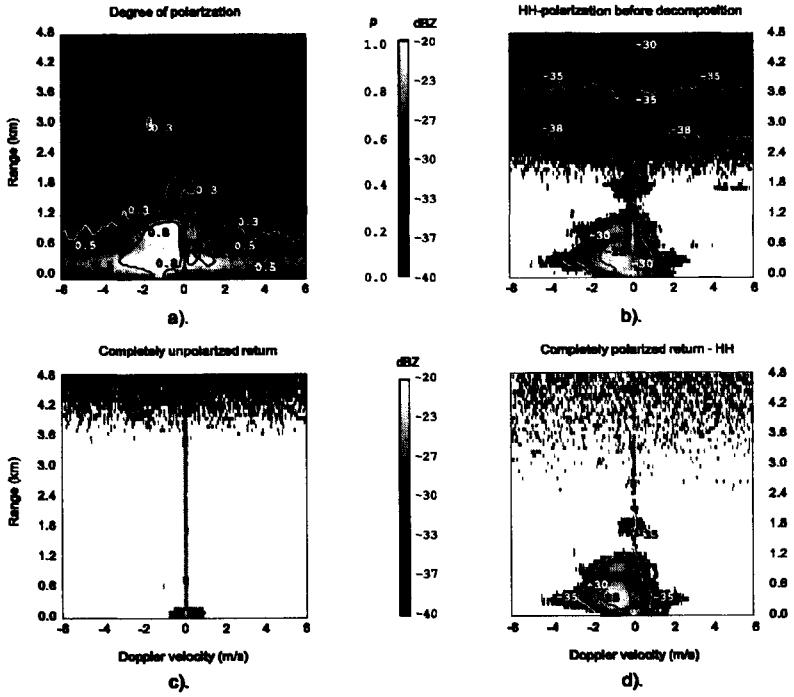

Figure 4.4: Vertical profile of precipitation (drizzle)

information on weather echoes and relatively large resolution cells to contain most of the ground clutter reflections in one Doppler cell. More details about Doppler polarimetric processing can be found in (Unal et al. 1998). A total of 8 spectra are obtained for each element of the coherence matrix. The number of spectra is a compromise between the good approximation of the degree of polarization and a good time resolution for real-time applications. Using (4.11), (4.12), (4.13) and (4.19) the degree of polarization, the completely polarized and completely unpolarized returns are calculated for every Doppler resolution cell.

The slant and the vertical profile of precipitation are shown in Fig. 4.3 and Fig. 4.4, respectively. Fig. 4.3 b) and 4.4 b) show the reflectivity of the precipitation versus range and Doppler velocity. The high reflectivity, between -5 and 5 dBZ, at 4.8 km in Fig. 4.3 b) corresponds to the melting layer of the precipitation. Reflections below the melting layer come from rain. Ice crystals falling from the

cloud cause reflections above the melting layer. Other features which can be clearly seen in Fig. 4.3 b) are measurement and processing artifacts. Such artifacts are spectral leakage and aliasing. The spectral leakage, caused by high reflection from the melting layer, can be clearly seen at a height of 4.8 km; it occupies all Doppler velocities and has a lower reflectivity than the melting layer itself. Since the maximum unambiguous velocity for these measurements was 6 m/s, all velocities which exceed this limit are aliased. This effect can be seen in Fig. 4.3 b) at ranges between 0 and 1.2 km and Doppler velocities between -2 and 6 m/s. Fig. 4.4 b) shows the Doppler spectrum of drizzle. The low reflectivity signal, about -38 dBZ, at 1.8 km come from a cloud and reflections between 0 and 1.2 km are caused by the drizzle itself.

Fig. 4.3 a) and 4.4 a) show the degree of polarization versus range and Doppler velocity. In Fig. 4.3 a) the grayscale gives values of the degree of polarization between 0.9 and 1 and contours show values between 0 and 0.8. As expected, reflections from the rain, the melting layer and the cloud have high degree of polarization values, which vary between 0.9 and 1. Reflections from the ground clutter and noise have lower values of degree of polarization. It is interesting to compare the degree of polarization values for areas in Fig. 4.3 a) and 4.4 a) which have no significant reflections. In Fig. 4.3 a) the degree of polarization values for such an area (range interval 5-8 km and Doppler velocities interval from -5 till -1 m/s) vary between 0.2 and 0.6. These rather high values can be explained by the influence of spectral leakage. So these values correspond not only to noise, but to a sum of noise and spectral leakage. As can be seen in Fig. 4.4 a), the values for the degree of polarization in areas which contain only noise lie between 0 and 0.2.

Fig. 4.3 d) and 4.4 d) show the completely polarized backscattering of the considered events. As can be seen, clutter reflections have been reduced by approximately 5 dB, while reflections from atmospheric targets are hardly affected at all (a reduction of 0.1 dB can be expected in the melting layer). Completely unpolarized returns in Fig. 4.3 c) and 4.4 c) show the difference in reflection before and after fluctuating-clutter suppression. Fig. 4.3 c) clearly shows that the main component of unpolarized reflections is clutter. However, it also shows that the lower part of the melting layer also contributes to unpolarized reflections. Thus, the melting-layer reflections are affected by this clutter suppression, but this influence is not large and coincides with our estimation made above. Fig. 4.4 c) shows approximately the same picture, only more clearly; note that due to the processing, noise is also suppressed.

4.6 Conclusions

It was shown that it is very useful to consider ground clutter as a sum of the stable and fluctuating (time-dependent) components. Moreover, the change of the polarimetric properties of ground clutter due to suppression of the stable part of the signal were also discussed. It was shown that the fluctuating part of ground clutter has low degree of polarization, while the degree of polarization of the complete clutter is close to unity. It was also shown that weather echoes have a high degree of polarization. Thus the degree of polarization is a parameter that can be used to discriminate between atmospheric targets and fluctuating ground clutter.

This study has led to a new ground-clutter suppression technique that preserves reflections from atmospheric targets. This clutter suppression technique shows good performance. It allows for separation of ground clutter and atmospheric objects even if they occupy the same Doppler spectrum area. This processing gives 16.35 dB of clutter suppression on average.

This new clutter suppression method is mainly applicable to cloud radars and wind profilers, since it requires suppression of the stable-clutter component, which is time-dependent in scanning weather radars. Nevertheless the polarimetric processing which is discussed in this chapter could be used to remove residuals of ground clutter, which are left after the standard Doppler processing in weather radars.

References

Borgeaud, M., R. Shin, and J. Kong: 1987, Theoretical models for polarimetric radar clutter. *J. Electromagn. Waves Appl.*, **1**, 67–86.

Chandrasekhar, S.: 1950, *Radiative Transfer*. Oxford Clarendon, Oxford, UK.

da Silveira, R. B. and A. R. Holt: 1997, A neural network application to discriminate between clutter and precipitation using polarization information as feature space. *Proc. Of 28th Conf. Radar Meteorol.*, Austin, TX, 57–58.

Davenport, W. B. and W. L. Root: 1958, *An Introduction to the Theory of Random Signals and Noise*. McGraw-Hill Book Company Inc., New York, NY.

Doviak, R. J. and D. S. Zrnic: 1993, *Doppler Radar and Weather Observations*. Academic Press, Inc., London.

Giuli, D., M. Fossi, and M. Gherardelli: 1991, Polarization behaviour of ground clutter during dwell time. *IEE Proceedings-F*, **138**, 211–217.

Gossard, E. E. and R. G. Strauch: 1983, *Radar Observation of Clear Air and Clouds*. Elsevier.

Hagen, M.: 1997, Identification of ground clutter by polarimetric radar. *Proc. Of 28th Conf. On Radar Meteorology*, Amer. Meteor. Soc., Austin, Texas, 67–68.

Lammeren, A. V., A. Feijt, D. Donovan, H. Bloemink, H. Russchenberg, V. Venema, J. Erkelens, A. Apituley, H. T. Brink, A. Khlystov, S. Jongen, G. Brussaard, and M. Herben: 1999, CLARA: Clouds and radiation- intensive measurement campaigns in the netherlands. *Symp. Proc.: Remote Sensing of Cloud Parameters: Retrieval and Validation*, Delft, The Netherlands, 5–10.

Moisseev, D., C. Unal, H. Russchenberg, and L. Ligthart: 2000, Doppler polarimetric ground clutter identification and suppression for atmospheric radars based on co-polar correlation. *Proc. MIKON*, Wroclaw, Poland, 94–97.

Perina, J.: 1972, *Coherence of Light*. Van Nostrand Reinhold Company Ltd., London.

Potechin, V. A. and V. N. Tatarinov: 1978, *Theory of Electromagnetic Field Coherence*. Izdatel'stvo Svjaz', Moscow, [in Russian].

Russchenberg, H. W. J.: 1992, *Ground-Based Remote Sensing of Precipiation Using a Multipolarized FM-CW Doppler Radar*. Ph.D. thesis, Delft University of Technology.

Ryzhkov, A. V.: 2001, Interpretation of polarimetric radar covariance matrix for meteorological scatterers: Theoretical analysis. *J. Atmos. Oceanic Technol.*, **18**, 315–328.

Ryzhkov, A. V. and D. S. Zrnic: 1998, Polarimetric rainfal estimation in the presence of anomalous propagation. *J. Atmos. Oceanic Technol.*, **15**, 1320–1330.

Swartz, A. A., H. A. Yueh, J. A. Kong, L. M. Novak, and R. T. Shin: 1988, Optimal polarizations for achieving maximum contrast in radar images. *J. Geophys. Res.*, **93**, 15252–15260.

Ulaby, F. T. and C. Elachi, eds.: 1990, *Radar Polarimetry for Geoscience Applications*. Artech House, Inc., Norwood, MA.

Unal, C. M. H., D. N. Moisseev, and L. P. Ligthart: 1998, Doppler-polarimetric measurements of precipitation. *Proc. Of JIPR'98*, Nantes, France, 429–438.

Venema, V., H. Russchenberg, and L. Ligthart: 1999, Correction for clipping of doppler spectra from clouds and other atmospheric targets. *Proc. IGARSS*, Hamburg, Germany, 1180–1182.

Vivekanandan, J., D. S. Zrnic, S. M. Ellis, R. Oye, A. V. Ryzhkov, and J. Straka: 1999, Cloud microphysics retrieval using S-band dual-polarization radar measurements. *Bull. Amer. Meteor. Soc.*, **80**, 381–388.

Zrnic, D. S. and A. V. Ryzhkov: 1999, Polarimetry for weather surveillance radars. *Bull. Amer. Meteor. Soc.*, **80**, 389–406.

Chapter 5

Radar Doppler polarimetry

Abstract: In this chapter a relation between Doppler and polarimetric characteristics of radar targets is studied. Based on this study a new formalism describing radar objects, radar Doppler polarimetry, is proposed. It is shown that based on this new polarimetric formulation a target enhancement problem can be generalized to the case of time varying transmit and receive polarization states, which results in an enhancement of the contrast between radar targets.

5.1 Introduction

The polarimetric description of radar targets is widely discussed in the scientific literature. It has been shown that stationary radar targets can be fully characterized by their characteristic polarization states, which are co-polar and cross-polar maxima and null polarizations (Kennaugh 1952; Huynen 1970; Agrawal and Boerner 1989). This target description originates from the work of Kennaugh (1952), and was further extended by Huynen (1970). The further development of the optimum polarization states and of the polarimetric description of stable targets was carried out in great part by Boerner et al. (Boerner et al. 1981; Boerner 1981; Kostinski and Boerner 1986). The main drawback of such a radar target representation is that it is only valid for stable radar targets and as a result, even small variations in the target properties lead to rather complicated behavior of the target characteristic polarizations (Mieras 1983).

In order to describe scattered waves from depolarizing radar targets as well as to characterize the targets themselves the second-order statistics is used. Usually for

characterizing partially polarized waves the Stokes vector and (or) wave coherency matrix are used (Born and Wolf 1965; Chandrasekhar 1950). For the description of random radar targets matrices of the second-order moments of the elements of the scattering matrix, such as Mueller, Kennaugh, target coherency and covariance matrices (Huynen 1970; Cloude 1986; van Zyl et al. 1987; Lüneburg et al. 1991; Boerner et al. 1991) are employed. Generally, the elements of these matrices are second order moments of the scattering matrix elements calculated at *zero time lags only*. As a result this formalism only fully characterizes the fluctuating radar target over a period of time which is smaller than the correlation time of the target as it will be shown further on in the chapter.

Modern radar systems commonly use Doppler power spectra to describe the dynamics of radar targets (Doviak and Zrnic 1993). Generally, the Doppler power spectrum of a radar target is related to the distribution of radial velocities as well as to the time variations in the scattering properties of the target. These fluctuations in the scattering properties of radar targets can often be associated with the change in orientation and shape of a target. If a radar target consists of more than one scattering center these time variations in the scattering properties can apply to all the centers and will result in rather chaotic radar signal and broaden the Doppler spectrum. Moreover, these fluctuations in target properties will also result in changes in the polarimetric properties of radar targets. Thus, we can expect that there is an interrelation between Doppler and polarimetric properties of radar targets.

Recent advances in the radar system design have allowed us to perform Doppler and polarimetric measurements simultaneously (Niemeijer 1996). This new measurement technique enables the study of the relation between Doppler and polarimetric properties of radar targets. As the result of this study we propose in this chapter a new polarimetric formalism, radar Doppler polarimetry, which takes advantage of the possibility to measure both Doppler and polarimetric properties of radar targets. It is shown in section 5.3 that this new formulation is more general than the conventional polarimetric one and includes radar polarimetric formulation as the limiting case.

Polarimetric target enhancement techniques are widely discussed in literature. The discussed methods enable an increase of the signal-to-clutter power ratio for stable (Kozlov 1979; Kostinski and Boerner 1986) and fluctuating targets (van Zyl et al. 1987; Swartz et al. 1988; Boerner and Kostinski 1989; McCormick and Hendry 1985; Tragl 1990). These target enhancement methods are based on the optimization problem of finding a pair of transmit and receive polarization states

that will obtain the maximum signal-to-clutter power ratio. Usually the sought polarization states are necessarily fully polarized states. In section 5.6 we generalize this approach to allow the polarization states of the transmitter and receiver to change on a pulse-to-pulse basis in order to obtain a better polarimetric contrast between objects.

This study is based on Doppler polarimetric measurements of precipitation and ground-based objects, carried out by the Delft Atmospheric Research Radar, which is an S-band Doppler polarimetric radar (Ligthart and Nieuwkerk 1980).

5.2 Radar polarimetry

If a set of orthonormal vectors $\{\overrightarrow{x}, \overrightarrow{y}\}$ which are lying in a plane perpendicular to the direction of radio wave propagation is defined, then the Jones vector of the scattered wave, $\overrightarrow{E^s(t)} = \begin{pmatrix} E_x^s(t) \\ E_y^s(t) \end{pmatrix}$, can be related to the Jones vector of the incident wave $\overrightarrow{e} = \begin{pmatrix} e_x \\ e_y \end{pmatrix}$ via the target scattering matrix $\mathbf{S}(t)$ (Kostinski and Boerner 1986; Ulaby and Elachi 1990)

$$\overrightarrow{E^s(t)} = \begin{pmatrix} S_{xx}(t) & S_{xy}(t) \\ S_{yx}(t) & S_{yy}(t) \end{pmatrix} \begin{pmatrix} e_x \\ e_y \end{pmatrix} = \tag{5.1}$$
$$= \mathbf{S}(t)\overrightarrow{e}$$

here we have assumed that the polarization state of the incident wave is not time dependent, which is the case for most radar sensing scenarios, and that the scattering matrix and hence the Jones vector of the scattered wave are time dependent.

Generally, the Stokes vector $\overrightarrow{g}$ is used for describing a wave scattered by a fluctuating target. The Stokes vector can be written in terms of the elements of the Jones vector as follows (Born and Wolf 1965)

$$\vec{g}(0) = \begin{pmatrix} \left\langle |E_x(t)|^2 \right\rangle + \left\langle |E_y(t)|^2 \right\rangle \\ \left\langle |E_x(t)|^2 \right\rangle - \left\langle |E_y(t)|^2 \right\rangle \\ \left\langle 2\,\mathrm{Re}(E_x(t)E_y^*(t)) \right\rangle \\ \left\langle 2\,\mathrm{Im}(E_x(t)E_y^*(t)) \right\rangle \end{pmatrix} \tag{5.2}$$

where * denotes complex conjugation and $\langle ... \rangle$ denotes ensemble average and is often substituted by the time average $\langle ... \rangle = \frac{1}{2T}\int_{-T}^{T}(...)\,dt$. It can be shown (Ulaby and Elachi 1990) that the scattered-wave Stokes vector $\vec{g^s}(0)$ is related to the incident-wave Stokes vector $\vec{g^i}(0)$ via the Kennaugh matrix $\mathbf{K}(0)$ as

$$\vec{g^s}(0) = \mathbf{K}(0)\vec{g^i}(0) \tag{5.3}$$

The Kennaugh matrix $\mathbf{K}(0)$ describes a fluctuating radar target and is a matrix consisting of second-order moments of linear combinations of the elements of the scattering matrix. Another conventional way of describing a fluctuating radar target is by means of the covariance matrix $\mathbf{C}(0)$, which can be written as follows (Lüneburg et al. 1991):

$$\mathbf{C}(0) = \left\langle \vec{k(t)} \otimes \vec{k(t)}^+ \right\rangle \tag{5.4}$$

where $\otimes$ denotes the Kronecker matrix multiplication and $\vec{k(t)} =$

$= \begin{pmatrix} S_{xx}(t) & \sqrt{2}S_{xy}(t) & S_{yy}(t) \end{pmatrix}^T$ is the time-dependent target scattering vector.

To conclude this section we can say that the description of the fluctuating targets as well as of the wave scattered by those targets is given by second-order moments calculated at zero time lags. This formulation is widely used in radar polarimetry for describing random radar targets (Agrawal and Boerner 1989; Cloude and Pottier 1996).

5.3 Radar Doppler polarimetry

5.3.1 Theoretical background

Since we would like to describe the behavior of all elements of a target scattering matrix together, it is convenient to consider them as a multivariate random process. Generally, a multivariate process can be characterized by its covariance

matrix (Priestley 1981), where every element is auto- (cross-) correlation function of the involved elementary random processes. In our case these elementary random processes are elements of a target scattering matrix. Now, if we assume that the elements of the scattering matrix are jointly stationary processes then the target covariance matrix expressed in an arbitrary polarization basis (x, y) will be

$$\mathbf{C}(\tau) = \left\langle \overrightarrow{k(t)} \otimes \overrightarrow{k(t+\tau)}^{+} \right\rangle \tag{5.5}$$

Further, we can define the spectral covariance matrix $\mathbf{F}(\omega)$, the elements of which are related to the elements of the covariance matrix by the Wiener-Khinchin theorem (Davenport and Root 1958) as follows:

$$\begin{aligned} F_{ij}(\omega) &= 2\int_{-\infty}^{+\infty} C_{ij}(\tau)\exp(-i\omega\tau)d\tau \\ C_{ij}(\tau) &= \frac{1}{4\pi}\cdot\int_{-\infty}^{+\infty} F_{ij}(\omega)\exp(i\omega\tau)d\omega \end{aligned} \tag{5.6}$$

where $i, j = 1, 2, 3$. It can be shown (Perina 1972) that the spectral covariance matrix $\mathbf{F}(\omega)$ is Hermitian semi-positive definite matrix for all frequencies ω, while the covariance matrix $\mathbf{C}(\tau)$ is Hermitian only for zero time lag.

Let us consider the main difference between proposed and conventional polarimetric techniques. We can easily see from (5.5) and (5.6) that if the time delays τ involved in (5.5) are restricted to $|\tau| \ll 1/\Delta\omega$, where $\Delta\omega$ is the maximum spectrum width of the $\mathbf{F}(\omega)$, then definition (5.5) converges to the definition (5.4). Thus it can be seen that the conventional polarimetric target description fully characterizes radar objects only for short observation times.

The standard Doppler processing (Doviak and Zrnic 1993), on the other hand, allows one to obtain Doppler power spectra $F_{ii}(\omega)$ for every element of the scattering matrix and as a result describes the time behavior of a target, but does not show the interrelations between polarimetric measures.

5.3.2 Doppler polarimetric coupling

Changes in polarimetric properties of radar targets will result in changes in the radar signal. Moreover, it will also result in different signal spectral properties for measurements with different polarization setups. To characterize this coupling between Doppler and polarimetric properties of radar targets, let us first consider

the ideal case, where there is no changes in polarimetric properties of a radar target and thus the polarimetric properties of a target are the same for all Doppler frequencies. In this case the spectral covariance matrix $\mathbf{F}(\omega)$ will be

$$F_{ij}(\omega) = \xi(\omega)F_{ij}(\omega_0) \quad i,j = 1..3$$

where $\mathbf{F}(\omega_0)$ is the spectral covariance matrix at some Doppler frequency ω_0 and $\xi(\omega)$ is a proportionality coefficient. Using (5.6) we can write the target covariance matrix $\mathbf{C}(0)$ as:

$$C_{ij}(0) = \frac{F_{ij}(\omega_0)}{4\pi} \int_{-\infty}^{+\infty} \xi(\omega) d\omega \tag{5.7}$$

From (5.7) it follows that in the case when the Doppler and polarimetric properties of targets are independent, the spectral covariance matrix $\mathbf{F}(\omega)$ is proportional to the covariance matrix $\mathbf{C}(0)$ for all Doppler frequencies:

$$F_{ij}(\omega) = \eta(\omega)C_{ij}(0) \tag{5.8}$$

where $\eta(\omega)$ is the proportionality coefficient. Thus, if the relation (5.8) is not valid, there is a coupling between Doppler and polarimetric properties of targets.

In order to derive the parameter which gives indication of the coupling between Doppler and polarimetric target properties we shall consider the spectra widths for all elements of the covariance matrix $\mathbf{C}(\tau)$. It is convenient to define the spectra widths σ_{ij} $(i,j = 1..3)$ as (Priestley 1981):

$$\sigma_{ij} = 0.5 \frac{\int_{-\infty}^{+\infty} |F_{ij}(\omega)|\, d\omega}{\max\limits_{\omega}(|F_{ij}(\omega)|)} \tag{5.9}$$

Remembering (5.8) we can easily see that for the case of no Doppler polarimetric coupling σ_{ij} will be the same for all i and j, and will be equal to

$$\sigma_{ij} = \sigma = 0.5 \frac{\int_{-\infty}^{+\infty} |\eta(\omega)|\, d\omega}{\max\limits_{\omega}(|\eta(\omega)|)} \quad \forall\, i,j = 1..3 \tag{5.10}$$

Thus condition (5.10) is the necessary condition to ensure that a target has no Doppler polarimetric coupling. Moreover, if the spectra width for the different elements of the covariance matrix $\mathbf{C}(\tau)$ are different, condition (5.10) is not valid, hence the Doppler and polarimetric properties of a target are related. Using (5.10) and (5.9) we can introduce the degree of the Doppler polarimetric coupling, W_σ,

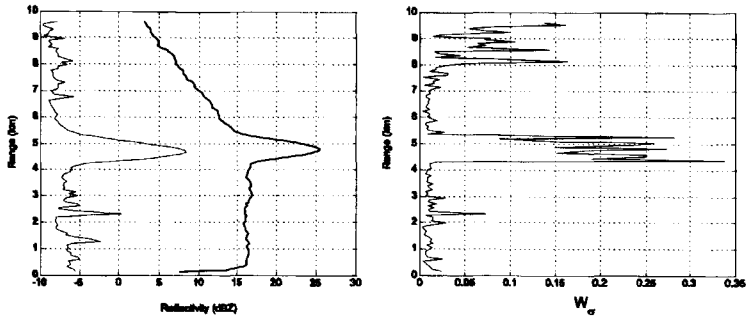

Figure 5.1: The slant profile of precipitation. The elevation angle is 20 degrees. The left figure shows the reflectivity profile. The thick solid line represents the *hh* measurement and the thin line shows the *hv* profile. The right figure gives the profile of the degree of Doppler polarimetric coupling of this event.

for a radar target:

$$W_\sigma = (\max_{i,j} \sigma_{ij} - \min_{i,j} \sigma_{ij})/(\max_{i,j} \sigma_{ij} + \min_{i,j} \sigma_{ij}) \tag{5.11}$$

The degree of Doppler polarimetric coupling gives a quantitative measure of the dependence between Doppler and polarimetric properties of radar targets. It lies in the interval from 0 to 1. The zero value of W_σ corresponds to no Doppler polarimetric coupling and if W_σ is equal to unity, it corresponds to the case where the Doppler and polarimetric target properties have a one-to-one relation.

5.4 Examples of Doppler polarimetric properties for different types of targets

5.4.1 Doppler polarimetric properties of precipitation

A good example to illustrate the effect of Doppler polarimetric coupling is polarimetric measurements of a stratiform precipitation. It was shown by Lüneburg et al. (1991) and by Bringi et al. (1991) that the polarimetric properties of a stratiform rain can considered to be deterministic, which results in near singular covariance matrix $\mathbf{C}(0)$. The polarimetric signatures of the melting layer of the precipitation, where precipitating snow melts into rain, on the other hand, are

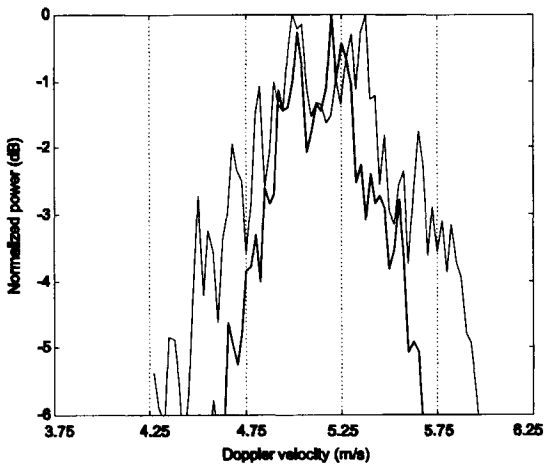

Figure 5.2: The Doppler spectra of the melting layer of precipitation. These spectra correspond to the range of 4.5 km where the maximum Ldr value is achieved. The thick solid line corresponds to the co-polar Doppler power spectrum and the thin line corresponds to the cross-polar spectrum.

less deterministic (Bringi et al. 1991; Ryzhkov 2001), hence all eigenvalues of the covariance matrix for the melting layer measurements are different from zero.

In Fig. 5.1 a). the slant profile of stratiform precipitation is shown. This measurement was carried out by DARR at a 20 degree elevation angle with a 75 m range resolution. The polarization switching was performed every 1.25 ms, which resulted in the set of hh, hv and vv measurements for every 3.75 ms.

For this measurement the degree of Doppler polarimetric coupling was calculated for all range cells and it is shown in Fig. 5.1 b). Since for the rain and cloud measurements the observed cross-polar power measurements are strongly predetermined by the imperfection of the antenna, all cross-polar measurements whose power was more than 20 dB lower than that of a co-polar channel were discarded. This thresholding explains the sharp increase in W_σ in the area of the melting layer. The increase of the degree of Doppler polarimetric coupling for ranges further than 8 km is determined by a poor signal-to-noise ratio.

It can be seen from Fig. 5.1 b) that in the area of rain and cloud the degree of Doppler polarimetric coupling is close to zero, which can be explained by the nearly deterministic behavior of light rain. It should be pointed out that the de-

terministic behavior of rain and cloud polarimetric signatures is not the result of the processing; on the contrary, the use of the thresholding on the measured cross-polar signal is the result of this deterministic behavior. The melting layer, on the other hand, has a non-zero cross-polar signal and as a result its polarimetric signature has more variability. It can be seen that W_σ varies from 0.1 till almost 0.35 for the melting layer. The signal-to-noise ratio for the cross-polar measurements in the melting-layer region is better than 20 dB.

Let us look in more detail at what causes these relatively high values of W_σ. In Fig. 5.2 the co-polar and cross-polar Doppler power spectra are shown for the range of 4.5 km. This range gate corresponds to the bottom of the melting layer where the highest Ldr value, a ratio of $\left\langle |S_{hv}|^2 \right\rangle$ to $\left\langle |S_{vv}|^2 \right\rangle$, is achieved. For this range gate the elements of the covariance matrix $\mathbf{C}(\tau)$ have the following relative Doppler widths

$$[\sigma_{ij}] = \begin{pmatrix} 1.00 & 1.04 & 0.95 \\ 1.04 & 1.59 & 1.00 \\ 0.95 & 1.00 & 0.96 \end{pmatrix} \tag{5.12}$$

and as a result $W_\sigma = 0.25$. It can be seen that the cross-polar signal has the widest spectrum $F_{22}(\omega)$. This result can be explained by the physical processes which take place in the melting layer (Russchenberg 1992). Due to the melting of snow flakes the particle shape changes. Moreover, the melting process leads to the exchange of the energy between the melting layer and the surrounding air, which results in an increase in turbulence in the area of the melting layer. The turbulent air causes variation in the orientation of the particles. Since the cross-polar measurements are more sensitive to changes in the shape and orientation of hydrometeors than the co-polar measurements, the broadening of the spectrum due to changes in polarimetric properties of particles will be more apparent in $F_{22}(\omega)$. This example illustrates the possibility of using Doppler polarimetry to retrieve the microphysical properties of precipitation, a more complete description of this problem is given by Verlinde et al. (2002).

5.4.2 Doppler polarimetric properties of ground targets

Another important class of radar targets is ground-based objects. The characterization of the scattered waves from these objects is important for many radar remote sensing applications such as for the retrieval of biophysical properties of

Table 5.1: Radar Specifications For the Ground Measurements

Parameter	Delftse Hout	Highway
Transmit power	- 20 dBW	- 20 dBW
Frequency deviation	2 MHz	2 MHz
Elevation	-2^o	-2.3^o
Antenna beamwidth	1.8^o	1.8^o
Number of samples per sweep	256	256
Number of samples for Doppler processing	512	512
Sweep time	5.12 ms	5.12 ms
Maximum range	9600 m	9600 m
Nearest point where radar beam hits ground	1780 m	1610 m
Furthest point where radar beam hits ground	4700 m	3700 m
Range resolution	75 m	75 m
Maximum Doppler velocity	$\pm$ 1.46 m/s	$\pm$ 1.46 m/s
Doppler velocity resolution	0.6 cm/s	0.6 cm/s
Radar distance to the presented range cell	1875 m	1875 m
Observation time for one Doppler spectrum	7.68 s	7.68 s
Total observation time	230.4 s	230.4 s

Table 5.2: Vehicles Velocities For the Highway Measurement

vehicle speed		vehicle path [m]		Doppler velocities [m/s]		
km/hr	m/s	7.68 s	230.4 s	v_{max}	v_o	v_{min}
80	22.22	170.6	5119.5	17.9	17.5	17.3
100	27.78	213.4	6400.5	22.2	21.9	21.6
120	33.33	256.0	7679.2	26.7	26.2	25.9

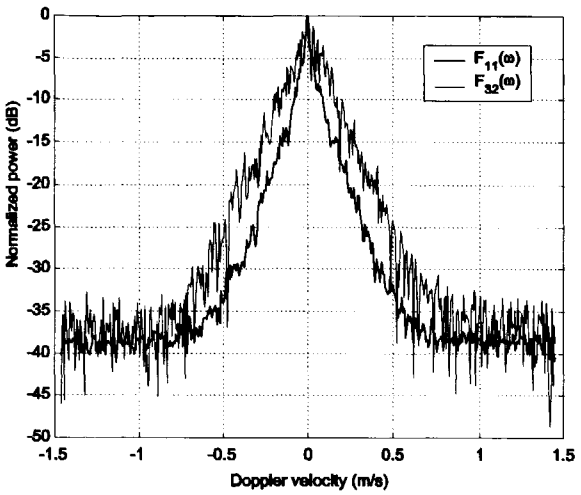

Figure 5.3: The Doppler spectra of park area measurements. The thick solid line corresponds to the co-polar Doppler power spectrum and the thin line corresponds to the $vv - hv$ cross spectrum.

vegetation and for ground-clutter suppression. In order to illustrate the use of Doppler polarimetry two measurements were carried out with DARR.

The first measurement concerned the park area in Delft known as the "Delftse Hout". The measurement was performed with a -2 degrees elevation angle, and the radar distance to the park was about 2 km. The same polarization switching scheme as discussed earlier was employed. The radar specifications for this measurement are given in Table 5.1. And the calculated widths give the following results

$$[\sigma_{ij}] = \begin{pmatrix} 1.00 & 0.61 & 0.77 \\ 0.61 & 1.45 & 2.02 \\ 0.77 & 2.02 & 1.12 \end{pmatrix} \tag{5.13}$$

As can be seen from (5.13) this measurement shows a completely different relation between Doppler and polarimetric properties than the precipitation measurement. The degree of Doppler polarimetric coupling for the park area was found to be 0.54 and as can be seen in (5.13) the minimum spectrum width is associated

with the covariance between S_{hh} and S_{vh}, while the maximum spectrum width is found for the covariance between S_{vv} and S_{hv}. These cross spectra are shown in Fig. 5.3. This result can be associated with the dynamic properties of ground clutter. One of the possible interpretations of these results is that wind induced movements of the trees can be approximated by a pendulum like oscillations. It is known that for a pendulum a point of the maximum velocity also corresponds to the minimum acceleration and thus at this point there is no relative movements between different parts of foliage and as a result the correlation between hh and vv signals will be the highest. This can be a possible explanation of the observed spectra.

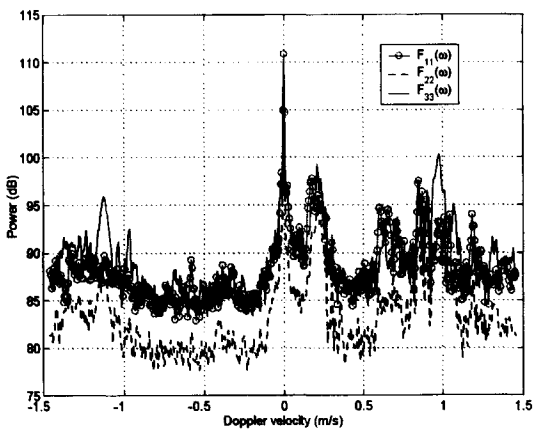

Figure 5.4: Doppler power spectra of the highway measurements. The solid line with circles represents the Doppler power spectrum of S_{hh}. The dashed line corresponds to the Doppler power spectrum of S_{hv} and the solid line corresponds to the power spectrum of S_{vv}.

The second measurement which was carried out to illustrate the coupling between Doppler and depolarization properties of radar targets is the measurement of the highway. This highway connects The Hague and Rotterdam. The speed limit on this highway is 120 km/hr for cars and of 80 km/hr for road-transport vehicles. The radar specifications for this measurement are similar to the previously discussed park measurement and also are given in Table 5.1. For this measurement

the calculated spectrum widths are:

$$[\sigma_{ij}] = \begin{pmatrix} 1.00 & 0.59 & 0.70 \\ 0.59 & 1.21 & 0.56 \\ 0.70 & 0.56 & 1.21 \end{pmatrix} \tag{5.14}$$

In Fig.5.4 Doppler power spectra of the co-polar elements $F_{11}(\omega), F_{33}(\omega)$ and the cross-polar element $F_{22}(\omega)$ of the scattering matrix are shown. It can be seen that there are four clear peaks at -1.2, 0.2, 0.7 and 1 m/s, which correspond to the reflections from vehicles and a peak around 0 m/s, which corresponds to the reflections from the ground. These observed vehicle velocities are not real Doppler velocities of cars, since the true velocities (see Table 5.2) are much higher than the maximum unambiguous Doppler velocity for this measurement setup. In Table 5.2 the observed Doppler velocities for different kinds of vehicles is given; $v_{\max}$ and $v_{\min}$ give the maximum and the minimum observed Doppler velocities for different types of vehicles and the v_o gives the value of the Doppler velocity for the middle point of a vehicle trajectory. The noise like signal at 85 dB for co-polar spectra and at 80 dB for the cross-polar spectrum is caused by the decorrelation of the measured signals due to continuous changes of targets in the radar volume. Because, the measurement time used to obtain one Doppler spectrum is 7.68 s and in total averaging is performed over 30 spectra in order to reduce the variance of the spectra estimate. Because of the different polarimetric properties of the vehicles the resulting Doppler power spectra are also different for different polarizations, as can clearly be seen in Fig. 5.4. The values of the spectrum width for different elements of the covariance matrix are given in (5.14) and the obtained value of the Doppler polarimetric coupling is 0.37. This example shows similar picture as the example of the compound target, presented in the beginning of this section. It shows that a compound target consisting of several scattering centers with different Doppler and polarimetric properties will have a rather high value of the degree of Doppler polarimetric coupling.

In this section the Doppler polarimetric properties of different types of targets were discussed. It was shown that most of the radar targets manifest strong coupling between the polarimetric and Doppler properties. The use of this coupling is shown further on in the chapter.

5.5 Depolarization and Doppler polarimetry

Often the target entropy H_s is used in order to characterize the depolarization properties of the scattering media (Cloude and Pottier 1996). It is defined as

$$H_s = -\sum_{i=1}^{3} p_i \log_3 p_i; \quad p_i = \frac{\lambda_i}{\sum_{j=1}^{3} \lambda_j} \tag{5.15}$$

where λ_i are the eigenvalues of $\mathbf{C}(0)$. If the target entropy is close to unity then the target can be considered as completely depolarizing and for the stationary target the entropy is zero. The target entropy originates from the coherent target decomposition (Cloude and Pottier 1996), where a depolarizing target is represented by the set of stationary targets with the RCS defined by the eigenvalues of $\mathbf{C}(0)$. Because the eigenvalues λ_i are related to the RCS of the elementary stationary radar targets, the target entropy is a power parameter.

Since the polarization dependence of radar targets Doppler properties takes place only for depolarizing targets, one would expect a relation between H_s and W_σ. However, on the one hand, the target entropy is a power parameter values of which are related to the RCS of the elementary radar targets and the degree of Doppler polarimetric coupling, on the other hand, characterizes differences in the statistical behavior of the radar signal for different antenna polarization states. Thus H_s and W_σ describe different aspects of the radar target depolarization process.

This conclusion coincides with the presented measurements. For the melting layer the entropy is found to be 0.17 and the degree of Doppler polarimetric coupling 0.25. For ground targets these values are $W_\sigma = 0.54$ and 0.37 and $H_s = 0.82$ and 0.83 for the park area and the highway respectively. It can be seen that there is no clear one-to-one dependence between the degree of Doppler polarimetric coupling and the target entropy. From these observations it can be concluded that the degree of Doppler polarimetric coupling is a new parameter which enables additional parametrization of the depolarizing properties of radar targets.

It is interesting to study dependence between depolarization properties of targets in time and spectral domain. Generally speaking Doppler polarimetric representation of a radar target can be considered as a coherent target decomposition. Though, in the case of the polarimetric target decomposition, as described by Cloude and Pottier (1996), a radar target is decomposed on a set of stochastic polarimetrically stable radar targets, as shown in (3.32). The Doppler polarimet-

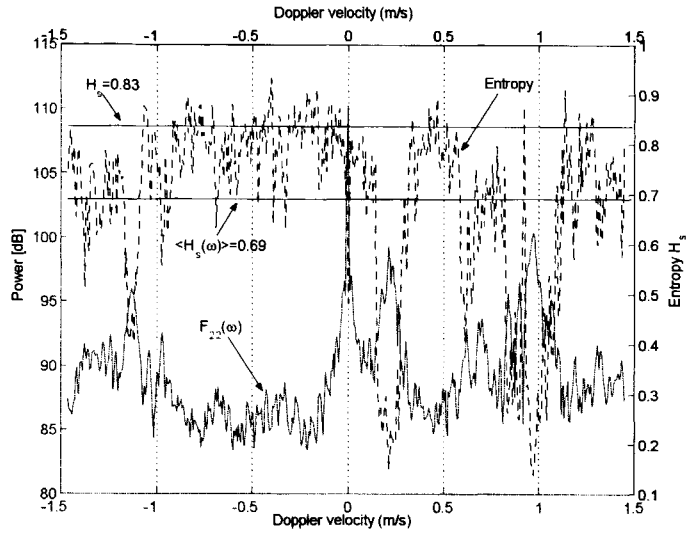

Figure 5.5: Highway measurement. Solid line is the Doppler power spectrum of HV ($F_{22}(\omega)$). And the dashed line is the entropy H_s as a function of Doppler velocity. It can be seen that vehicles have low entropy, and that the entropy of the combined target is much higher than the entropy of any individual target.

ric representation of radar targets, on the other hand, gives a set of depolarizing targets with deterministic Doppler properties. Nonetheless, it should be noted that in case of Doppler polarimetric representation of radar target, the elementary targets are less depolarizing than the whole radar target.

Let us demonstrate this conclusion on real life measurements. In Fig.5.5 the entropy as a function of the Doppler velocity for the highway measurements is shown. It can be seen that the entropy of cars is relatively low between 0.4, for reflections at -1.2 and 0.2 m/s, and 0.15 for the signals at 0.7 and 1 m/s. For the ground the entropy is about 0.5. The entropy for the noise like target is around 0.8. The average value of the entropy for all these targets is 0.69. If the combination of all these targets is considered to be one complex target the resulting entropy of this target is 0.83. As is expected, the entropy of the set of targets is larger than the averaged entropy of all separate targets. This property of Doppler polarimetric representation has a very important consequences for target contrast enhancement techniques as will be shown further on.

5.6 Doppler polarimetric target enhancement and voltage equation

5.6.1 Generalized contrast enhancement problem

One of the important applications of radar polarimetry is polarimetric target contrast enhancement. Where for stationary radar targets great enhancement of the target contrast can be achieved (Kozlov 1979; Giuli 1986; Yang et al. 2001), the case of time-varying radar targets is more complicated and the resulting contrast enhancement is greatly affected by the depolarization properties of radar targets (Ioannidis and Hammers 1979; van Zyl et al. 1987; Swartz et al. 1988).

It was shown above that for any depolarizing radar target the polarization properties are different for different Doppler frequencies. As a result the Doppler processing can be treated as a coherent target decomposition technique which represents a target as a set of less depolarizing targets. Thus, the application of the polarimetric optimization procedure for every Doppler cell generally will give a better contrast enhancement than the polarization enhancement technique applied to the complete target.

Let us assume that we have two radar objects with spectral covariance matrices $\mathbf{F}_t(\omega)$ and $\mathbf{F}_c(\omega)$. The ratio of the powers, P_t and P_c, in the radar signals received of these targets is

$$R_{tc} = \frac{P_t}{P_c} = \frac{\int_{-\infty}^{+\infty} \vec{\vartheta}_3^{+}(\omega)\mathbf{F}_t(\omega)\vec{\vartheta}_3(\omega)d\omega}{\int_{-\infty}^{+\infty} \vec{\vartheta}_3^{+}(\omega)\mathbf{F}_c(\omega)\vec{\vartheta}_3(\omega)d\omega}, \tag{5.16}$$

where $\vec{\vartheta}_3(\omega)$ represents a polarization state defined for every Doppler frequency cell. For the simplicity sake we have restricted ourselves to the case of reciprocal targets and as a result the spectral covariance matrices are 3x3 matrices. If we want to increase the contrast of the target, given by the spectral covariance matrix $\mathbf{F}_t(\omega)$, with respect to clutter, $\mathbf{F}_c(\omega)$, we should maximize the ratio R_{tc}. This optimization procedure can be solved by applying the method of Lagrangian multipliers. In this case Lagrangian L is:

$$L = \int_{-\infty}^{+\infty} \vec{\vartheta}_3^{+}(\omega)\mathbf{F}_t(\omega)\vec{\vartheta}_3(\omega)d\omega + \lambda\left(\int_{-\infty}^{+\infty} \vec{\vartheta}_3^{+}(\omega)\mathbf{F}_c(\omega)\vec{\vartheta}_3(\omega)d\omega - c\right) \tag{5.17}$$

where λ is the Lagrangian multiplier and c is a constant. Or we can rewrite (5.17)

as

$$L = \int_{-\infty}^{+\infty} \left[\vec{\vartheta}_3^{+}(\omega) \mathbf{F}_t(\omega) \vec{\vartheta}_3(\omega) + \lambda (\vec{\vartheta}_3^{+}(\omega) \mathbf{F}_c(\omega) \vec{\vartheta}_3(\omega) - \frac{c}{4\pi}) \right] d\omega \qquad (5.18)$$

Reminding that the spectral covariance matrices are Hermitian semi-positive definite and thus in (5.18) the integral sign can be omitted, hence we can solve this problem by finding optimum polarization vectors for every Doppler frequency. This solution can be achieved by setting the partial derivative $\frac{\partial L(\omega)}{\partial \vec{\vartheta}_3^{+}}$, where $L(\omega)$ is the Lagrangian for every Doppler frequency, to zero:

$$\frac{\partial L(\omega)}{\partial \vec{\vartheta}_3^{+}(\omega)} = \mathbf{F}_t(\omega) \vec{\vartheta}_3(\omega) + \lambda \mathbf{F}_c(\omega) \vec{\vartheta}_3(\omega) = 0 \qquad (5.19)$$

This leads us to the generalized eigenvalue problem (Searle 1982):

$$\mathbf{F}_t(\omega) \vec{\vartheta}_3(\omega) = -\lambda \mathbf{F}_c(\omega) \vec{\vartheta}_3(\omega) \qquad (5.20)$$

and thus optimum polarization vectors $\vec{\vartheta}_{3opt}(\omega)$ are the eigenvectors determined from (5.20). The maximum ratio R_{tc} is given by (5.16), where the polarization state vectors are substituted by $\vec{\vartheta}_{3opt}(\omega)$. This procedure (5.16 - 5.20) is a generalization of the target covariance matrix optimization approach, which is given in (Swartz et al. 1988; Mott 1995; Boerner et al. 1998) for the case of time-dependent antenna polarization states, as will be shown further on.

5.6.2 Voltage equation for optimum reception

Generally all the polarization optimization solutions should give an appropriate formulation for the antenna polarization states. In order to find such a formulation let us consider the time behavior of the optimum received power, P_t:

$$P_t(t) = \frac{1}{4\pi} \int_{-\infty}^{+\infty} \vec{\vartheta}_{3opt}^{+}(\omega) \mathbf{F}_t(\omega) \vec{\vartheta}_{3opt}(\omega) e^{i\omega t} d\omega = \qquad (5.21)$$

$$= \frac{1}{4\pi} \int_{-\infty}^{+\infty} [\vec{\vartheta}_{3opt}^{+}(\omega) \otimes \vec{\vartheta}_{3opt}^{T}(\omega)] vec(\mathbf{F}_t(\omega)) e^{i\omega t} d\omega$$

where $vec(\mathbf{F}_t(\omega))$ is the vector representation of $\mathbf{F}_t(\omega)$. Further the received power can be connected to the target covariance matrix $\mathbf{C}(\tau)$ as follows

$$P_t(t) = \int_{-\infty}^{+\infty} \vec{b}_w(z) vec(\mathbf{C}(t-z)) dz \tag{5.22}$$

$$\vec{b}_w(z) = \int_{-\infty}^{+\infty} [\vec{w}^+_{3opt}(x) \otimes \vec{w}^T_{3opt}(x+z)] dx$$

$$\vec{w}_{3opt}(t) = \frac{1}{4\pi} \int_{-\infty}^{+\infty} \vec{\vartheta}_{3opt}(\omega) e^{i\omega t} d\omega$$

where $\vec{w}_{3opt}(t) = [\, h_x(t)e_x(t) \;\; \frac{1}{\sqrt{2}}(h_x(t)e_y(t) + h_y(t)e_x(t)) \;\; h_y(t)e_y(t) \,]^+$ and defines the time-dependent antenna polarization states $\vec{h}(t)$ and $\vec{e}(t)$ on the transmit and receive sides respectively. From (5.22) it follows that the received voltage, $v(t)$, will be

$$v_t(t) = \int_{-\infty}^{+\infty} \vec{w}^+_{3opt}(x) \vec{k}(t-x) dx \tag{5.23}$$

and reminding that $\vec{k}(t) = vec(\mathbf{S}(t))$ we can rewrite (5.23) as:

$$v_t(t) = \int_{-\infty}^{+\infty} \vec{h}^T(x) \mathbf{S}(t-x) \vec{e}(x) dx \tag{5.24}$$

The formula (5.24) gives a new formulation for the radar voltage equation, which takes into account the spectral characteristics of a target. Moreover, the optimization procedure (5.16 - 5.24) can be interpreted as a linear predictive filter where $\vec{w}^+_{3opt}(t)$ is the impulse response of the filter and $[\vec{\vartheta}^+_{3opt}(\omega) \otimes \vec{\vartheta}^T_{3opt}(\omega)]$ is its frequency response. This interpretation indicates that the physical meaning of the proposed optimization approach and the resulting voltage equation is that we are trying to predict the polarimetric properties of the target, namely its scattering matrix, at the moment of measurement on the basis of the previously measured scattering matrices of this target. We then use the predicted target polarimetric properties to select our optimum polarization states. This prediction approach assumes that there is a correlation between the polarimetric properties of targets from measurement to measurement. On the other hand the conventional polarimetric optimization approach does not consider correlation between consecutive polarimetric measurements and as a result the optimum antenna polarization

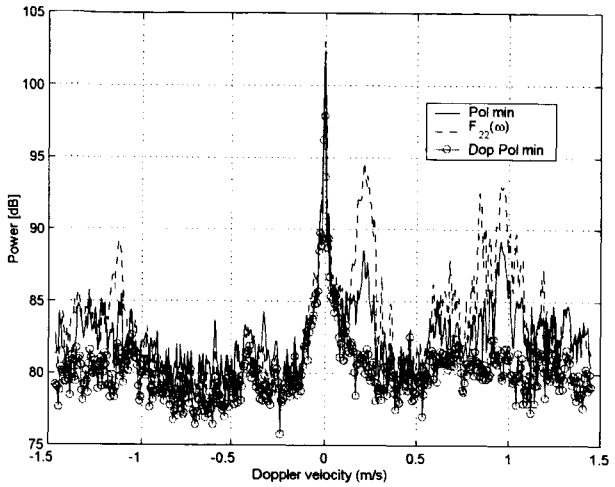

Figure 5.6: Comparison between clutter suppression results polarimetric and Doppler polarimetric methods. The dashed line shows the Doppler power spectrum of S_{hv}. The solid line corresponds to the minimum power obtained by the polarimetric technique and the solid line with circles corresponds to the Doppler polarimetric minimum.

states are constant and the resulting voltage equation is

$$v_t(t) = \overrightarrow{h}^T \mathbf{S}(t) \overrightarrow{e}$$

and the target covariance matrix $\mathbf{C}(0)$ (or Kennaugh matrix $\mathbf{K}(0)$) is used to calculate the optimum polarization states (Boerner et al. 1998).

5.7 Example of the use of Doppler polarimetric optimization method

To illustrate the use of the Doppler polarimetric optimization procedure we shall apply the proposed technique to the highway measurement, which is described in section 5.4.3. In this example the minimum power of the receive signal is sought. Once it is found using (5.16) - (5.20) we can determine $\overrightarrow{\vartheta}_{3opt}(\omega)$ and the $P_{\min}$.

In Fig.5.6 the results of Doppler polarimetric and polarimetric minimizations

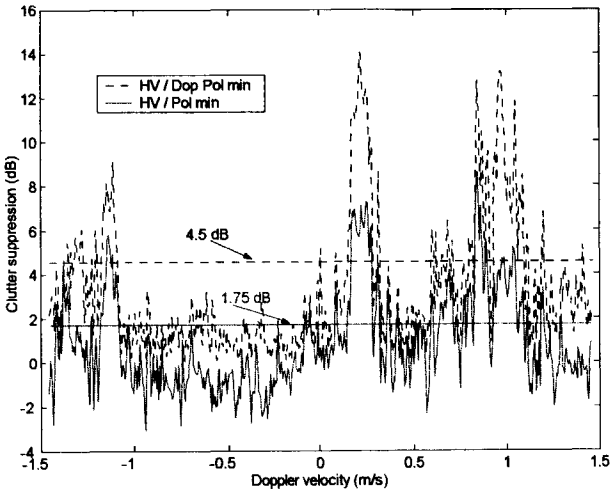

Figure 5.7: Results of the polarimetric clutter suppression. The dashed line shows the ratio of $F_{22}(\omega)$ to the Doppler polarimetric minimum of the signal. The solid line shows the ratio of $F_{22}(\omega)$ to the polarimetric minimum of the signal. The straight solid line shows the mean value of the clutter suppression by the polarimetric technique, and the straight dashed line shows the mean value of the clutter suppression by the Doppler polarimetric method.

are shown. With polarimetric minimum we imply $\vec{w}_{3opt}^{+}\mathbf{F}(\omega)\vec{w}_{3opt}$ where $\vec{w}_{3opt}$ is found from the minimization problem $\min_{\vec{w_3}}[\vec{w_3}^{+}\mathbf{C}(0)\vec{w_3}]$. As can be seen in Fig.5.6 both polarimetric and Doppler polarimetric methods have reduced the power of the signal received from cars. However, the Doppler polarimetric suppression is more efficient in all the cases. In Fig.5.7 the comparison between the power reduction by polarimetric and Doppler polarimetric approaches is given.

Comparing Doppler polarimetric and polarimetric methods, we can conclude that for this example Doppler polarimetry gives an improvement of 2.75 dB in suppression on average. Moreover, in this example differences as large as 10 dB between the performances of these techniques were obtained for the separate targets.

5.8 Conclusions

In this chapter the new polarimetric formulation Doppler polarimetry was introduced. It was shown that this formulation is more general than the common polarimetric one. It was also shown that the Doppler polarimetric target characterization converges to the polarimetric one for short observation times. Moreover, it was shown that Doppler and polarimetric properties of depolarizing radar targets are interrelated. To characterize this interrelation we introduced the degree of Doppler polarimetric coupling. It was shown that this new parameter gives extra information about polarimetric behavior of radar targets and can be used to describe the depolarization properties of radar targets better. These conclusions were illustrated by Doppler polarimetric measurements of precipitation and ground-based objects.

Using a new polarimetric formulation we solved the polarimetric optimization for a general case, where antenna polarization states are allowed to change on pulse-to-pulse basis. It was shown that this optimization procedure can be interpreted as a construction of a linear predictive filter, the characteristics of which are determined in order to obtain maximum signal-to-clutter power ratio. It was shown in the example of the highway measurements that Doppler polarimetric optimization procedure gives better results than the conventional polarimetric one. Moreover, based on this study the new radar voltage equation was derived. This new voltage equation takes into account the spectral polarimetric properties of radar targets.

Appendix A. Estimation of spectral properties from the measurements

The Doppler polarimetric formulation which was introduced above is based on infinitely long and continuous measurements. In the case of real radar measurements we deal with the estimation of spectral characteristics from finite measurement samples. If the shapes of the spectra $F_{ij}(\omega)$ are not known it is common to use periodogram spectrum estimation. In this case the estimated Doppler spectrum $I_{ij}^N(\omega)$ is connected to the true spectrum $F_{ij}(\omega)$ as follows (Doviak and Zrnic 1993; Priestley 1981):

$$I_{ij}^N(\omega) = \int_{-\pi/T_s}^{\pi/T_s} W_N(\theta - \omega) F_{ij}(\theta) d\theta \tag{5.25}$$

where T_s is the sampling interval ($\frac{\pi}{T_s}$ is the maximum unambiguous Doppler frequency), $W_N(\omega)$ is the spectrum of the covariance lag window and N is the number of samples (NT_s gives the observation time). Because of this, Doppler polarimetry has some limitations when describing real radar targets. These limitations can be illustrated by the following examples:

1. If N is so small that the spectral width of $W_N(\omega)$ is much larger than the one of $F_{ij}(\omega)$ then

$$I_{ij}^N(\omega) = W_N(0) \int_{-\sigma_w}^{\sigma_w} F_{ij}(\theta) d\theta = \tag{5.26}$$
$$= W_N(0) \cdot C_{ij}(0)$$

2. If N (and thus the observation time) goes to infinity, then $W_N(\omega)$ will behave like a δ- function and this will lead to

$$\lim_{N\to\infty} I_{ij}^N(\omega) = \int_{-\pi/T_s}^{\pi/T_s} \lim_{N\to\infty} W_N(\theta-\omega) F_{ij}(\theta) d\theta = \tag{5.27}$$
$$= F_{ij}(\omega)$$

thus the estimated spectrum will coincide with the actual spectrum.

Based on these examples we can conclude that Doppler polarimetric formalism gives the most complete description when we deal with targets which have discrete spectra $F_{ij}(\omega_k) = F_{ij}^k$ and the minimum distance between spectral components is larger than the spectral width of the covariance lag window, i.e. when the following inequality is satisfied:

$$\min_{i,j} |\omega_i - \omega_j| \geq \frac{\int |W_N(\omega)|\, d\omega}{2 \cdot W_N(0)} \tag{5.28}$$

For such targets every $\mathbf{F}^k$ is uniquely connected to a scattering matrix $\mathbf{S}^k$ and the target can be described as a set of deterministic targets.

References

Agrawal, A. P. and W.-M. Boerner: 1989, Redevelopment of Kennaugh's target characteristic polarization state theory using the polarization transformation ratio formalism for the coherent case. *IEEE Trans. Geosci. Remote Sens.*, **27**, 2–14.

Boerner, W.-M.: 1981, Use of polarization in electromagnetic inverse scattering. *Radio Sci.*, **16**, 1037–1045.

Boerner, W.-M., M. B. El-Arini, C.-Y. Chan, and P. M. Mastoris: 1981, Polarization dependence in electromagnetic inverse problems. *IEEE Trans. Antennas Propagat.*, **29**, 262–271.

Boerner, W.-M. and A. B. Kostinski: 1989, Optimal reception of partially polarized waves in radar meteorology. *Proc. Of 24th Conference on Radar Meteorology*, American Meteorological Society, Tallahassee, Florida, 407–410.

Boerner, W.-M., H. Mott, E. Luneburg, C. Livingstone, B. Brisco, R. Brown, and J. S. Paterson: 1998, *Manual of Remote Sensing. Principles and Applications of Imaging Radar*, John Wiley and Sons., chapter 5. Polarimetry in Radar Remote Sensing: Basic and Applied Concepts. 271–357.

Boerner, W.-M., W.-L. Yan, A.-Q. Xi, and Y. Yamaguchi: 1991, On the basic principles of radar polarimetry: The target characteristic polarization state theory of Kennaugh, Huynen's polarization fork concept, and its extension to the partially polarized case. *Proc. IEEE*, **79**, 1538–1550.

Born, M. and E. Wolf: 1965, *Principles of Optics*. Pergamon Press Ltd., London.

Bringi, V. N., V. Chandrasekar, P. Meischner, J. Hubbert, and Y. Golestani: 1991, Polarimetric radar signatures of precipitation at S- and C-bands. *IEE Proc. F. Commun. Radar Signal Process.*, **138**, 109–119.

Chandrasekhar, S.: 1950, *Radiative Transfer*. Oxford Clarendon, Oxford, UK.

Cloude, S. R.: 1986, *Polarimetry: The Characterization of Polarization Effects in EM Scattering*. Ph.D. thesis, Univ. of Birmingham.

Cloude, S. R. and E. Pottier: 1996, A review of target decomposition theorems in radar polarimetry. *IEEE Trans. Geosci. Remote Sens.*, **34**, 498–518.

Davenport, W. B. and W. L. Root: 1958, *An Introduction to the Theory of Random Signals and Noise*. McGraw-Hill Book Company Inc., New York, NY.

Doviak, R. J. and D. S. Zrnic: 1993, *Doppler Radar and Weather Observations*. Academic Press, Inc., London.

Giuli, D.: 1986, Polarization diversity in radars. *Proc. IEEE*, **74**, 245–269.

Huynen, J. R.: 1970, *Phenomenological Theory of Radar Targets*. Ph.D. thesis, Delft University of Technology.

Ioannidis, G. A. and D. E. Hammers: 1979, Optimum antenna polarizations for target discrimination in clutter. *IEEE Trans. Antennas Propagat.*, **27**, 357–363.

Kennaugh, E. M.: 1952, Polarization properties of radar reflections. Project Rep. 389-12, Ohio State Univ.

Kostinski, A. B. and W.-M. Boerner: 1986, On foundations of radar polarimetry. *IEEE Trans. Antennas Propagat.*, **34**, 1395–1404.

Kozlov, A. I.: 1979, Radar contrast between two objects. *Radioelectronika*, **22**, 63–67.

Ligthart, L. P. and L. R. Nieuwkerk: 1980, FM-CW Delft atmospheric research radar. *IEE Proc. F. Commun. Radar Signal Process.*, **127**, 421–426.

Lüneburg, E., V. Ziegler, A. Schroth, and K. Tragl: 1991, Polarimetric covariance matrix analysis of random radar targets. *Target and Clutter Scattering and Their Effects on Military Radar Performance*, AGARD-CP-501, Ottawa, Canada, 27–1–27–12.

McCormick, G. C. and A. Hendry: 1985, Optimal polarizations for partially polarized backscatter. *IEEE Trans. Antennas Propagat.*, **33**, 33–40.

Mieras, H.: 1983, Optimal polarizations of simple compound targets. *IEEE Trans. Antennas Propagat.*, **31**, 996–999.

Mott, H.: 1995, Polarimetric contrast optimization. *IGARSS*, 2011–2013.

Niemeijer, R. J.: 1996, *Doppler-Polarimetric Radar Signal Processing*. Ph.D. thesis, Delft Univ. Technology.

Perina, J.: 1972, *Coherence of Light*. Van Nostrand Reinhold Company Ltd., London.

Priestley, M. B.: 1981, *Spectral Analysis and Time Series*. Academic Press, London.

Russchenberg, H. W. J.: 1992, *Ground-Based Remote Sensing of Precipiation Using a Multipolarized FM-CW Doppler Radar*. Ph.D. thesis, Delft University of Technology.

Ryzhkov, A. V.: 2001, Interpretation of polarimetric radar covariance matrix for meteorological scatterers: Theoretical analysis. *J. Atmos. Oceanic Technol.*, **18**, 315–328.

Searle, S. R.: 1982, *Matrix Algebra Useful for Statistics*. Wiley Series in Probability and Mathematical Statistics, John Wiley and Sons, Inc., New York.

Swartz, A. A., H. A. Yueh, J. A. Kong, L. M. Novak, and R. T. Shin: 1988, Optimal polarizations for achieving maximum contrast in radar images. *J. Geophys. Res.*, **93**, 15252–15260.

Tragl, K.: 1990, Polarimetric radar backscattering from reciprocal random targets. *IEEE Tr. Geosci. Remote Sens.*, **28**, 856–864.

Ulaby, F. T. and C. Elachi, eds.: 1990, *Radar Polarimetry for Geoscience Applications*. Artech House, Inc., Norwood, MA.

van Zyl, J. J., C. H. Papas, and C. Elachi: 1987, On the optimum polarizations of incoherently reflected waves. *IEEE Trans. Antennas Propagat.*, **35**, 818–825.

Verlinde, J., D. Moisseev, N. Skaropoulos, S. H. Heijnen, W. F. V. Zwan, and H. Russchenberg: 2002, Spectral polarimetric measurements in the radar bright band. *Proc. Of URSI-F Open Symp. Propagat. and Remote Sens. (CDROM)*, Germany.

Yang, J., Y. Yamaguchi, H. Yamada, W.-M. Boerner, H. Mott, and Y. Peng: 2001, Development of target null theory. *IEEE Trans. Geosci. Remote Sens.*, **39**, 330–338.

Chapter 6

Ground clutter suppression using correlation analysis

Abstract: In this chapter two new clutter suppression techniques are introduced. In the first method polarimetric properties of the target and clutter are calculated per Doppler frequency cell and based on this information clutter is suppressed. As a result only Doppler resolution cells that are affected by ground clutter are suppressed and thus a more accurate Doppler notch filter can be constructed. The second technique is based on the use of two pairs of transmit and receive polarization states such that the measured clutter is linearly independent for these two settings. It is shown that this contrast enhancement method suppresses clutter better than the common polarimetric enhancement techniques, which are based on the optimization of the signal-to-clutter power ratio. In both methods we employ a correlation analysis of polarimetric measurands.

6.1 Introduction

Chapter 4 of this thesis introduced a new clutter suppression method which enables separation between ground clutter and atmospheric echoes in the case of similar Doppler spectra properties. On average this method can suppress 16 dB of ground clutter. However, in some atmospheric radar studies, the ground-clutter component of the measured signal exceed the weather echoes component with more than 20 dB. As a result in these cases the performance of the proposed suppression technique is not sufficient for the effective suppression of ground clutter. In order to solve this problem in this chapter we introduce two new ground clutter

suppression technique which allows us to improve the performance of polarimetric radars in the case of strong ground clutter.

The most common clutter suppression technique, Doppler clutter suppression, uses a notch filter to suppress signals with Doppler frequencies close to zero (Doviak and Zrnic 1993). However, the characteristics of this filter depend on the width of the ground clutter Doppler spectra and as a result should be adapted for every measurement. This adaptation of the filter is required since the ground clutter spectrum width depends on weather conditions, e.g. wind speed (Doviak and Zrnic 1993).

The other common clutter suppression approach is to use polarimetry to identify range bins affected by ground clutter, see for example (Zrnic and Ryzhkov 1999; Hagen 1997; Ryzhkov and Zrnic 1998; Yanovsky 1995; da Silveira and Holt 1997). However, the main disadvantage of this technique is that it rejects all range bins which are affected by the ground clutter and therefore may results in substantial loss of data.

In order to overcome the drawbacks of the polarimetric and Doppler ground clutter suppression techniques we shall combine them. Using a combination of polarimetry and Doppler information, we can accurately identify the range Doppler bins that are affected by clutter; as a result, only a few Doppler cells need to be suppressed instead of a complete range bin. In this way the proposed technique overcomes the disadvantages of the separately used Doppler and polarimetric clutter detection techniques.

Even though the proposed technique does reduce the loss of data it still can fail in cases where clutter and signal have similar Doppler properties. In these cases neither conventional Doppler processing techniques nor polarimetric clutter rejection methods nor the techniques which are discussed in chapters 4 will allow us to separate ground clutter from atmospheric echoes. The potential solution of this problem can be the use of a polarimetric contrast-enhancement method to improve the contrast between atmospheric objects and ground clutter.

In most of the cases the scattered radar waves from both targets and clutter are partially polarized. The common polarimetric contrast-enhancement technique used for such a case is to maximizing the signal-to-clutter power ratio. There are different approaches for the solving this optimization problem (Boerner et al. 1991; van Zyl et al. 1987; Swartz et al. 1988). However, the performances of these techniques are restricted by the randomness of the observed objects. This chapter introduces a new method to improve the contrast between objects even if they have completely random behavior.

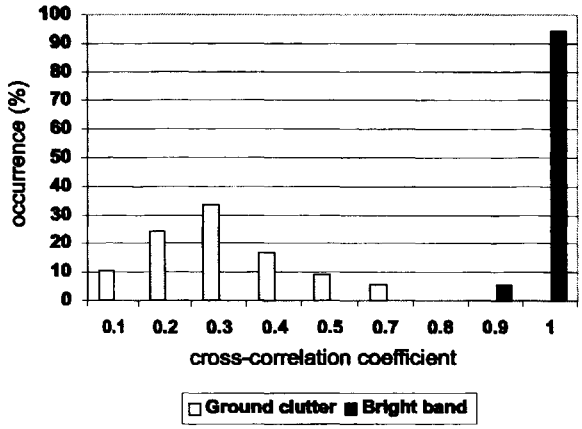

Figure 6.1: Histogram of the co-polar cross-correlation coefficient for ground clutter and bright band. Melting layer measurements were performed with the radar pointing to the zenith, the rain reflectivities for these measurements were smaller than 20 dBZ. Ground clutter was collected from both direct measurements of ground objects with the radar pointing to the to the ground and from measurements of ground clutter via sidelobes, when no atmospheric signal was present.

6.2 Co-polar coherency spectrum

Several methods for identifying ground clutter using polarimetric radars have been reported in the literature. Hagen (1997) discussed the use of Ldr, which is the ratio of cross-polar reflection to the co-polar one expressed in the linear $v-h$ polarization basis, for ground clutter detection. He noticed that for ground clutter, the Ldr is larger than for most meteorological echoes. However, for the melting layer of precipitation Ldr can be rather high and comparable to the one for ground clutter. Another approach described in (Ryzhkov and Zrnic 1998; Yanovsky 1995) uses a cross-correlation coefficient $\rho_{hv}(0)$ between horizontal and vertical co-polar returns. It was reported that for weather echoes, values of the modulus of the cross-correlation coefficient are usually larger than 0.7 but lower for areas contaminated with ground clutter. Note that even for the melting layer reflections, $|\rho_{hv}(0)|$ is larger than 0.9, as was presented by Bringi et al. (1991); this can also be clearly seen in Fig. 6.1. Therefore, the cross-correlation coefficient gives a high contrast between ground and weather echoes and is well suited for ground clutter identification.

In this section the theoretical formulation is introduced to expand the use of co-polar cross-correlation coefficient in the Doppler frequency domain. Using this formulation, we can detect the Doppler range bins affected by ground clutter.

6.2.1 Theoretical formulation

The cross-correlation coefficient $\rho_{hv}(0)$ of horizontal and vertical co-polar returns can be related to power and cross spectra (see Chapter 5):

$$\rho_{hv}(0) = \frac{C_{13}(0)}{\sqrt{C_{11}(0)C_{33}(0)}} = \tag{6.1}$$
$$= \frac{\int_{-\infty}^{+\infty} F_{13}(\omega)d\omega}{\sqrt{\int_{-\infty}^{+\infty} F_{11}(\omega)d\omega \cdot \int_{-\infty}^{+\infty} F_{33}(\omega)d\omega}}$$

Keeping in mind that $F_{ij}(\omega)d\omega$ gives the variance if $j = i$ and covariance if $j \neq i$ of the signal with the frequency ω, we can introduce the spectral co-polar correlation coefficient $w_{hv}(\omega)$

$$w_{hv}(\omega) = \frac{F_{13}(\omega)}{\sqrt{F_{11}(\omega) \cdot F_{33}(\omega)}} \tag{6.2}$$

The graph showing the modules of the co-polar correlation coefficient $w_{hv}(\omega)$ as a function of frequency is called the co-polar coherency spectrum, after Priestley (1981). The co-polar coherency spectrum $|w_{hv}(\omega)|$ shows the extent to which the hh and vv elements of the scattering matrix are linearly related. The use of this spectrum for ground-clutter suppression is discussed further in this chapter.

6.2.2 Estimation of co-polar coherency spectrum

In the case of real radar measurements we deal with the estimation of spectral characteristics from finite measurement samples. In this case the estimated Doppler spectrum $I_{ij}^N(\omega)$ is connected to the actual spectrum $F_{ij}(\omega)$ as follows (Doviak and Zrnic 1993; Priestley 1981):

$$I_{ij}^N(\omega) = \int_{-\frac{\pi}{T_s}}^{\frac{\pi}{T_s}} W_N(\theta - \omega)F_{ij}(\theta)d\theta \tag{6.3}$$

where T_s is the sampling interval ($\frac{\pi}{T_s}$ is the maximum unambiguous Doppler

frequency), $W_N(\omega)$ is the spectrum of the covariance lag window and N is the number of samples.

If $N \to \infty$, $W_N(\omega)$ will behave like a δ-function and this will lead to

$$\lim_{N\to\infty} I_{ij}^N(\omega) = \int_{-\frac{\pi}{T_s}}^{\frac{\pi}{T_s}} \lim_{N\to\infty} W_N(\theta-\omega)F_{ij}(\theta)d\theta = \tag{6.4}$$
$$= F_{ij}(\omega)$$

If N is so small that the spectral width of $W_N(\omega)$ is much larger than that of $F_{ij}(\omega)$ then

$$I_{ij}^N(\omega) = W_N(0)\int_{-\sigma_w}^{\sigma_w} F_{ij}(\theta)d\theta = \tag{6.5}$$
$$= W_N(0)\cdot C_{ij}(0)$$

Based on (6.4) and (6.5) we can conclude that if the number of samples is large enough, the spectrum width of the lag window will be much smaller than the width of $F_{ij}(\omega)$, and the estimated Doppler spectrum $I_{ij}^N(\omega)$ will converge to the actual spectrum $F_{ij}(\omega)$. Moreover, if N is so small that the spectrum width of $W_N(\omega)$ is much larger than the width of $F_{ij}(\omega)$, then the estimated $I_{ij}^N(\omega)$ spectrum will be proportional to $C_{ij}(0)$ and the estimated co-polar coherency spectrum will coincide with the modulus of the correlation coefficient $|\rho_{hv}(0)|$.

In the chapter 5 it was shown that polarimetric properties of radar targets are different for different Doppler cells. As a result also polarimetric properties of targets in time and Doppler domains will be different. Therefore the acquired statistics of polarimetric properties of the weather echoes and ground clutter cannot be used directly to identify Doppler cells affected by ground clutter.

In order to estimate how large are differences between polarimetric properties of radar targets in Doppler and in time domains we should consider both the degree of Doppler polarimetric coupling and the polarization entropy. As we have shown in chapter 5 the degree of Doppler polarimetric coupling for atmospheric echoes is low except the melting layer region where W_σ is about 0.25. This shows us that the polarimetric properties of the melting layer vary have strong dependence on Doppler velocity. However, if we will consider the values of entropy, which are given in chapter 5, or values of the degree of polarization, as discussed in chapter 4,

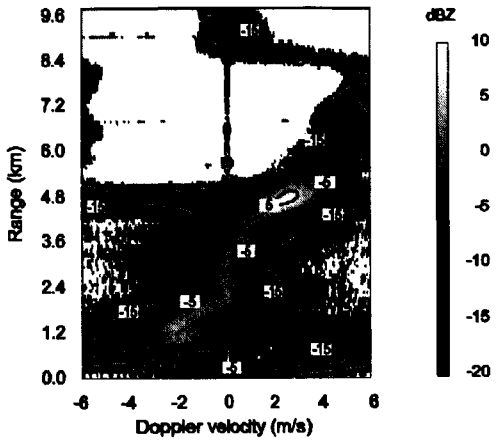

Figure 6.2: Doppler spectrum of the precipitation event (HH-polarization). High reflectivity at 4.8 km corresponds to the melting layer. Reflections below the melting layer come from rain. Ice crystals falling out of the cloud cause reflections above the melting layer.

we will see that this variations in polarization properties are small in comparison to total signal and thus can be neglected. It can be shown that the signal in the varying part is 18 dB lower than the total signal.

Ground clutter on the other hand has high values for both the degree of Doppler polarimetric coupling and the entropy. As a result the changes in polarization properties as a function of Doppler velocity cannot be neglected. But in most cases of atmospheric remote sensing ground clutter has a narrow Doppler spectrum and, according to (6.5) $|w_{hv}(\omega)|$, is roughly equal to $\rho_{hv}(0)$ and thus, the co-polar coherency spectrum can be used to identify areas of the Doppler spectrum, which are affected by clutter.

6.2.3 Signal-to-noise problem

The estimation of the spectral correlation coefficient for weak targets is influenced by the noise; as a result the estimated correlation coefficient $\widetilde{w_{hv}}(\omega)$ is related to

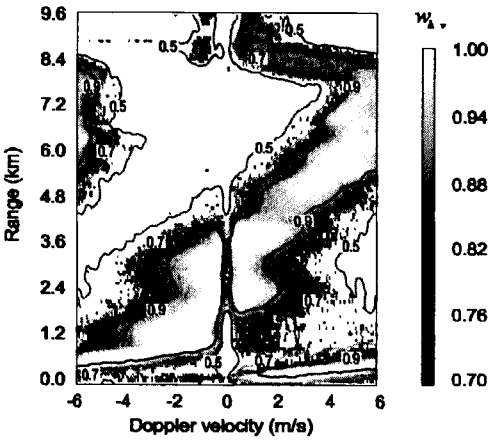

Figure 6.3: Co-polar coherency spectrum $|w_{hv}(\omega)|$. The contours represent $|w_{hv}(\omega)|$ values between 0.5 and 1. The gray scaling shows values of between 0.7 and 1. As expected the values of $|w_{hv}(\omega)|$ for weather echoes are larger than 0.7 and for areas affected by ground clutter they are less than 0.7.

the actual correlation coefficient $w_{hv}(\omega)$ as (Illingworth and Caylor 1991):

$$\widetilde{w_{hv}}(\omega) = \frac{w_{hv}(\omega)}{\sqrt{(1+\frac{1}{SNR})(1+\frac{Zdr}{SNR})}} \tag{6.6}$$

This effect can be reduced rather efficiently by subtracting the mean noise power from $F_{11}(\omega)$ and $F_{33}(\omega)$.

6.3 Clutter identification and suppression

To test this new clutter suppression technique, we measured the slant profile of precipitation. The elevation angle of the radar was 20 degrees.

The scattering matrix measurements are carried out in three consecutive sweeps of alternating linear polarizations on the receiving and transmitting channels; this cycle takes 3.75 ms. For this particular example about one minute of data is collected. Prior to the Doppler processing, averaged values of the scattering-matrix elements are subtracted from the corresponding time series of scattering-matrix elements. This processing is applied to the complete data set. This subtraction is

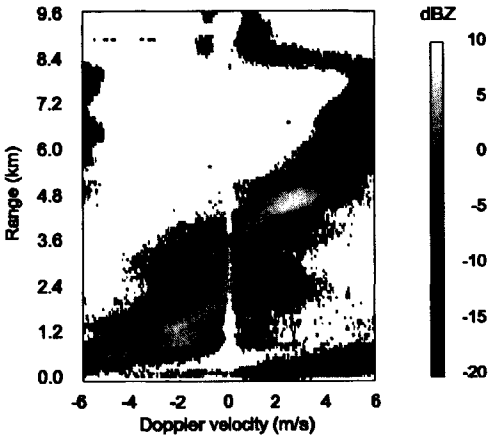

Figure 6.4: Doppler spectrum of the precipitation event after clutter suppression. The reflections that have $|w_{hv}(\omega)|$ values below 0.7 are clipped away. This new clutter suppression method shows good performance. It is interesting to note that this suppression has also removed spectral leakage like signal in the area of the melting layer. This signal corresponds to transient effects which take place in the melting layer as argued in (Verlinde et al. 2002)

identical to suppression of the stable ground clutter, which is discussed in chapter 4.

To obtain Doppler spectra we used 256 sweeps. A total of 40 spectra is obtained for each element of the scattering matrix. Based on these spectra the spectral covariance matrix $\mathbf{F}(\omega)$ is obtained and the co-polar coherency spectrum is estimated. In Fig. 6.2 the Doppler power spectrum for hh polarization (the element of the spectral covariance matrix) is shown. Fig. 6.3 presents the modulus of the co-polar coherency spectrum $w_{hv}(\omega)$. A clear contrast can be seen between ground clutter and atmospheric targets. Therefore, in order to suppress the ground clutter, we have suppressed all areas that have a cross-correlation coefficient below 0.7. The result is shown in Fig. 6.4. As it can clearly be seen in Fig. 6.4 this clutter suppression shows a good performance in the areas where target signal is mixed with clutter. However, we can also see that as a result of this processing also leakage like signal at the height 4.5 km is suppressed, it is argued that this signal corresponds to reflections from rocking hydrometeors in the melting layer (Verlinde et al. 2002). But as it was explained above this suppressed signal is much

weaker than the total signal, thus the application of this technique is preferable if strong clutter with relatively narrow spectrum to be suppressed.

6.4 Zero-correlation method

Now let us consider the situation when Doppler properties of a target and clutter are similar. In this case if we want to improve the signal-to-clutter ratio without substantial loss of data we can use a polarimetric contrast enhancement technique. The performance of the conventional polarimetric enhancement techniques, however, is restricted by the randomness of the targets, hence a new approach should be sought. As we have seen in previous sections, the co-polar correlation coefficients for ground clutter and atmospheric echoes are different. So the logical question that arises is whether we can find a measurement setup in which the observed cross-correlations between two measurements for ground clutter is zero and for atmospheric objects different from zero. This new approach we call the *zero-correlation method.*

The zero-correlation method can be formulated as follows: it is necessary to find two pairs of antenna polarization states $\vec{e}_r^{\,1}, \vec{e}_t^{\,1}$ and $\vec{e}_r^{\,2}, \vec{e}_t^{\,2}$ such that the corresponding measured complex voltages b_1^c, b_2^c of the unwanted target are uncorrelated with each other. The measured complex voltages b_1^c, b_2^c are related to the time-dependent clutter-scattering matrix $\mathbf{S}_c(t)$ as

$$\begin{aligned} b_1^c(t) &= \left(\vec{e}_r^{\,1}\right)^T \mathbf{S}_c(t)\vec{e}_t^{\,1} \\ b_2^c(t) &= \left(\vec{e}_r^{\,2}\right)^T \mathbf{S}_c(t)\vec{e}_t^{\,2} \end{aligned} \tag{6.7}$$

and the covariance between these voltages is

$$\left\langle b_1^c(t) b_2^{c*}(t) \right\rangle = 0 \tag{6.8}$$

The other requirement for this method is that the measured voltages of the wanted target must have some degree of linear dependency:

$$\left\langle b_1^t(t) b_2^{t*}(t) \right\rangle \neq 0 \tag{6.9}$$

The appropriate antenna polarization states can be derived from the coherent target decomposition. Using coherent decomposition of the covariance matrix $\mathbf{C}_4$ as presented in (Cloude and Pottier 1996; Unal and Ligthart 1998), one can

decompose the time-dependent scattering matrix $\mathbf{S}(t)$ of a radar target into k stable linearly independent radar targets as:

$$\mathbf{S}(t) = \sum_{i=1}^{k} \gamma_i(t)\mathbf{S}_i \text{ or} \tag{6.10}$$

$$\overrightarrow{s}(t) = \sum_{i=1}^{k} \gamma_i(t)\overrightarrow{s}_i = \sum_{i=1}^{k} \gamma_i(t)\overrightarrow{w_{4i}} \tag{6.11}$$

where k is the rank of $\mathbf{C}_4$, λ_i is the i-th eigenvalue of $\mathbf{C}_4$, $\overrightarrow{w_{4i}} = \overrightarrow{e}_r^* \otimes \overrightarrow{e}_t^* = \begin{bmatrix} e_{r1}e_{t1} & e_{r1}e_{t2} & e_{r2}e_{t1} & e_{r2}e_{t2} \end{bmatrix}^{*T}$ is the corresponding eigenvector. Since this coherent decomposition represents a random target as a set of polarimetrically stable targets, the only time-dependent variables in (6.10) are the coefficient $\gamma_i(t)$. To satisfy linear independence of these characteristic targets the covariance $\langle \gamma_i(t)\gamma_j^*(t) \rangle$ should be zero for all i, j such that $i \neq j$.

From (6.10) it follows that the complex voltages b_1^c, b_2^c, in order to satisfy condition (6.8) should be:

$$\begin{aligned} b_1^c(t) &= \gamma_1(t) \\ b_2^c(t) &= \gamma_2(t) \end{aligned} \tag{6.12}$$

then the covariance between them is:

$$\langle b_1^c(t)b_2^{c*}(t) \rangle = \langle \gamma_1(t)\gamma_2^*(t) \rangle = 0 \tag{6.13}$$

Thus, the sought antenna polarization states $\overrightarrow{e}_r^1, \overrightarrow{e}_t^1$ and $\overrightarrow{e}_r^2, \overrightarrow{e}_t^2$ are directly connected to the eigenvectors of the clutter covariance matrix $\mathbf{C}_c$. In order to satisfy condition (6.9) the target and clutter should be polarimetrically different, meaning that the target and the clutter eigenvectors should not be collinear. In this case even if $\langle b_1^t(t)b_2^{t*}(t) \rangle$ is much smaller than the averaged power of any element of the scattering matrix, the contrast between the target and the clutter is very high, since $\langle b_1^c(t)b_2^{c*}(t) \rangle$ is zero.

6.5 Statistical model

The proposed method will achieve the best performance, i.e. zero correlation between two polarization measurements of ground clutter, only if averaging over infinite number of samples will be performed. In reality, however, this requirement is not fulfilled and thus we should study the sensitivity of this enhancement technique to the number of averages.

It is common to model the response of a range resolution cell by the multivariate complex Gaussian distribution (Goodman 1963). This model is based on three main assumptions:

The resolution cell consists of many individual scatterers and no single one of them dominate the others. To fulfill this assumption in our case we subtract the mean signals from all elements of the scattering matrix, as a result the reflections from large targets, such as buildings, are suppressed.

The phase of every individual scatterer must be uniformly distributed between $-\pi$ and π.

The phases of all scatterers must be uncorrelated between each other.

If these three assumptions hold then we can write a probability density function of the scattering matrix , **S**, as follows (Lee et al. 1994):

$$pdf(\vec{s}) = \frac{1}{\pi^3 |\mathbf{C}|} \exp\left(-\vec{s}^{+}\mathbf{C}^{-1}\vec{s}\right) \tag{6.14}$$

where **C** is the covariance matrix and $\vec{s} = vec(\mathbf{S})$.

By further developing the equation (6.14) and introducing correlation coefficient, ρ:

$$\rho = \frac{\left|\frac{1}{n}\sum_{k=1}^{n} s_i(k)s_j^*(k)\right|}{\sqrt{E[|s_i|^2]E[|s_j|^2]}} \tag{6.15}$$

where n is number of averages taken for the estimation of the covariance, $s_i(k)$ is the $i-th$ element of the target scattering vector $\vec{s}$ and $E[|s_i|^2]$ represents the mathematical expectation of the power of this element, we can obtain probability density function of the correlation coefficient (Lee et al. 1994):

$$pdf(\rho) = \frac{4n^{n+1}\rho^n}{\Gamma(n)(1-|\rho_c|^2)} I_o\left(\frac{2|\rho_c|n\rho}{1-|\rho_c|^2}\right) K_{n-1}\left(\frac{2n\rho}{1-|\rho_c|^2}\right) \tag{6.16}$$

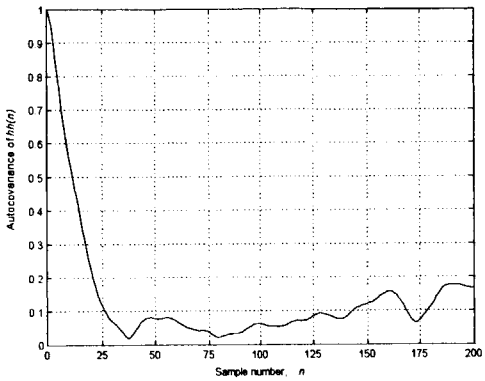

Figure 6.5: Autocovariance function of ground clutter. It can be seen that the correlation time is about 15 samples. Every sample is 7.5 ms.

where ρ_c is the expectation value of the correlation coefficient, in our case it is 0, $I_o(\ )$ and $K_{n-1}\ ()$ are modified Bessel functions.

Based on the formulation (6.16) we can also estimate the dependence of the estimated correlation coefficient, $\langle\rho\rangle$, and the variance, σ_ρ, of this estimate on number of averages as:

$$\langle\rho\rangle = \int \rho \cdot pdf(\rho)d\rho \tag{6.17}$$

$$\langle\sigma_\rho\rangle = \int \rho^2 \cdot pdf(\rho)d\rho$$

To illustrate the presented model we have used the measurements of the park area "Delftse Hout" as presented in chapter 5. Prior to this comparison we should estimate a number of independent samples which were taken for a calculation of the correlation coefficient. In Fig. 6.5 we can see the autocovariance function of the co-polar signal from one resolution cell. It can be seen that this signal is correlated over 15 samples, and thus the effective number of independent samples is 15 times smaller than number of samples used to estimate the correlation.

We have compared this statistical model to the measurements of "Delftse hout". These measurements contain more than 70000 samples. Based on all these samples we have estimated the target covariance matrix and the eigenvectors of this matrix. In order to obtain a distribution of the estimated correlation coefficients we have

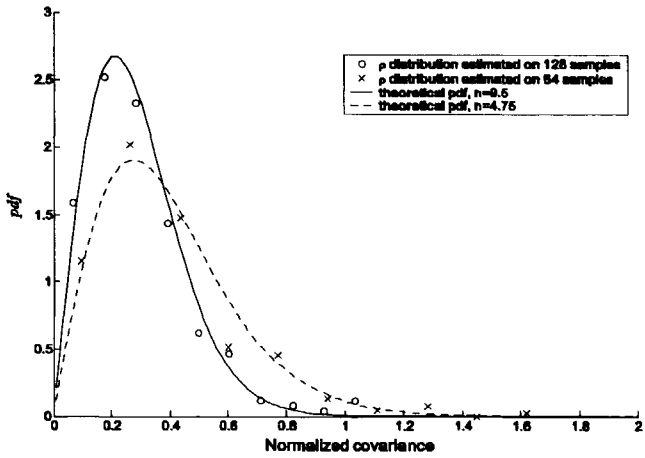

Figure 6.6: Probability density function of the correlation coefficient ρ. The mathematical expectation of the correlation coefficient is 0. Crosses represent the histogram of the measured correlation coefficients if averaged over 64 samples. Circles represent the histogram of the measured correlation coefficient if averaged over 128 samples. It can be seen that due to correlation between samples the effective averaging values are 4.75 and 9.5 respectively. The corresponding pdf are given by dashed and solid lines.

applied the eigenvectors on calculated covariance matrices as given in (6.7), these matrices are estimated over 64 and 128 samples. The result of this calculations shown in Fig. 6.6. It can be seen that the measured distributions fit well to the modeled density functions. Moreover, as it was expected the effective number of averages is smaller than the number of samples, n, taken for the estimation of the covariance matrices, and approximately coincides with the expected value of $n/15$. Also we have calculated the dependence of the calculated correlation coefficient and the variance of this estimation on the number of independent averages. In Fig. 6.7 the results of these calculations are plotted, it can be seen that if we would use more than 80 independent samples for the zero-correlation method we will suppress clutter by 10 dB. It should be noted that we do not include the improvement of the signal-to-clutter ratio by the stable clutter suppression, which is presented in chapter 4, and also applied here prior to the zero-correlation processing. The combined clutter suppresion will be about 23 dB.

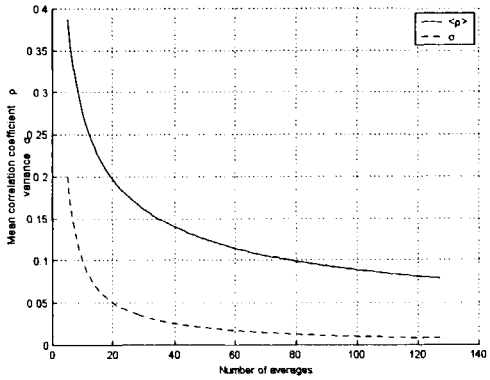

Figure 6.7: The predicted behavior of the estimated correlation coefficient and the variance of the estimate as a function of number of averages.

6.6 Comparison between zero-correlation method and polarization matched filter (PMF)

To compare the performance of zero-correlation method and a standard polarimetric optimization technique, we have used a complete range profile of the "Delftse hout" measurements. As an example of the standard contrast enhancement technique we have used the covariance matrix optimization procedure, PMF, (Swartz et al. 1988; Mott 1995). We have used over 70000 samples to estimate the covariance matrix of the target and to estimate the optimum polarization states. These calculation were performed for every range cell. Then PMF and the zero-correlation methods were applied on target covariance matrices, which were estimated over 1000 samples. In Fig. 6.8 the results of this processing is given. We can see that the performance of PMF is poor that can be explained by highly depolarizing nature of ground clutter. The zero-correlation method, on the other hand, shows rather good results, with the average clutter suppression of about 8 dB.

Based on these results we can conclude that the proposed zero-correlation method is well suited for the cases of highly depolarizing targets. Its performance mainly depends on the number of independent samples taken for the estimation of zero-correlation and does not depend on depolarization properties of targets.

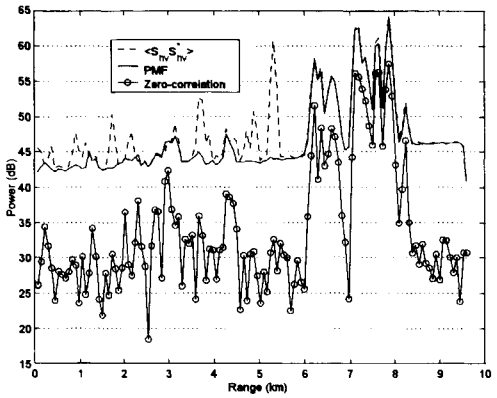

Figure 6.8: Comparison between zero correlation method and the covariance matrix optimum solution, PMF. This is the measurement of the park area "Delftse Hout", the measurement setup is described in chapter 5. The correlation is estimated on 1000 measurement samples, approximately 60 independent samples.

6.7 Conclusions and recommendations

In this chapter two new ground-clutter suppression technique were presented. The first one uses both Doppler and polarimetric information to identify Doppler cells affected by clutter. This proposed method has all the advantages of the use of Doppler clutter suppression without the problem of having to select the characteristics of the notch filter for every measurement. Also this new method has less effect on the measurements of the weather echoes than the common Doppler clutter rejection technique. Based on the above we propose to use this new clutter suppression method as the successor of the conventional Doppler clutter suppression method.

Although this new clutter suppression procedure has solved most of the problems of the conventional Doppler and polarimetric suppression methods it still suffers from the common pitfall, namely suppression of the useful data. When the Doppler spectra of the weather echoes and ground clutter overlaps the proposed method will not only suppress clutter but also some part of the atmospheric signal.

To overcome this problem we have proposed the zero-correlation method. It was shown that this method do not depend on depolarization properties of radar targets and can suppress clutter very efficiently. As a result it can be used to

obtain target information even if the signal-to-clutter ratio is extremely low.

However, the optimal performance of the proposed method as well as that of any polarimetric contrast-enhancement technique requires accurate knowledge of the polarimetric properties of target and clutter. Thus, accurate modeling as well as development of appropriate adaptive techniques is crucial for the success of polarimetric clutter-suppression techniques. Also the use of whitening techniques to increase number of independent samples can be very useful for the proposed technique, and should the topic for the further studies.

References

Boerner, W.-M., W.-L. Yan, A.-Q. Xi, and Y. Yamaguchi: 1991, On the basic principles of radar polarimetry: The target characteristic polarization state theory of Kennaugh, Huynen's polarization fork concept, and its extension to the partially polarized case. *Proc. IEEE*, **79**, 1538–1550.

Bringi, V. N., V. Chandrasekar, P. Meischner, J. Hubbert, and Y. Golestani: 1991, Polarimetric radar signatures of precipitation at S- and C-bands. *IEE Proc. F. Commun. Radar Signal Process.*, **138**, 109–119.

Cloude, S. R. and E. Pottier: 1996, A review of target decomposition theorems in radar polarimetry. *IEEE Trans. Geosci. Remote Sens.*, **34**, 498–518.

da Silveira, R. B. and A. R. Holt: 1997, A neural network application to discriminate between clutter and precipitation using polarization information as feature space. *Proc. Of 28th Conf. Radar Meteorol.*, Austin, TX, 57–58.

Doviak, R. J. and D. S. Zrnic: 1993, *Doppler Radar and Weather Observations*. Academic Press, Inc., London.

Goodman, N. R.: 1963, Statistical analysis based on a certain complex Gaussian distribution (an introduction). *Ann. Mathemat. Statist.*, **34**, 152–177.

Hagen, M.: 1997, Identification of ground clutter by polarimetric radar. *Proc. Of 28th Conf. On Radar Meteorology*, Amer. Meteor. Soc., Austin, Texas, 67–68.

Illingworth, A. J. and I. J. Caylor: 1991, Co-polar correlation measurements of precipitation. *Proc. Of 25th Conference on Radar Meteorology*, American Meteorological Society, Paris, France, 650–653.

Lee, J.-S., K. W. Hoppel, S. A. Mango, and A. R. Miller: 1994, Intensity and phase statistics of multilook polarimetric and interferometric SAR imagery. *IEEE Trans. Geosci. Remote Sens.*, **32**, 1017–1028.

Mott, H.: 1995, Polarimetric contrast optimization. *IGARSS*, 2011–2013.

Priestley, M. B.: 1981, *Spectral Analysis and Time Series*. Academic Press, London.

Ryzhkov, A. V. and D. S. Zrnic: 1998, Polarimetric rainfal estimation in the presence of anomalous propagation. *J. Atmos. Oceanic Technol.*, **15**, 1320–1330.

Swartz, A. A., H. A. Yueh, J. A. Kong, L. M. Novak, and R. T. Shin: 1988, Optimal polarizations for achieving maximum contrast in radar images. *J. Geophys. Res.*, **93**, 15252–15260.

Unal, C. M. H. and L. Ligthart: 1998, Decomposition theorems applied to random and stationary radar targets. *PIER*, **18**, 45–66.

van Zyl, J. J., C. H. Papas, and C. Elachi: 1987, On the optimum polarizations of incoherently reflected waves. *IEEE Trans. Antennas Propagat.*, **35**, 818–825.

Verlinde, J., D. Moisseev, N. Skaropoulos, S. H. Heijnen, W. F. V. Zwan, and H. Russchenberg: 2002, Spectral polarimetric measurements in the radar bright band. *Proc. Of URSI-F Open Symp. Propagat. and Remote Sens. (CDROM)*, Germany.

Yanovsky, F. J.: 1995, Use of signal polarization properties - the way to improvement of weather radar's parameters. *Proc. Of the Third International Workshop on Radar Polarimetry*, Nantes, France, 578–589.

Zrnic, D. S. and A. V. Ryzhkov: 1999, Polarimetry for weather surveillance radars. *Bull. Amer. Meteor. Soc.*, **80**, 389–406.

Chapter 7

Conclusions and discussion

7.1 Contributions of this research

7.1.1 Polarimetric radar calibration

The motivation for the study presented in chapter 2 is the need for an accurate description of the effects a radar system has on polarimetric measurements of distributed targets. This study showed that the commonly used method to calibrate polarimetric measurements of extended targets, the point-target calibration approach, does not give reliable results. The effect of this can clearly be observed in the measurements of low depolarizing targets, such as precipitation.

It was shown that due to imperfection of the antennas and due to the spatial structure of radar targets the resulting polarization cannot be regarded as fully polarized. For the case of atmospheric measurements with DARR, the antenna polarization states have a degree of polarization of 0.997, or, in other words, 0.3% of the transmitted wave is unpolarized. It may seem a small number, but since there is a need for more precise polarimetric measurements of meteorological targets, this effect must be taken into account. By considering this depolarizing effect as a part of the antenna system we were able to improve the sensitivity of the radar for cross-polar measurements by 7 dB on average.

7.1.2 Polarimetric formulation

The other important issue which was considered in this thesis is the more complete polarimetric formulation for the description of depolarizing radar targets. This

study is divided into two main parts: one where optimum polarization states for depolarizing targets are determined and one where the statistical and polarimetric target properties are combined.

In the first part we considered common polarimetric formulations, i.e. Mueller matrix and covariance matrix approaches. It was shown that even though it is hard sometimes to realize the optimum polarization states for the covariance matrix method, it is still more advantageous to use this method for solving the polarimetric optimization problem than the Mueller matrix one. This study is given in chapter 3.

In chapter 5 the combination of Doppler and polarimetric target information for a better target description is studied. It was shown that by combining these two information sources one can obtain a better polarimetric formulation. Moreover this formulation includes the common polarimetric formalism as the limiting case. It was also shown that both Doppler and polarimetric properties of targets are interrelated, and thus by means of Doppler processing polarimetric properties of targets can be changed, as discussed in chapter 4. It was also indicated that the reverse effect should be expected as well: polarimetric processing can affect Doppler signatures of targets. Another important conclusion which arose from the new Doppler polarimetric formulation is that if a more complete radar target description is required, all elements of the scattering matrix should be measured simultaneously.

7.1.3 Target enhancement

In this thesis four new target enhancement techniques are proposed. In most of the cases they are complimentary and can be used for different circumstances of radar sounding. The two first techniques are mainly dedicated to suppressing ground clutter in atmospheric studies. The first one of this group gives on average 16 dB of ground-clutter suppression and does not affect the weather echoes, and is presented in chapter 4. This technique is mainly limited to the cases of a relatively high signal-to-clutter ratio.

In cases where ground clutter is much stronger than the atmospheric signal it is useful to apply another technique, which is shown in chapter 6. In this chapter we propose the use of polarimetry to identify Doppler cells affected by ground clutter. In this case a notch filter that is much more accurate than the traditional one can be constructed, which will reduce the effect of the processing on atmospheric targets. However, if ground clutter and weather echoes have very similar Doppler

properties, i.e. they occupy the same area in the Doppler spectrum, this processing will result in suppression of the atmospheric signal.

The other two proposed target enhancement methods are more general and can be applied for different radar sounding circumstances. The first one in this group is the generalized method for target enhancement which originates from the traditional covariance matrix approach and from radar Doppler polarimetric formulation. The main principe of this method arises from the radar Doppler polarimetric formulation. It was also shown in chapter 5 that Doppler polarimetry allows for the representation of radar targets as a set of elementary targets defined for every Doppler frequency resolution cell. It also shown that in the case of depolarizing radar targets these elementary targets have different polarimetric properties. And hence it is more efficient to apply the polarimetric optimization techniques to every Doppler resolution cell, as shown in chapter 5. Moreover, this new formulation led to the development of the new voltage equation for optimum reception, which can be interpreted as the expression for the signal at the output of the linear predictive filter.

The other contrast enhancement technique, which is given in chapter 6, enables very efficient enhancement of targets contrast even in the case where targets are strongly depolarizing. This novel method can be useful for many radar remote sensing applications. It is shown that this technique can potentially provide a very high clutter suppression level and is not limited by depolarization properties of targets as the standard polarimetric contrast techniques.

7.2 Recommendations for future studies

In this Ph.D. thesis a statistical approach was used to describe polarimetric properties of targets. It was shown that this method gives a better description of radar targets. However, the spectral and time series analysis which was adopted in this thesis does not fully use the developed statistical apparatus for describing random processes. The reason behind it are the measurement limitations. The most severe one is that the elements of the scattering matrix are not measured simultaneously and thus only second-order statistics can be used for describing the polarimetric properties of targets. So for more complete description of the behavior a new radar system should be developed which is capable of measuring all elements of the scattering matrix simultaneously. However, it was shown that in the general case the transmit and receive polarization states of a radar system are partially polarized and thus the use of the second-order statistics is necessary to compensate

for the effect of the antenna on the polarimetric measurements. And thus in the case where the investigated targets are distributed targets with a small degree of depolarization, only averaged polarimetric parameters can be used. This conclusion leads to one more recommendation for future radar systems: if such systems are to investigate distributed lightly depolarizing targets, such as meteorological objects, new advanced antenna systems should be developed. These new antenna systems should have either low coupling (<-40 dB) between polarization channels or similar antenna patterns for co- and cross-polar channels.

As was shown, polarimetry can play a very important role in clutter suppression. However, the main step which separates it from being used in real-time applications is the absence of an appropriate adaptive algorithm for evaluating the polarimetric properties of targets and clutter.

These recommendations could be the basis of a new generation radar systems which are able to operate in heavy clutter environments.

Atmospheric studies can also benefit from a further research in the field of Doppler polarimetry. The degree of Doppler polarimetric coupling which was introduced in this thesis can be a convenient tool for a characterization of atmospheric echoes. As we have discussed different polarimetric measures have different Doppler properties. Thus by combining Doppler and polarimetric observations we may be able to decouple which part of a Doppler spectrum corresponds to the fall velocities of hydrometeors and which part is related to their shape and orientation changes. This study would be of great importance to hydrology, severe weather observations and cloud physics.

Samenvatting

Het belang van polarimetrische metingen binnen het radaronderzoek groeit daar op deze wijze meer informatie over het meetobject kan worden verkregen. Met gepolariseerde metingen kunnen niet alleen de microfysische eigenschappen van radarobjecten beter bepaald worden (zoals vorm en oriëntatie), ze geven ook meer informatie over de temporele eigenschappen van de radarobjecten en over het voortplantingsmedium. Radarpolarimetrie kan ook gebruikt worden om de kwaliteit van radarmetingen te verbeteren. Het kan bijvoorbeeld de signaalruisverhouding verbeteren en het contrast tussen object en achtergrond vergroten.

De hoofdvragen die in dit werk worden bestudeerd zijn de polarimetrische calibratie van radars en het gebruik van Dopplerpolarimetrie voor het karakteriseren van doelen en het verhogen van contrasten.

List of symbols and acronyms

List of acronyms

2D	Two-Dimensional
CLARA	CLouds and RAdiation measurement campaign
DARR	Delft Atmospheric Research Radar
FFT	Fast Fourier Transform
FM-CW	Frequency Modulated Continuos Wave
Ldr	Linear depolarization ratio
PDF	Probability Density Function
PMF	Polarization Match Filter
RCS	Radar Cross Section
SNR	Signal-to-Noise Ratio
Zdr	Differential reflectivity

List of symbols

$\mathbf{A}$	Kronecker expansion matrix
b_1, b_2	Bilinear forms of target scattering matrix
$\mathbf{C}$	Target covariance matrix
$\mathbf{C}_4$	4x4 target covariance matrix for general scattering case
$\mathbf{C}_3$	3x3 target covariance matrix for backscattering monostatic scattering case
$\mathbf{C}_m$	Measured uncalibrated covariance matrix
$\mathbf{C}_s$	Calibrated covariance matrix
$\mathbf{D}$	Combined antenna distortion matrix for Point target measurement case
$\widehat{\mathbf{D}}$	Combined antenna distortion matrix for distributed target measurement case
$\overrightarrow{e}_t$	Transmitting antenna polarization state
$\mathbf{F}$	Spectral target covariance matrix
$[f_t(\theta,\phi)]$, $[f_r(\theta,\phi)]$	Transmit (or receive) distortion matrix, elements of which are antenna gain patterns for different polarization states
f	Co-polar channel imbalance
$\mathbf{G}$	Graves power matrix
$\overrightarrow{g}$	Stokes vector
H_s	Target entropy
$\overrightarrow{h}$	Receive antenna polarization state
I^N	Periodogram spectrum estimation
$\mathbf{J}$	Wave coherency matrix
$\mathbf{K}_4$	Kennaugh matrix
$\overrightarrow{k}$	Target scattering vector

L	Lagrangian
$\mathbf{M}$	Measured uncalibrated scattering matrix
$\mathbf{M}_4$	Mueller matrix
p	Degree of polarization
$\mathbf{R}$	Receive distortion matrix
R	Autocovariance function
$\mathbf{S}$	Calibrated target scattering matrix
$\overrightarrow{s}$	Target scattering vector
$\mathbf{T}$	Transmit distortion matrix
v	Receive voltage (voltage equation)
$\overrightarrow{w}_3$ ($\overrightarrow{w}_4$)	Eigenvector of target covariance matrix
W_N	Spectrum of a covariance lag window
W_σ	Degree of Doppler polarimetric coupling
w_{hv}	Co-polar coherency spectrum
δ_1, δ_2	Radar polarization channels coupling terms
θ	Azimuth angle
$\overrightarrow{\vartheta}_3$	Spectral polarization state vector
λ_i	Eigenvalue of target covariance matrix
ρ_a	Antenna polarization isolation in boresight direction
$\widetilde{\rho}_a$	Complete antenna polarization isolation
ρ_{hv}	Co-polar correlation coefficient
ρ_{xh}, ρ_{xv}	Co-cross-polar correlation coefficient
σ_{ij}	Doppler width for different polarization states
τ	Time lag
ϕ	Elevation angle

Curriculum vitae

Ph.D.	1997-2001	International Research Centre for Telecommunication-transmission and Radar, Department of Information Technology and Systems, Delft University of Technology
M.Sc.	1995-1997	Department of Aerodynamics and Space Research, Moscow Institute of Physics and Technology
B.Sc.	1991-1995	Moscow Institute of Physics and Technology

Professional Experience

Nov. 2001-present	Postdoctoral Fellow, Department of Civil Engineering and Geosciences, Delft University of Technology,
1997-2001	Research Assistant, IRCTR, Department of Information Technology and Systems, Delft University of Technology
1996-1997	Student Research Assistant, Center for Program Studies, Russian Academy of Science, Moscow

Awards

2001 Conference travel grant awarded to 10 best student papers, IEEE Radar Conference, Atlanta, May 1-3, 2001
Granted for the work entitled: *"Target-to-Clutter Contrast Enhancement Using Radar Doppler Polarimetry"*

2000 1st Prize in Young Scientist Contest, MIKON, Wroclaw, Poland, May 22-24, 2000
Awarded for the work entitled *"Doppler polarimetric ground clutter identification and suppression for atmospheric radars based on co-polar correlation"*

Research Interests

Radar polarimetry, radar signal processing, SAR interferometry, and their application to atmospheric studies

List of Publications

Journal Articles

Moisseev, D. N., C. M. H. Unal, H. W. J. Russchenberg and L. P. Ligthart: 2000, The influence of the antenna pattern on cross polarization measurements of atmospheric targets. *Phys. Chem. Earth (B)*, **25**, 843-848.

Moisseev, D. N., C. M. H. Unal, H. W. J. Russchenberg and L. P. Ligthart: 2002, A new method to separate ground clutter and atmospheric reflections in the case of similar Doppler velocities. *IEEE Trans. Geosci. Remote Sens*, **40**, 239-246.

Moisseev, D. N., C. M. H. Unal, H. W. J. Russchenberg and L. P. Ligthart: 2002, Doppler polarimetric ground clutter identification and suppression for atmospheric radars based on co-polar correlation. To be published in *J. Telecom. Inform. Technol.*

Moisseev, D. N., C. M. H. Unal, H. W. J. Russchenberg and L. P. Ligthart: 2002, Improved polarimetric calibration for atmospheric radars. To be published in *J. Atmos. Oceanic Technol.*

Moisseev, D. N., C. M. H. Unal, H. W. J. Russchenberg and L. P. Ligthart: Radar Doppler polarimetry. Submitted to *IEEE Trans. Geosci. Remote Sens.*

Moisseev, D. N., C. M. H. Unal, H. W. J. Russchenberg and L. P. Ligthart: Zero-correlation approach for polarimetric target enhancement. In preparation for *IEEE Trans. Geosci. Remote Sens.*

Conference Articles

Moisseev, D. N., C. M. H. Unal, H. W. J. Russchenberg and L. P. Ligthart: 2002, Characterization of depolarizing behavior of radar targets; introduction of

the degree of Doppler polarimetric coupling. *Proc. URSI General Assembly*, Maastricht, The Netherlands.

Moisseev, D. N., C. M. H. Unal, S.H. Heijnen, H. W. J. Russchenberg and L. P. Ligthart: 2002, Realizability of optimum polarization states provided by the target covariance matrix. *Proc. URSI General Assembly*, Maastricht, The Netherlands.

Verlinde, J., D. Moisseev, N. Skaropoulos, S. H. Heijnen, W. F. v.d. Zwan and H.W.J. Russchenberg: 2002, Spectral polarimetric measurements in mixed phased cloud. *Proc. 11th Conference on Cloud Physics*, Ogden, UT

Moisseev, D. N., C. M. H. Unal, H. W. J. Russchenberg and L. P. Ligthart: 2002, Polarimetric contrast enhancement for highly depolarizing targets. *Proc. URSI-F Meeting (CDROM)*, Germany.

Moisseev, D. N., C. M. H. Unal, H. W. J. Russchenberg and L. P. Ligthart: 2002, Linear predictive approach for polarimetric contrast enhancement of radar targets. *Proc. URSI-F Meeting (CDROM)*, Germany.

Verlinde, J., D. Moisseev, N. Skaropoulos, S. H. Heijnen, W. F. v.d. Zwan and H.W.J. Russchenberg: 2002, Spectral polarimetric Measurements in the Radar Bright Band. *Proc. URSI-F Meeting (CDROM)*, Germany.

Unal C.M.H., D. N. Moisseev: 2002, Improved Doppler processing for polarimetric radars: application to precipitation measurements. *Proc. URSI-F Meeting (CDROM)*, Germany.

Moisseev, D. N., C. M. H. Unal, H. W. J. Russchenberg and L. P. Ligthart: 2001, Improvement of polarimetric radar calibration for atmospheric radars. *Proc. 30th Conf. on Radar Meteorology*, Munich, Germany, Amer. Meteor. Soc., 26-28.

Unal, Christine, Dmitri Moisseev, Herman Russchenberg and Leo Ligthart: 2001, Radar Doppler polarimetry applied to precipitation measurements: introduction of the spectral differential reflectivity. *Proc. 30th Conf. on Radar Meteorology*, Munich, Germany, Amer. Meteor. Soc., 316-318.

Moisseev, Dmitri, Christine Unal, Herman Russchenberg and Leo Ligthart: 2001, Target-to-Clutter Contrast Enhancement Using Radar Doppler Polarimetry. *Proc. IEEE Radar Conference*, Atlanta, GA, 321-325.

Moisseev, Dmitri, Christine Unal, Herman Russchenberg and Leo Ligthart: 2000, Radar Doppler polarimetry: a new approach for characterization of radar targets, *Proc. SPIE Annual meeting*, San Diego, CA, **4133**, 261-269.

Moisseev, Dmitri, Christine Unal, Herman Russchenberg and Leo Ligthart, 2000: Doppler polarimetric ground clutter identification and suppression for atmospheric radars based on co-polar correlation. *Proc. MIKON*, Wroclaw, Poland, 94-97.

Moisseev, Dmitri, Christine Unal, Herman Russchenberg, and Leo Ligthart, 1991: Polarimetric radar calibration using distributed target. *Proc. IGARSS*, Hamburg, Germany, 434-436.

Unal, C.M.H., D.N. Moisseev, and L.P. Ligthart, 1998: Doppler-polarimetric radar measurements of precipitation. *Proc. J.I.P.R.'4, Radar Polarimetry workshop*, 429-438.

Acknowledgments

Working on a PhD thesis requires not only a major effort from the PhD student himself but also a lot of support and understanding from other people. This PhD thesis is a proof that people who were surrounding me for these four years were carrying and kind enough to make this thesis possible.

First of all I would like to thank my professor, Leo Ligthart, who not only believed in me but also kept encouraging me through all these years. I also wish to thank my day-to-day supervisor, Herman Russchenberg, for keeping me on track and for providing me with very helpful and practical comments on my work.

I learned a lot from my colleagues. I am indebted to Christine Unal who taught me basics of radar polarimetry and who provided many valuable comments on my work. I am grateful to Felix Yanovsky, who was visiting IRCTR in the fall of 1997, for explaining to me a clutter suppression method that became the basis for the work presented in Chapter 6. I am thankful to Viktor N. Tatarinov for our long discussions that have contributed to my understanding of radar polarimetry. Alex Yarovoy, Oleg Krasnov, Silvester Heijnen and Nikolaos Skaropoulos were kind enough to tolerate my interference in their work and to discuss many issues of my research; thank you very much for your patience and help. My friend and roommate Victor Venema has provided a nice working environment and helped me to adjust to the Dutch culture. At the last stage of writing a PhD thesis when motivation reaches its minimum it was inspiring to communicate with Hans Verlinde, who was visiting IRCTR at the time. I would also like to thank Ezio Pusone for making late night working more pleasant. I am thankful to my new colleague at the Department of Geodesie, Rens Swart, for teaching me the proper Dutch language.

I am grateful to Mirjam Nieman for proofreading and polishing the manuscript of this thesis. I also want to acknowledge members of my defense committee for devoting their time to read and comment on my thesis.

I am thankful to all my friends who supported me during all these years. I especially would like to thank members of the Wednesday night jogging club, Yngve, Karl, Ivo, Sander and Javier. Thank you guys for keeping me in shape. I also wish to thank Elise, Sharm, Aude, Jean-Marie, Christophe, Cecile, Claire, Nikos and Elena for making my stay in the Netherlands such a great fun.

I am grateful to my parents for their love and support. I am indebted to my wife Svetlana who has surrounded me with atmosphere of love and encouragement, which made this thesis possible.

Dmitri Moisseev
Delft, March 2002

ISBN 90-77017-64-X